FCTUC DEPARTAMENTO DE FÍSICA
FACULDADE DE CIÊNCIAS E TECNOLOGIA
UNIVERSIDADE DE COIMBRA

Monitoring Wine Fermentation Process

Paulo Gonçalves Marques

Student Number 2005112061

FCTUC DEPARTAMENTO DE FÍSICA
FACULDADE DE CIÊNCIAS E TECNOLOGIA
UNIVERSIDADE DE COIMBRA

Monitoring Wine Fermentation Process

Dissertation presented to the Department of Physics of the Faculty of Sciences and Technology of the University of Coimbra to complete the requirements to obtain the degree of Master of Physics Engineering

Paulo Gonçalves Marques
Student Number: 2005112061

Coimbra, 31 August, 2010

FCTUC DEPARTAMENTO DE FÍSICA
FACULDADE DE CIÊNCIAS E TECNOLOGIA
UNIVERSIDADE DE COIMBRA

activespace technologies

making space a global endeavour

“Your persistence is your measure of faith in yourself.”

Unknown Source

ABSTRACT

Alcoholic fermentation in wine-making industry is a process in which grape sugars are transformed in alcohol and carbon dioxide by the yeasts metabolic processes, who consume them. This plays an important role in wine-making, since it is during fermentation that wines gain their exquisite properties and a failed fermentation results in a failed wine, with associated losses. Monitoring wine fermentation process is still a long and costly process, since it is required to extract samples from tanks, send them to specialized labs and perform all required tests. Some of the most important parameters to monitor during the fermentation process are temperature, pH, density, carbon dioxide concentration,, alcoholic concentration, sugars concentration and colour, to quote only a few. In order to monitor these parameters, several periodic measurements are made, using specific sensors.

The present project, named UVAS, intends to develop an automatic system which integrates all required sensors in one single system, from which information regarding all important variables can be consulted, allowing to save both time and money.

Keywords: Alcoholic Fermentation, Wine-making, yeasts, temperature, pH, density, carbon dioxide concentration, alcoholic concentration, sugars concentration, colour, UVAS.

RESUMO

A fermentação alcoólica na indústria vinícola é um processo em que os açúcares da uva são transformados em álcool e dióxido de carbono através dos processos metabólicos das leveduras que os consomem. Este processo é extremamente importante, uma vez que é com a fermentação que os vinhos ganham as suas propriedades únicas, que os valorizam o que significa que se a fermentação falhar, há um prejuízo considerável. O processo de monitorização da fermentação resulta num grande custo, uma vez que é necessário extrair amostras dos tanques e enviá-los para laboratórios especializados, onde os diversos testes serão efectuados. Alguns dos parâmetros da fermentação considerados mais importantes são a temperatura, o pH, a densidade, concentração de dióxido de carbono, a concentração alcoólica, concentração de açúcares e a cor, para citar apenas alguns. Para monitorizar estes parâmetros, diversas medições são efectuadas, fazendo uso de sensores específicos.

O presente projecto, chamado UVAS, pretende desenvolver um sistema automático que integre todos os sensores necessários num único sistema, através do qual a informação relativamente às variáveis mais importantes poderá ser consultada.

Palavras-chave: Fermentação alcoólica, vinícola, leveduras, temperatura, pH, densidade, condutividade, permitividade, concentração alcoólica, concentração de açúcares, cor, UVAS.

ACKNOWLEDGEMENTS

This work is dedicated to all those who have ever support and believed in me, for my parents who gave me this opportunity five years ago, to Active Space Technologies, whose members took me as part of the family and finally to me, for proving that I can do it.

Thank you, everyone, for everything.

Paulo Marques

TABLE OF CONTENTS

ABSTRACT II

RESUMO III

ACKNOWLEDGEMENTS IV

TABLE OF CONTENTS V

LIST OF FIGURES VII

LIST OF TABLES X

1 INTRODUCTION 1

1.1 PURPOSE 1
1.2 DOCUMENT STRUCTURE 2
1.3 PROJECT GROUP 3
1.4 PROJECT SCHEDULE 4

2 PARAMETERS MEASUREMENT 5

2.1 MEASURING PH 5
2.1.1 GLASS ELECTRODES 7
2.1.2 ISFET TRANSISTORS 9
2.2 MEASURING TEMPERATURE 11
2.2.1 THERMOCOUPLES 11
2.2.2 RESISTIVE THERMAL DEVICES 14
2.2.3 TEMPERATURE COEFFICIENT DEVICES 17
2.3 MEASURING DENSITY 18
2.3.1 SPECIFIC GRAVITY 18
2.3.2 BUOYANCY 18
2.3.3 REFRACTOMETERS 19
2.3.4 NUCLEAR DENSITY SENSORS 20
2.4 MEASURING VISCOSITY 21
2.4.1.1 Dynamic viscosity 22
2.4.1.2 Kinematic viscosity 23
2.4.1.3 Acoustic Wave Measurement Overview 23
2.4.1.4 SAW and STW technology 24
2.4.1.5 BAW Technology 25
2.4.1.6 Shear-Horizontal Acoustic Plate Mode (SH-APM) 27
2.5 MEASURING SUGARS CONCENTRATION 28
2.5.1 STECHIOMETRIC MEASUREMENTS 29
2.5.2 BRIX SENSORS 29
2.5.2.1 Refractometry 30
2.5.2.2 Refractometers 30
2.6 MEASURING ALCOHOLIC CONCENTRATION 33
2.6.1 STECHIOMETRIC MEASUREMENT 34
2.6.2 SPECTROPHOTOMETRY 35
2.6.3 REFRACTOMETRY 36
2.7 MEASURING GLUCOSE AND FRUCTOSE CONCENTRATION 36
2.7.1 POLARIMETRY 36

2.7.2 POLARIMETERS 37
2.7.2.1 Polarimeter Using Optoelectronic methods 39
2.7.2.2 Polarimeter Using Mobile parts method 40
2.7.3 IDENTIFYING FRUCTOSE AND GLUCOSE 40
2.8 MEASURING CONDUCTIVITY 41
2.8.1 OHM'S LAW CONDUCTIVITY MEASUREMENT 42
2.8.2 RELAXATION PROBE METHOD 42
2.9 MEASURING PERMITTIVITY 43
2.9.1 MUTUAL IMPEDANCE PROBE 44
3 SYSTEM OVERVIEW 47
3.1 SYSTEM ARCHITECTURE 47
3.2 SYSTEM FUNCTIONAL BREAKDOWN 48
3.3 SYSTEM SEQUENCE DIAGRAM 51
3.3.1 FUNCTIONAL BLOCKS ANALYSIS 52
4 SENSORS DEVELOPMENT 56
4.1 SENSORS DEVELOPMENT OVERVIEW 56
4.1.1 MEASURING PH 56
4.1.2 MEASURING TEMPERATURE 58
4.1.3 MEASURING VISCOSITY 60
4.1.4 MEASURING SUGARS AND ALCOHOLIC CONCENTRATION 60
4.1.5 MEASURING GLUCOSE AND FRUCTOSE CONCENTRATION 62
4.1.5.1 Sample Vial 63
4.1.5.2 Guide Troughs and Mounts 64
4.1.5.3 Light Source and Light Detector 65
4.1.5.4 Collimator 68
4.1.5.5 Polarizers 69
4.1.5.6 Detector/ Analyzer 70
4.1.5.7 Polarimeter Assembly and Programming 75
4.1.5.8 Tests and Validation 78
4.2 SENSOR'S PLACEMENT AND LIQUID ISOLATION 82
5 CONCLUSIONS 83
6 GLOSSARY 84
6.1 TERMS AND DEFINITIONS 84
6.2 ACRONYMS 84
7 APPLICABLE AND REFERENCE DOCUMENTS 87
7.1 APPLICABLE DOCUMENTS 87
7.2 REFERENCE DOCUMENTS 92

LIST OF FIGURES

FIGURE 2-1: PH SENSOR GLASS ELECTRODES ARCHITECTURE. 7
FIGURE 2-2: REFERENCE ELECTRODE SCHEME 9
FIGURE 2-3: MEASUREMENT ELECTRODE SCHEME 9
FIGURE 2-4: SCHEMATIC REPRESENTATION OF A A) MOSFET AND AN B) ISFET STRUCTURE. 10
FIGURE 2-5: THERMOCOUPLE WORKING PRINCIPLE. 12
FIGURE 2-6: 2-WIRE RTD CONFIGURATION 15
FIGURE 2-7: 3-WIRE RTD CONFIGURATION 15
FIGURE 2-8: 4-WIRE RTD CONFIGURATION 15
FIGURE 2-9: GRAPHICAL REPRESENTATION OF TOLERANCE VALUES FOR RESISTANCE WITH TEMPERATURE FOR CLASS A AND CLASS B RTD. 16
FIGURE 2-10: FORCES ACTING IN A BODY IMMERSED IN A FLUID 19
FIGURE 2-11: VISCOSITY CALCULATION DIAGRAM. 22
FIGURE 2-12: SAW SENSOR SCHEME 25
FIGURE 2-13: STW SENSOR SCHEME 25
FIGURE 2-14: TSM REPRESENTATION 26
FIGURE 2-15: BAW DEVICE WITH DIRECT CONTACT WITH LIQUIDS 26
FIGURE 2-16: BAW DEVICE WITH A THIN FILM ACTING AS CONTACT BETWEEN ELECTRODE AND LIQUID 27
FIGURE 2-17: SHEAR-HORIZONTAL ACOUSTIC PLATE MODE SCHEMATIC 27
FIGURE 2-18: TYPICAL NORMAL AND STUCK (•) FERMENTATIONS OF CABERNET SAUVIGNON. 28
FIGURE 2-19: DIAGRAM OF THE REFRACTOMETER OUTPUT THE WHITE SECTION REPRESENTS THE SECTION WITH INCIDENT LIGHT AND THE DARK PATH REPRESENTS THE AREA WITH NO INCIDENT LIGHT 30
FIGURE 2-20: REFRACTOMETER SENSOR SCHEMATICS 31
FIGURE 2-21: BRIX (SUCROSE CONCENTRATION) RELATION WITH THE REFRACTIVE INDEX 32
FIGURE 2-22: SCHEME OF A SOLUTION READING GIVEN BY AN ANALOGICAL REFRACTOMETER. 32
FIGURE 2-23: ANALOGICAL REFRACTOMETER 32
FIGURE 2-24: PORTABLE BRIX REFRACTOMETER 33
FIGURE 2-25: IN LINE BRIX REFRACTOMETER 33
FIGURE 2-26:EVOLUTION OF ALCOHOL CONTENT (DETERMINED BY 4 DIFFERENT METHODS, HPLC, MUST ANALYSIS, WINE ANALYSIS AND CONCENTRATION RATIO ANALYSIS) DURING THE FERMENTATION OF A RED MUST OF CABERNET SAUVIGNON 34
FIGURE 2-27: LIQUID ETHANOL SPECTRUM IN THE NEAR IR REGION 35
FIGURE 2-28: SCHEMATIC REPRESENTATION OF A POLARIMETER 37
FIGURE 2-29: LIGHT'S ELECTRIC FIELD VECTOR DECOMPOSITION 40
FIGURE 2-30: RELATION BETWEEN CARBON DIOXIDE CONCENTRATION AND TOTAL WINE IMPEDANCE 42
FIGURE 2-31: RELAXATION PROBE CIRCUIT SCHEMATICS 43
FIGURE 2-32: FOUR ELECTRODE WORKING SCHEMATIC 44
FIGURE 2-33: MUTUAL IMPEDANCE PROBE WORKING SCHEMATIC 45

FIGURE 3-1: UVAS SYSTEM ARCHITECTURE 47
FIGURE 3-2: UVAS SYSTEM NETWORK ARCHITECTURE 48
FIGURE 3-3: UVAS SYSTEM FUNCTIONAL BREAKDOWN 50
FIGURE 3-4: UVAS SYSTEM SEQUENCE DIAGRAM 51
FIGURE 3-5: FUNCTIONAL BLOCK DIAGRAM – TOP LEVEL. 52
FIGURE 3-6: FUNCTIONAL BLOCK DIAGRAM – TIER 1. 53
FIGURE 3-7: FUNCTIONAL BLOCK DIAGRAM- TIER 2, MASTER UVAS 53
FIGURE 3-8: FUNCTIONAL BLOCK DIAGRAM- TIER 2, SLAVE UVAS. 54
FIGURE 3-9: FUNCTIONAL BLOCK DIAGRAM – TIER 3, MASTER HMI 55
FIGURE 4-1: ISFET CHIP OII1 57
FIGURE 4-2: ISFET CHIP CIRCUIT 57
FIGURE 4-3: RTD SENSOR IMAGE 58
FIGURE 4-4: RTD RELATION BETWEEN RESISTANCE AND TEMPERATURE 59
FIGURE 4-5: VISCOSIMETER SCHEMATIC 60
FIGURE 4-6: ATAGO PAL-86S BRIXMETER 61
FIGURE 4-7: ATAGO PAL-34S ALCOHOLMETER 61
FIGURE 4-8: POLARIMETER SCHEMATICS 63
FIGURE 4-9: POLARIMETER SAMPLE VIAL 64
FIGURE 4-10: DRYLIN® N - LOW PROFILE LINEAR GUIDE SYSTEM WITH ONE SKATE 64
FIGURE 4-11: SKATE MOUNT USED 65
FIGURE 4-12: OPTICAL MOUNTS USED IN THE POLARIMETER: A) STANDARD MOUNT; B) ANALYSER MOUNT 65
FIGURE 4-13: LED USED AS LIGHT SOURCE IN THE POLARIMETER 66
FIGURE 4-14: PHOTODIODE AND TRANSISTOR CIRCUIT COMPARISON WITH THE PHOTOTRANSISTOR 66
FIGURE 4-15: PHOTOTRANSISTOR USED AS PHOTODETECTOR IN POLARIMETER 66
FIGURE 4-16: OSRAM 3310 PHOTOTRANSISTOR RELATIVE SENSITIVITY GRAPHIC 67
FIGURE 4-17: LED AND PHOTOTRANSISTOR CIRCUITS 67
FIGURE 4-18: LED ARRAY AND PHOTOTRANSISTOR CIRCUITS IN PROTOBOARDS ASSEMBLIES 68
FIGURE 4-19: PRECISION PINHOLE COLLIMATOR MOUNT 69
FIGURE 4-20: TECHSPEC LINEAR POLARIZING LAMINATED FILM SHEET 69
FIGURE 4-21: A) FIRST POLARIZER MOUNT; B) ANALYSER MOUNT 70
FIGURE 4-22: SCHEMATICS OF THE ANALYSER ROTATION SYSTEM 70
FIGURE 4-23: ANALYSER BRACKET ASSEMBLY FROM DIFFERENT VIEWS 71
FIGURE 4-24: L293E AND STEPPER MOTOR CIRCUIT SCHEMATIC 72
FIGURE 4-25: BIPOLAR STEPPER MOTOR SCHEMATICS 73
FIGURE 4-26: UNIPOLAR STEPPER MOTOR SCHEMATICS WITH 5 AND 6 WIRES 73
FIGURE 4-27: STEP MOTOR DRIVE CIRCUIT ASSEMBLED 74
FIGURE 4-28: POSITION SENSOR CIRCUIT SCHEMATICS 74
FIGURE 4-29: POSITION SENSOR CIRCUIT 75
FIGURE 4-30: POLARIMETER CIRCUIT SCHEMATIC 75
FIGURE 4-31: POLARIMETER FULL PROTOTYPE ASSEMBLY 76
FIGURE 4-32: PICDEM 2 PLUS DEMO BOARD 76
FIGURE 4-33: POLARIMETER SOFTWARE FLOW DIAGRAM 77
FIGURE 4-34: RESULTS OF THE POLARIMETER 81

FIGURE 4-35: TUBE CONNECTIONS USED FOR SENSORS IMPLEMENTATION 82

LIST OF TABLES

TABLE I: PROJECT TEAM....3
TABLE II: UVAS PROJECT SCHEDULE....4
TABLE III: LIST OF IMPORTANT PARAMETERS TO MONITOR DURING WINE FERMENTATION....5
TABLE IV: RTD RESISTANCE WITH TEMPERATURE RELATION....58
TABLE V: SUCROSE CONCENTRATION MEASUREMENT USING POLARIMETRY....80

1 Introduction

1.1 Purpose

The entire process of wine-making is a very complex biological process, which involves several stages and several reactions, where the metabolization of grape sugars in carbon dioxide and ethanol by yeasts action is the most important:

- Microbiological reactions – the number and the yeast species change during the fermentation. The concentration of yeasts increases to a maximum value as a consequence of the fermentation process, after which the concentration of bacteria will decrease again. After this point, the sugar concentrations are not enough to sustain the high bacteria population and the yeasts will start to die. Ideally, at the end of the fermentation process, there will be no more yeasts alive in the wine.
- Biochemical and chemical reactions – many biochemical and chemical reactions take place during fermentation process. The most important is the sugar degradation, which results in ethanol and carbon dioxide production. However, many secondary metabolites, such as aroma compounds, are formed as consequence of this transformation. Others reactions such as colour extraction, oxidations, precipitations etc. take place during fermentation process.
- Physical reactions - the occurred transformations lead to several physical modifications, namely the decrease of density, the increase of temperature and the carbon dioxide liberation.

Although this process is common in all wine-making, it is through slight variations in this fermentation process that all different and more exquisite wines are created, varying in different parameters from each others, such as pH, density, alcoholic content, colour and remaining sugar concentration after fermentation. Yeasts, the microorganisms responsible for the fermentation process are very fragile and very susceptible to environment variations. For this reason, it becomes also important to monitor and control all environmental parameters in order to avoid the yeasts deaths and therefore stop the fermentation process, achieving a low quality wine. By means of this continuous monitoring, it is possible to control the fermentation process and even actuate over it if necessary, in order to achieve a good quality wine.

For these reasons, it is intended to develop a system to monitor the fermentation parameters considered the most important for the fermentation process.

In order to do this, the UVAS system shall acquire and provide relevant information regarding the state of the fermentation process, in order to allow a better process control.

1.2 Document Structure

The present document has been organized in several sections, each one presenting important information regarding the project.

In section 1, a brief introduction to the project is made, as well as an exposition of the motivation and the purposes of the project. The project team and project schedule are also introduced.

In section 2, a theoretical background regarding the working principles of the UVAS system is presented, as well as a brief list of possible sensors to measure all the most important parameters.

Section 3 presents a system overview, specifying the functionalities of the system and the chosen architecture to implement UVAS system.

In section 4, all information regarding the assembly and validation of the sensors is presented, as well as all communication protocols, configurations of the master computer and all other functionalities of the UVAS system.

In section 5, the conclusions of all the work done in the UVAS system are presented.

In section 6, a list of all terms, definitions and acronyms used while writing the present document are listed.

Section 7 presents a complete list with all documents consulted while researching and writing this document during project development.

1.3 Project Group

Table I: Project Team

Name	Role
Paulo Marques	Trainee
Abel Mendes	Chief Supervisor
Rui Sousa	Electronics Engineer
Joaquim Varandas	Electronics Engineer
André Tenreiro	IT support
Rui Henriques	Quality assurance
Fernando Simões	Consultant, PHD

In the first months of the UVAS project, during which research was made, the project team was mainly composed by the trainee Paulo Marques, supervised by Eng. Abel Mendes. Eng. Rui Henriques granted support in quality assurance, Eng. André Tenreiro granted support in IT, and Dr. Fernando Simões provided as a consultant during the development of the UVAS project.

In the final months of the phase one of the project, during which the system design has been performed, the project team has been increased with Eng. Rui Sousa and Eng. Joaquim Varandas.

1.4 Project Schedule

Table II: UVAS Project Schedule

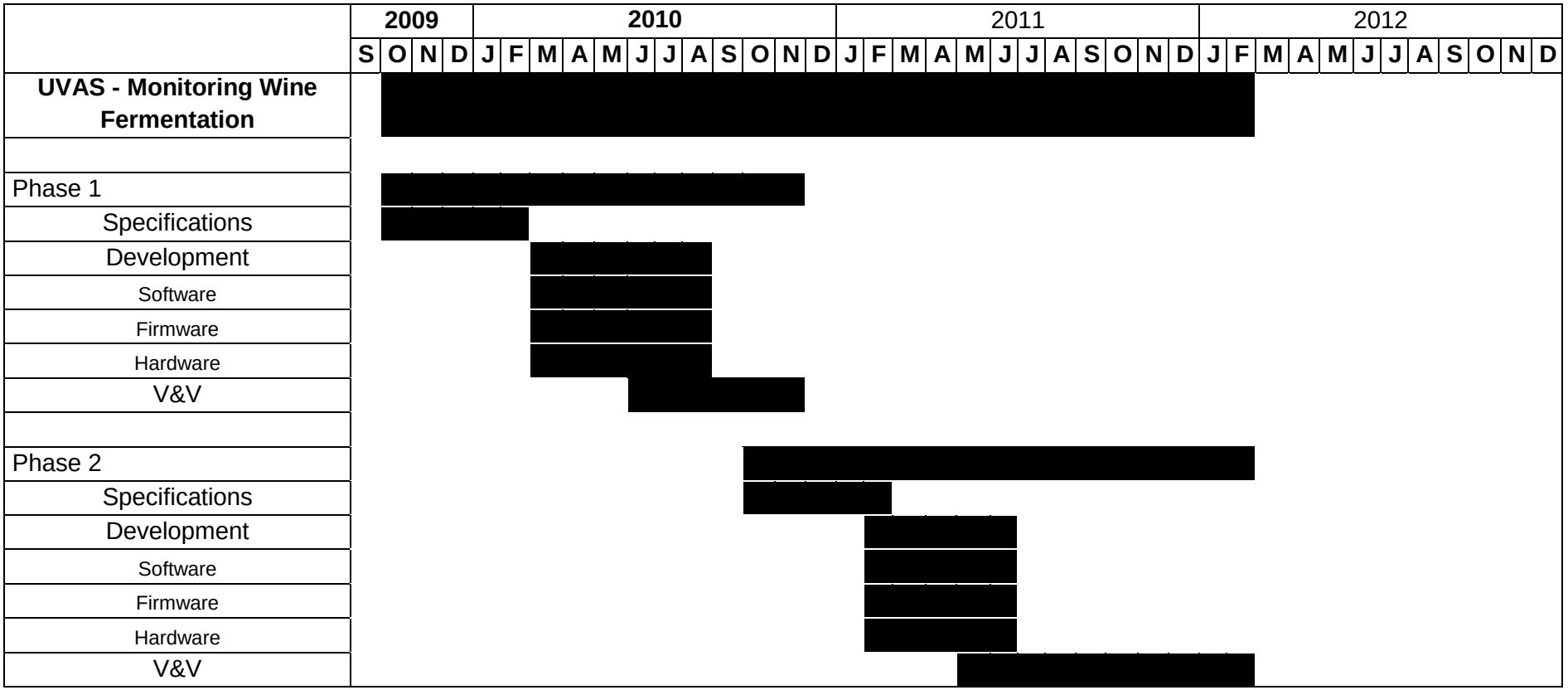

2 Parameters Measurement

As it was said before, the fermentation is a complex process, which involves several other sub reactions and processes. All these cause significant changes into the grape juice, turning it into a good or not so good wine. There are several important parameters which are affected and are considered essential to monitor during the fermentation process, being these pH, total acidity, temperature, density, total sugar concentration, glucose and fructose concentrations, alcoholic concentration and colour intensity of the wine. There are also other parameters considered desirable to measure. These are carbon dioxide concentration, nitrogen concentration, yeast concentration, sulfur dioxide concentration and viscosity. If all these parameters are known either quantitatively or qualitatively, it becomes possible to extract information about the fermentation process and determine how it is best to actuate.

Table III: List of Important Parameters to Monitor During Wine Fermentation

Parameter	Level before fermentation (must)	Level after fermentation (wine)	Analytical method	Importance

Due to confidentiality agreements, Table 3 can not be properly be displayed. For more information, regarding this table, Activespace Technologies must be contacted.

In the following chapter, the physical parameters to measure will not be approached in the wine's perspective, but in an instrumentation perspective, in which the analysis is made considering the most suitable technology to measure the wine's parameters.

2.1 Measuring pH

The pH of a solution is a characteristic which indicates its acidic or alkaline properties. This is an important parameter in industrial and pharmaceutical areas, food processing, agriculture and many more. The term pH is derived from "p", the mathematical symbol of the negative logarithm, and "H", the chemical symbol of Hydrogen. The formal definition of pH is the negative logarithm of the Hydrogen ion activity. It is measured on a scale from 0 to 14.

The pH value of a substance is directly related to the ratio of the hydrogen ion [H^+] and the hydroxyl ion [OH^-] concentrations. If the H^+ concentration is greater than OH^-, the solution is acidic; i.e., the pH value is less than 7. If the OH^- concentration is greater than H^+, the solution is basic, with a pH value greater than 7. If equal amounts of H^+ and OH^- ions are present, the solution is neutral, with a pH of 7. Since the relationship between hydrogen ions and hydroxyl ions in a given solution is constant for a given set of conditions, either one can be determined by knowing the other. Thus, pH is a measurement of both acidity and alkalinity, even though by definition it is a selective measurement of hydrogen ion activity. Since pH is a logarithmic function, a change of one pH unit represents a ten-fold change in hydrogen ion concentration.

Temperature also has a great influence in pH measurement. pH is a temperature dependant characteristic and the slightest temperature variation can cause pH variation which alters the entire thermal equilibrium, which will cause significant changes to the chemical equilibrium, producing more OH^- and H^+, altering the pH. Temperature also affects the output of the electrode, which use ionic movement to interpolate the pH, as will be explained.

The response of an ideal pH electrode is given by Nernst equation:

$$\mathrm{E} = \mathrm{E}_0 - 2.3\left(\frac{\mathrm{RT}}{\mathrm{nF}}\right)\log \mathrm{H}^+ \qquad (1)$$

where E is the total potential developed, E_0 is the potential developed with $[\mathrm{H}^+]$ $1\ \mathrm{mol/dm^3}$, R is the gas constant, n is the valence of the ion, F is the Faraday constant, $\mathrm{H}^+$is the concentration of hydrogen ion and T is the temperature. All these being constants, T is the only variable which can truly influence the potential. This variation also influences calibrations. To solve this problem, both pH and temperature are measured to provide external compensation, or automatic temperature compensation is performed by the sensor and the output data is already compensated for thermal effects.

2.1.1 Glass Electrodes

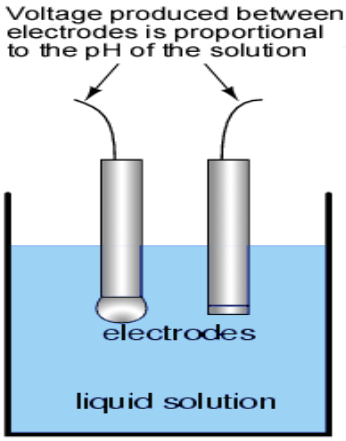

Figure 2-1: pH Sensor Glass Electrodes Architecture.

[AD1]

A glass bulb pH probe is made of two special electrodes, one to act as a reference and one to measure the voltage in relation to the reference.

Inside these electrodes there is a special solution acting as a buffer. These are solutions that have constant pH values and the ability to resist changes in that pH level, being used to calibrate the pH measurement system (electrode and meter). There can be small differences between the output of one electrode and another, as well as changes in the output of electrodes over time. Therefore, the system must be periodically calibrated. Most pH meters require calibration at several specific pH values. One calibration is usually performed near the isopotential point (the signal produced by an electrode at pH 7 is 0 mV at 25℃), and a second is typically performed at either pH 4 or pH 10. It is best to select a buffer as close as possible to the actual pH value of the sample to be measured.

Having an inner and an outer tube, the reference electrode is in the inner tube and it is only good while it stays electrically static through the duration of the measurement. The outer tube contains the measurement electrode and it is in contact with the medium. As such, the buffer solution requires to be periodically replenished due to ion losses and evaporation.

The measurement electrode is constructed using special materials in order to allow the ion selective barrier needed to attract the hydrogen ions from the solution being measured. Usually it is made of glass, filled with a buffer solution, with a bulb like extremity. However, glass is a dielectric material and therefore has high impedance, which raises some problems regarding ionic conductivity. To solve these problems, special types of glasses, doped with different elements, are used for the glass bulb. These glasses are based in silicate matrixes or chalcogenide matrixes. In the case that

the glass is based in silicate matrixes, it can be doped with Li, Na, K, Al, B or Ca. In the case of chalcogenide matrixes, the dopants are based in molecular networks of AsS, AsSe or AsTe. These structures are such that the dopants (metal cations) have mobility in the glass network.

These doped glasses have a thin layer (~10nm) of hydrated gel inside and outside of the bulb, which will make it an ion selective electrode. When in contact with the gel, the metal cations diffuse out of the glass and into the solution, to be measured while H^+ from the solution to be measured can diffuse into the hydrated gel. H^+ does not cross through the glass membrane of the pH electrode. Instead, it is the dopant that crosses it and suffers a change in its free energy. When an ion diffuses from a region of activity to another region of activity, there is a free energy change and this is what the pH meter actually measures. The hydrated gel membrane is connected by cation transport and thus the concentration of H^+ on the outside of the membrane is 'relayed' to the inside of the membrane by the dopant.

Also inside the inner tube is the cathode terminus of the reference probe. The anodic terminus wraps itself around the outside of the inner tube and ends with the same sort of reference probe as was on the inside of the inner tube. Both the inner tube and the outer tube contain a reference solution but only the outer tube has contact with the solution on the outside of the pH probe by way of a porous plug that serves as a salt bridge.

The pH output may vary with the temperature so it should also be monitored, adding a temperature sensor and adding a temperature value to each of pH measurements. This system should generate a voltage directly proportional to the pH of the solution. As such, with a pH 7, the electrodes return 0V. With an acid pH (below 7), the voltage will have one polarity and with an alkaline pH (above 7), with opposite polarity.

All glass pH electrodes have extremely high electric resistance from 50 to 500 MΩ. Therefore, the glass electrode can be used only with a high input-impedance measuring device like a pH meter, or, more generically, a high input-impedance voltmeter which is called an electrometer.

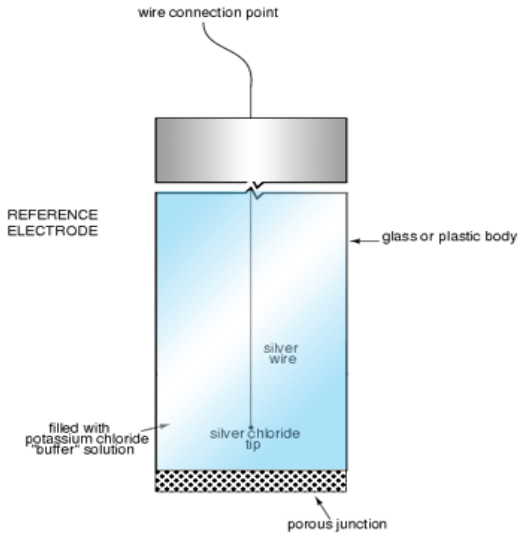

Figure 2-2: Reference Electrode scheme

[AD1]

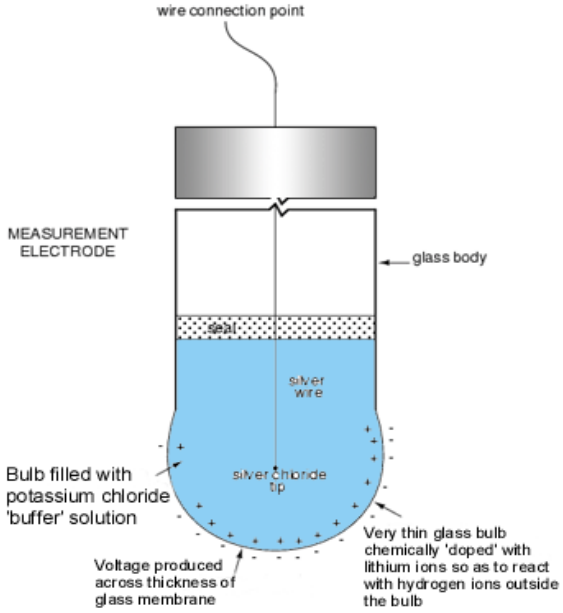

Figure 2-3: Measurement Electrode Scheme

[AD1]

2.1.2 ISFET Transistors

In the simplest version, (i.e. a metal oxide semiconductor field effect transistor, n-channel MOSFET), a p-type silicon substrate (bulk) contains two n-type diffusion regions (source and drain). The structure is covered with a silicon dioxide insulating layer on top of which a metal gate electrode is deposited (figure 2-4a).

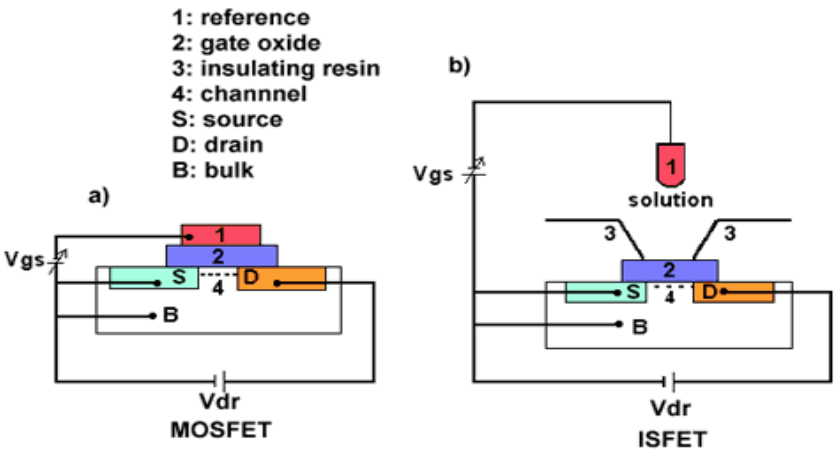

Figure 2-4: Schematic representation of a a) MOSFET and an b) ISFET structure. [AD2]

When a positive voltage is applied to the gate electrode, electrons (which are the minority carriers in the substrate) are attracted to the surface of the semiconductor. Consequently, a conducting channel is created between the source and the drain, near the silicon dioxide interface. The conductivity of this channel can be modulated by adjusting the strength of electrical field between the gate electrode and the silicon, perpendicular to the substrate surface. At the same time a voltage can be applied between the drain and the source (V_{ds}), which results in a drain current (I_d) between the n-regions.

In the case of the ISFET (figure 2-4b), the gate metal electrode of the MOSFET is replaced by an electrolyte solution which is contacted by reference electrode (then the SiO_2 gate oxide is placed directly in an aqueous electrolyte solution. The metal part of reference electrode can be considered as the gate of the MOSFET).

The electric current (I_d) flows from the source to the drain. Like in MOSFET the channel resistance will depend of the voltage applied to the gate. Therefore, the source-drain current, I_d, is influenced by the interface potential at the oxide/aqueous solution. Although the electric resistance of the channel provides a measure for the gate oxide potential, the direct measurement of this resistance gives no indication of the absolute value of this potential. However at a fixed source-drain potential (V_{ds}), changes in the gate potential can be compensated by modulation of the V_{gs}. This adjustment should be carried out in such a way that the changes in V_{gs} applied to the reference electrode are exactly opposite to the changes in the gate oxide potential. This is automatically performed by ISFET amplifier with feedback which allows obtaining a constant source-drain current. In this particular case, the gate-source potential is determined by the surface potential at the insulator/electrolyte interface.

When SiO_2 is used as the insulator, the chemical nature of the interface oxide is reflected in the measured source-drain current. The surface of the gate oxide contains OH^- functionalities, which are in electrochemical equilibrium with ions in the sample solutions (H^+ and OH^-). The hydroxyl groups at the gate oxide surface can be protonated and deprotonated and thus, when the gate oxide contacts an aqueous solution, a change of pH will change the SiO_2 surface potential. The selectivity and chemical sensitivity of the ISFET are completely controlled by the properties of the electrolyte/insulator interface. Other inorganic gate materials for pH sensors like Al_2O_3, Si_3N_4 and Ta_2O_5 have better than SiO_2 properties in relation with pH response, hysteresis and drift. In practice, these layers are deposited on the top of the first layer of SiO_2 by means of chemical vapour deposition (CVD).

2.2 Measuring Temperature

The wine quality is highly dependent of fermentation temperature. Values of temperature off the range presented in table 3 may lead to some problems, like unfinished fermentations, the deaths of the fermenting yeast, and the loss of volatile aroma compounds and ethanol [RD31].

2.2.1 Thermocouples

The thermocouple is one of the applications of the thermoelectric effect, more specifically, of the Seebeck effect. This effect was first observed when Seebeck discovered that a compass needle would be deflected when a closed loop was formed of two metals joined in two places with a temperature difference in them. By this gradient, an electric current is created, producing as well a magnetic field, which altered the compass.

Thermocouples are used to measure temperatures. To achieve this, one of the thermocouple's endings is placed at a known temperature, usually a much colder than the one desired to measure while the other ending is placed at the desired temperature. In the early days of thermocouples, the cold junction would be in an ice-bath but today, this solution is impractical in most situations. Therefore, when the cold junction is not at 0℃, the temperature of this jun ction must be known in order to determine the actual hot-junction temperature. The output voltage of the thermocouple must also be compensated to account for the voltage created by the nonzero cold-junction temperature. This process is known as cold-junction compensation.

Thermocouples are the most popular temperature sensors. They are cheap, interchangeable, have standard connectors and can measure a wide range of temperatures. The main limitation is accuracy since system errors of less than 1℃ can

be difficult to achieve. They are less suitable for applications where smaller temperature differences need to be measured with high accuracy, for example the range 0–100 ℃ with 0.1 ℃ accuracy. For such applications thermistors and resistance temperature detectors are more suitable.

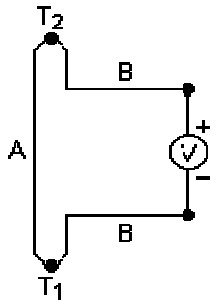

Figure 2-5: Thermocouple working principle.
[AD12]

A wide variety of thermocouples is available for several applications. These are chosen according with project specifications and with the thermocouple's own characteristics, e.g. if the device is made out of magnetic materials and its own material inertness:

- Type K (chromel–alumel) is the most common general purpose thermocouple. It is inexpensive and available in a wide variety of probes. They are available in the −200ºC to +1350ºC range. The type K was specified at a time when metallurgy was less advanced than it is today and, consequently, probes' characteristics vary considerably. Another potential problem arises in some situations since one of the constituent metals, nickel, is magnetic. One characteristic of thermocouples made with magnetic material is that they undergo a deviation in output when the material reaches its Curie point; this occurs for type K thermocouples at around 150℃. Se nsitivity is approximately 41µV/℃. For K type thermocouples, the chromel cond uctor is positive and the alumel conductor is negative.
- Type E (chromel–constantan) has a high output (68µV/℃) which makes it well suited to cryogenic use. Additionally, it is non-magnetic.
- Type J (iron–constantan) is less popular than type K due to its limited range (−40 to +750℃). The Curie point of the iron (770℃) causes an abrupt change to the characteristic and it is this that provides the upper temperature limit. Type J thermocouples have a sensitivity of about 55µV/℃ .
- Type N (Nicrosil–Nisil) (Nickel-Chromium-Silicon/Nickel-Silicon) thermocouples are suitable for use at high temperatures, exceeding 1200ºC, due to their

stability and ability to resist high temperature oxidation. Sensitivity is about 39µV/℃ at 900℃, slightly lower than type K. Desig ned to be an improved type K, it is becoming more popular.

- Types B, R, and S thermocouples use platinum or a platinum–rhodium alloy for each conductor. These are among the most stable thermocouples, but have lower sensitivity, approximately 10µV/℃, than othe r types. The high cost of these makes them unsuitable for general use. Generally, type B, R, and S thermocouples are used only for high temperature measurements.
- Type B thermocouples use a platinum–rhodium alloy for each conductor. One conductor contains 30% rhodium while the other conductor contains 6% rhodium. These thermocouples' range goes to 1800ºC, however, these produce the same output at 0ºC and 42ºC. This makes that these devices are discarded for applications with temperatures below 50ºC.
- Type R thermocouples use a platinum–rhodium alloy containing 13% rhodium for one conductor and pure platinum for the other conductor. Type R thermocouples are used up to 1600ºC.
- Type S thermocouples are constructed using one wire of 90% Platinum and 10% Rhodium (the positive or "+" wire) and a second wire of 100% platinum (the negative or "-" wire). Like type R, type S thermocouples are used up to 1600℃. In particular, type S is used as the standa rd of calibration for the melting point of gold (1064.43ºC).
- Type T (copper–constantan) thermocouples are suited for measurements in the −200 to 350℃ range. Often used as a differential m easurement since only copper wire touches the probes. Since both conductors are non-magnetic, there is no Curie point and thus no abrupt change in characteristics. Type T thermocouples have a sensitivity of about 43 µV/℃.
- Type C (tungsten 5% rhenium – tungsten 26% rhenium) thermocouples are suited for measurements in the 0ºC to 2320℃ range. This thermocouple is well-suited for vacuum furnaces at extremely high temperatures and must never be used in the presence of oxygen at temperatures above 260℃.
- Type M thermocouples use a nickel alloy for each wire. The positive wire contains 18% molybdenum while the negative wire contains 0.8% cobalt. These thermocouples are used in the vacuum furnaces for the same reasons as with type C. Upper temperature is limited to 1400ºC. Though it is a less common type of thermocouple, look-up tables to correlate temperature to EMF (milli-volt output) are available.

- In chromel-gold/iron thermocouples, the positive wire is chromel and the negative wire is gold with a small fraction (0.03–0.15 atom percent) of iron. It can be used for cryogenic applications (1.2–300K and even up to 600K). Both the sensitivity and the temperature range depend on the iron concentration. The sensitivity is typically around 15μV/K at low temperatures and the lowest usable temperature varies between 1.2 and 4.2K.

2.2.2 Resistive Thermal Devices

RTDs are sensors used to measure temperature by correlating the resistance of the resistive material with temperature. These sensors have been used for many years to measure temperature in laboratory and industrial processes, and have developed a reputation for accuracy, repeatability, and stability. As an example, there is the PT100, which has a resistance of 100Ω at 0ºC, and 138.4Ω at 100℃. There are also PT1000 sensors that have a resistance of 1000Ω at 0℃.

RTDs are constructed by one of the next manufacturing configurations. Most RTD elements consist of a length of fine coiled wire wrapped around a ceramic or glass core. This construction is usually quite fragile, so it is often placed inside a sheathed probe to protect it. A more common configuration is the thin-film element, which consists of a very thin layer of metal laid out on a plastic or ceramic substrate. Thin-film elements are cheaper and more widely available because they can achieve higher nominal resistances with less platinum. To protect the RTD, a metal sheath encloses the RTD element and the lead wires connected to it.

RTDs are the most accurate sensors for industrial applications and also offer the best long-term stability. Since RTDs offer a high resistance to external electromagnetic noise sources, these are well suited for temperature measurement in industrial environments. A representative value for the accuracy of a platinum resistance is +0.5% of the measured temperature. After one year there may be a shift of +0.05ºC through aging. Platinum resistance thermometers can cover temperature ranges from -200 to 800ºC. Because of this excellent stability and linear response to temperature, RTDs are a very popular choice. However, RTDs are also characterized by a slow response time and low sensitivity; and because they require current excitation, they can be prone to self-heating.

The easiest way to connect an RTD or thermistor to a measurement device is with a 2-wire connection.

With this method, the two wires that provide the RTD or thermistor with its excitation current are also used to measure the voltage across the sensor. Because of the low nominal resistance of RTDs, measurement accuracy can be drastically affected

by lead wire resistance. For example, lead wires with a resistance of 1Ω connected to 100Ω platinum RTD cause a 1% measurement error.

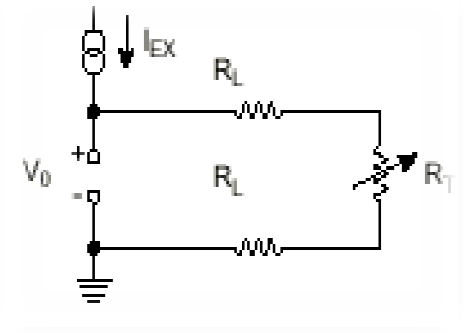

Figure 2-6: 2-wire RTD configuration
[AD66]

A 3-wire or 4-wire connection method can eliminate the effects of lead wire resistance. The connection places leads on a high impedance path through the measurement device, effectively eliminating error caused by lead wire resistance. It is not necessary to use a 3 or 4-wire connection method for thermistors because they typically have much higher nominal resistance values than RTDs.

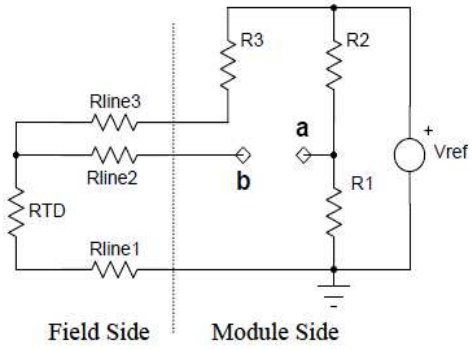

Figure 2-7: 3-wire RTD configuration
[AD66]

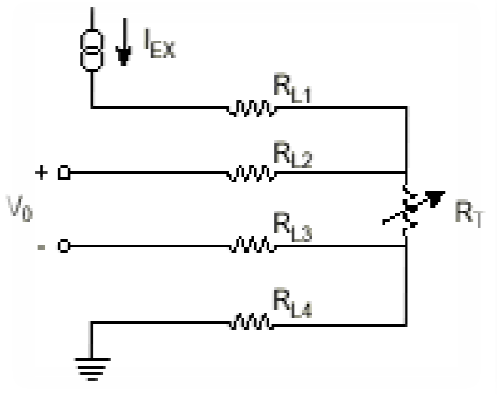

Figure 2-8: 4-wire RTD configuration
[AD66]

RTD and thermistor output signals are typically in the millivolt range, which are susceptible to internal noise influences. Lowpass filters are commonly used in RTD and thermistor data acquisition systems to effectively eliminate high frequency noise in measurements. For instance, lowpass filters are useful for removing the 50 Hz power line noise (in european power grids) that is prevalent in most laboratory and plant settings.

There are two standards for platinum RTDs: the European standard (also known as the DIN or IEC standard) and the American standard.

The European standard is considered the world-wide standard for platinum RTDs. This standard, DIN/IEC 60751 (or simply IEC751), specify an electrical resistance of 100.00Ω at 0℃ and a temperature coefficient of resistance (TCR) of 0.00385Ω/Ω/℃ between 0 and 100℃.

The American standard, used mostly in North America, has a resistance of 100.00 ±0.10Ω at 0℃ and a temperature coefficient of resistance (TCR) of 0.00392Ω/Ω/℃ nominal (between 0 and 100℃).

Actually the resistance variation with temperature is not absolutely linear although it is commonly assumed as such, this raises the appearance of two classes based on the deviation of the actual response to the linear model. These are class A and class B, the two classifications give information about the RTD's tolerance and accuracy. A class A RTD has a smaller slope of its tolerance-temperature response, while a class B RTD has a higher tolerance variation with the temperature. Class B RTDs are the most common RTD and both classes have an equal thermal coefficient∝=0.00385 for the linear model. This variation can be expressed through the following graphic:

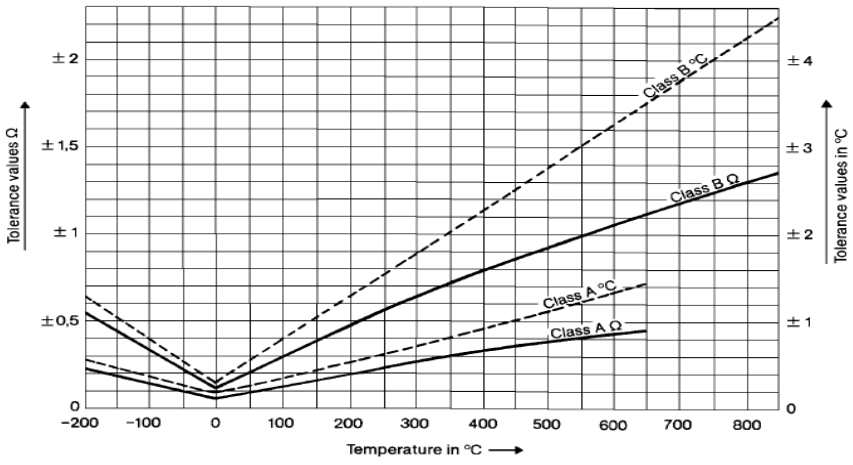

Figure 2-9: Graphical representation of tolerance values for resistance with Temperature for class A and class B RTD

[AD16]

2.2.3 Temperature Coefficient Devices

The temperature coefficient of materials is defined as being is the relative change of properties when the temperature of the material is changed by 1K. In the case of temperature detectors, the variation is of the electrical resistance.

The variation in the electrical resistance may be given by

$$R(T) = R(T_0)(1 + \alpha \Delta T) \quad (2)$$

where R(T) is the resistance at a temperature T, T_0 is the reference temperature, ΔT is the temperature variation and α is the temperature coefficient of a given material.

There are two possible cases when dealing with temperature coefficients: it is possible to have negative temperature coefficients or positive temperature coefficients.

2.2.3.1 Negative Temperature Coefficients

A negative temperature coefficient (NTC) occurs when the resistance of a semiconductor decreases with the temperature. This way, the relation between the electrical resistance and the temperature is given by:

$$R = R_0 e^{\frac{B}{T}} \quad (3)$$

where R is the resistance, R_0 is the initial resistance, B is a constant related with the conduction (if B decreases, the material tends to be insulating) and T is the absolute temperature (in Kelvin).

NTC temperature detectors have a large sensitivity and are available in many physical forms for application. NTCs are connected with a standard two-wires connection, have a good electrical noise immunity, are easy to interface and are easily modelled.

These have a vast application and are easily found in integrated circuits, acting as temperature detectors, such as in household electronics, automotive electronics, heating and air conditioning electronics, industrial electronics, communications and several more.

2.2.3.2 Positive Temperature Coefficients

The positive temperature coefficient differs from the negative temperature coefficient in a manner that when the temperature of the material increases, the material experiences an increase as well in its electrical resistance. The higher the coefficient, the higher the electrical resistance increase. These however, are often used for high temperature ranges and applications where a greater sensitivity is required.

2.3 Measuring Density

When the fermentation occurs, the density of the wine decreases as sugar is transformed into alcohol. Because of this, the evolution of the fermentation reaction may be supervised by measuring the liquid density.

2.3.1 Specific Gravity

The Specific Gravity (SG) is a dimensionless unit defined as the ratio of density of the material to the density of water at a specified temperature. Specific Gravity can be expressed as:

$$SG = \frac{\rho}{\rho_{H_2O}} \quad (4)$$

It is common to use the density of water at 4 ºC as reference. At this temperature, the water density is 1000 kg/m^3.

2.3.2 Buoyancy

When placed in fluids, objects behave differently. Some float, others sink, and there are some that act somewhere in the between. This behave can be expressed with buoyancy.

Buoyancy was first discovered by Archimedes of Syracuse, which formulated it as:

"Any object, wholly or partially immersed in a fluid, is buoyed up by a force equal to the weight of the fluid displaced by the object."

According with this law, it is valid to say that buoyancy is the force acting on a submerged body by the fluid, which depends on the immersed volume of the object and fluid density. This force can be expressed as

$$F = V\gamma = V\rho g \quad (5)$$

where F is the buoyant force (N), V is the body volume (m^3), γ is the specific weight of fluid (N/m^3), ρ is the density of fluid (kg/m^3) and g is the acceleration of gravity.

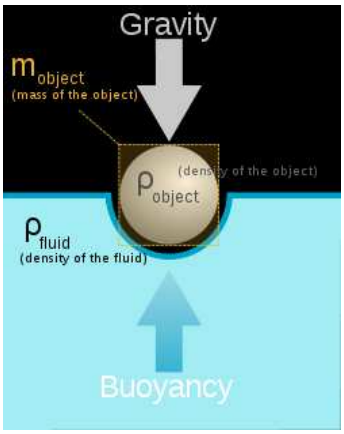

Figure 2-10: Forces acting in a body immersed in a fluid
[AD43]

Archimedes' principle does not consider the surface tension acting on the body and although this is an important parameter, it is still valid, used in several applications where surface tensions are not required.

It is because of buoyancy that the apparent weight of objects that have sunk completely in fluids is reduced. This explains why it is easier to lift an object up through the water than it is to pull it out of the water, since there is always a force opposing its weight.

It is important to note that the buoyant force does not depend on the weight or shape of the submerged object, only on the density of the displaced fluid. Archimedes' principle applies to object of all densities. If the density of the object is greater than that of the fluid, the object will sink. If the density of the object is equal to that of the fluid, the object will neither sink nor float. If the density of the object is less than that of the fluid, the object will float.

Some applications of buoyancy are the determination of density by water immersion, determination of density by immersion in a general liquid and determination of liquid density by immersion of a standard object. Though old, this is still one of the best methods used to determine densities. For that, one only needs to know the net force, the weight, the fluid volume displaced or the body volume and the specific weight. However, the problem while using this method is to know the total net force.

2.3.3 Refractometers

One other known relation is that the refractive index increases with density and as such, it can be said that the refractive index is proportional to the density.

Using these concepts, photoelectric density sensors were created, which make use of the correlation between the refractive index of the fluid to determine density. The

measurement of the index of refraction of a substance is provided with a refractometer, which allows observation of an interference pattern produced by passing light through the substance.

This topic will be better explained in the section regarding sugar concentration measurement.

2.3.4 Nuclear density sensors

Gamma radiation is one of the three types of natural radioactivity. The other two types of natural radioactivity are alpha and beta radiation, which are in the form of particles. Gamma rays are the most energetic form of electromagnetic radiation, with a very high energy.

Depending upon the ratio of neutrons to protons within atomic nucleus, an isotope of a particular element may be stable or unstable. When the binding energy is not strong enough to hold the nucleus of an atom together, the atom is said to be unstable. Atoms with unstable nuclei are constantly changing as a result of the imbalance of energy within the nucleus. Over time, the nuclei of unstable isotopes spontaneously disintegrate, or transform, in a process known as radioactive decay. Various types of penetrating radiation may be emitted from the nucleus and/or its surrounding electrons. Nuclides which undergo radioactive decay are called radionuclides. Any material which contains measurable amounts of one or more radionuclides is a radioactive material.

A nucleus which is in an excited state may emit one or more photons (packets of electromagnetic radiation) of discrete energies. The emission of gamma rays does not alter the number of protons or neutrons in the nucleus but instead has the effect of moving the nucleus from a higher to a lower energy state (unstable to stable).

The intensity of the beam formed after these photons will be:

$$I(d) = I_0 e^{-\mu d} \quad (6)$$

$$\mu = n\sigma \quad (7)$$

in which I is the intensity of the photon beam after cross a material of thickness d, I_0 is the initial intensity of the beam, when the photon is emitted from the nucleus and μ is absorption coefficient, measured in cm^{-1}, given by $\mu = n\sigma$, where n the number of atoms per cm^3 in the material, σ the absorption cross section in cm^2. Knowing n, it is only a matter of math to determine density in quilograms per cubic meter.

Using these relations, it is possible to correlate the energy of the photons with the thickness of the material and determine de density of the material. This is the principle behind nuclear density sensors.

However, because gamma radiation is a form of ionizing radiation, gamma rays can cause serious damage when absorbed by living tissue, and cause biological hazards against bacteria in wine.

2.4 Measuring Viscosity

Viscosity (also known as rheology) is a quantity that describes a fluid's resistance to flow or to be deformed by either shear stress or extensional stress, being an important property in the analysis of liquid behaviour and fluid motion near solid boundaries. This is an important measurement requirement in industrial process control since these measures are beneficial for quality control, where raw materials must be consistent from batch to batch. For this purpose, viscosity is an indirect measure of product consistency and quality, which varies inversely with temperature so all viscosity measures must be accompanied by the value of temperature they are determined.

In everyday terms (and for fluids only), viscosity is "thickness." Thus, water is "thin," having a lower viscosity, while honey is "thick" having a higher viscosity. Put simply, the more viscous something is, the greater its resistance to movement (fluidity). This resistance is caused by intermolecular friction exerted when layers of fluids attempt to slide by one another and varies with temperature and sometimes with pressure. This is to remember when is required to compare viscosity of different fluids: fluids must be compared at same temperatures and pressures. Close temperature control of the fluid is essential to accurate measurements. For some fluids, viscosity is a constant over a wide range of shear rates. These are Newtonian fluids.

The fluids without a constant viscosity are called non-Newtonian fluids. Their viscosity cannot be described by a single number. Non-Newtonian fluids exhibit a variety of different correlations between shear stress and shear rate.

There are several methods that could be used to measure viscosity. The method based on the viscosity definition is to measure the fluids velocity in response to a known torque. This is Newton's definition for viscosity, simplified in Figure 2-11: Viscosity calculation diagram. Two parallel planes of fluid of equal area A are separated by a distance dx and are moving in the same direction at different velocities V_1 and V_2. Newton assumed that the force required to maintain this difference in speed was proportional to the difference in speed through the liquid, or the velocity gradient. Having these values, it is easy to calculate the viscosity of the fluid by substituting the proper values in (8):

$$\tau = \frac{\mathrm{F}}{\mathrm{A}} = \mu \frac{\mathrm{dv}}{\mathrm{dy}}. \quad (8)$$

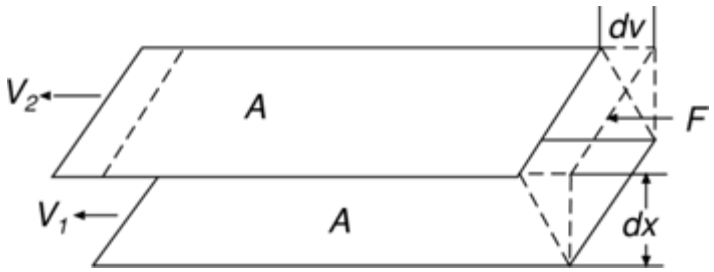

Figure 2-11: Viscosity calculation diagram.

[AD22]

This is the most common method, although there are other possibilities, such as:

- Measuring the power input necessary to keep the oscillator vibrating at constant amplitude. The higher the viscosity, the more power is needed to maintain the amplitude of oscillation.
- Measuring the decay time of the oscillation once the excitation is switched off. The higher the viscosity of the fluid, the faster the signal decays.

2.4.1.1 Dynamic viscosity

Dynamic viscosity, also known as absolute viscosity, represented by the greek symbol μ, is determined by the ratio of the shearing stress τ and the velocity gradient $\frac{dv}{dy}$.

$$\tau = \frac{F}{A} = \mu\left(\frac{dv}{dy}\right) \quad (9)$$

The more usual form of this relationship, obtained with Newton's equation, states that the resulting shear of a fluid is directly proportional to the force applied and inversely proportional to its viscosity. The similarity to Newton's second law of motion ($F = ma$) should be apparent.

$$\frac{\mathrm{F}}{\mathrm{A}} = \mu \frac{\mathrm{dv_x}}{\mathrm{dy}} \Leftrightarrow \mathrm{m} \frac{\mathrm{dv}}{\mathrm{dt}} \quad (10)$$

The velocity gradient (dv/dx) is a measure of the change in speed at which the intermediate layers move with respect to each other. It describes the shearing the liquid experiences and is thus called shear rate (γ). Its unit of measure is called the reciprocal second [sec^{-1}]. The term F/A indicates the force per unit area required to produce the

shearing action. It is referred to as shear stress (τ). Its unit of measurement is dynes per square centimeter [$dynes/cm^2$].
Using these simplified terms, dynamic viscosity may be defined mathematically by:

$$\mu = \frac{\tau}{\gamma} \qquad (11)$$

The SI unit of dynamic viscosity is the pascal second [$Pa \cdot s$], which has no special name. Despite its self-proclaimed title as an international system, the International System of Units has had very little international impact on viscosity. The pascal second is rarely used in scientific and technical publications today. The most common unit of viscosity is the dyne second per square centimetre [$dyne \cdot s/cm^2$], which is given the name poise [P] after the French physiologist Jean Louis Poiseuille (1799-1869). Ten poise equal one pascal second [$Pa \cdot s$] making the centipoise [cP] and millipascal second [$mPa \cdot s$] identical.

2.4.1.2 Kinematic viscosity

Kinematic viscosity is defined as the dynamic viscosity divided by the density of the fluid.

$$\nu = \frac{\mu}{\rho} \qquad (12)$$

Because density is itself an intrinsic property, it can be argued that kinematic viscosity is not a precise measure of internal fluid friction. However, kinematic viscosity is the preferred unit when the shear stress and shear rate of the fluid is influenced by the density.

The SI unit of kinematic viscosity is the square meter per second [m^2/s], which has no special name. This unit is so large that it is rarely used. A more common unit of kinematic viscosity is the square centimetre per second [cm^2/s], which is given the name stokes [St] after the Irish mathematician and physicist George Gabriel Stokes (1819-1903).

2.4.1.3 Acoustic Wave Measurement Overview

The classical method previously described is not the only method to measure viscosity. In the past years, new sensing methods were developed, some of which were adapted to measure viscosity, intending to replace mobile part sensors. One of these methods is acoustic wave sensing, which utilizes Surface Acoustic Wave (SAW) properties and Bulk Acoustic Wave (BAW) properties.

Acoustic wave sensors are so named because their detection mechanism is an acoustic wave. As the acoustic wave propagates through the material, any changes to the characteristics of the propagation path affect the velocity and/or amplitude of the wave. Changes in velocity can be monitored by measuring the frequency or phase characteristics of the sensor and can then be correlated to the corresponding physical quantity being measured.

The importance of this method lies in the possibility to create sensors that use different measurement principles. The classical viscosimeters use mobile parts to perform the measurements and because of that, are very susceptible to wear.

This new method to measure viscosity lies in the definition of acoustic impedance. This impedance is defined as being

$$Z = \sqrt{\omega \cdot \rho \cdot \mu} \qquad (13)$$

in which Z is the acoustic impedance, ω is the angular frequency, ρ is the density of the sensor material and μ is the viscosity. A closed loop will be formed, with the output wave, the fluid, the input wave and the sensor.

The determination of Z is made by calculating the power losses of the acoustic resonator into the fluid, e.g. the power differences between the output wave and the input wave. This can be made since the required parameters of the wave are known in both cases and relating them, Z can be calculated.

Using this method, the creation of solid state viscosity sensors is possible. This means these sensors have no moving parts, are sealed so they can be completely immersed in process stream. Due to the high frequency of the atomic vibration related with the standing wave propagation, several millions of vibrations per second, the sensor is independent of flow conditions of the liquid and immune to vibration effects of the environment. Electronics resistant to high temperatures and advanced packaging techniques are used that allow a very wide operating temperature range for the sensor, and there is no need for calibration.

2.4.1.4 SAW and STW technology

A surface acoustic wave (SAW) is an acoustic wave travelling along the surface of a material exhibiting elasticity, with amplitude that typically decays exponentially with depth into the substrate, while the Surface Transverse Wave (STW) follows the same definition. The main difference is that the STW device uses a metal grating structure between the IDT, Figure 2-12 and Figure 2-13, which intends to trap the propagating wave to the surface of the substrate. Without the grating, the wave propagates at a

slight angle into the substrate, resulting in its attenuation. Secondly, the displacement of the propagating STW is in the plane of the substrate with no vertical component of displacement.

Since there is no vertical component of displacement, the STW could theoretically be used for liquid-based applications. In a practical sense, use as a liquid-based sensor is very unlikely. Placing water on the surface of the device will dielectrically short out the IDT electrodes preventing the excitation of the STW. Isolation of the IDTs from the liquid has been tried with various types of packaging (i.e. passivation coatings or o-ring sealed flow cavity), but this usually results in significant losses in the device characteristics. For this reason, the STW is typically only used for gas sensing.

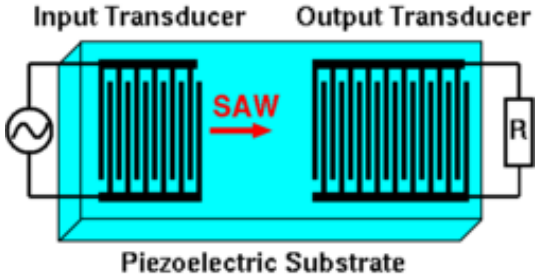

Figure 2-12: SAW sensor scheme

[AD35]

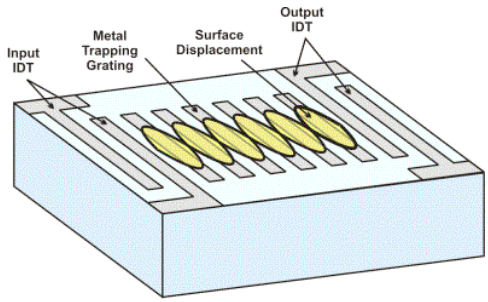

Figure 2-13: STW sensor scheme

[AD35]

2.4.1.5 BAW Technology

A wave propagating through the substrate is called a bulk wave. The most commonly used bulk acoustic wave (BAW) devices are the thickness shear mode (TSM) resonator and the shear-horizontal acoustic plate mode (SH-APM) sensor. Both these devices have the same working principles. As all acoustic wave devices, these are sensors sensitive to perturbations of many different physical parameters. Any change in the characteristics of the path over which the acoustic wave propagates will result in a change in output.

The TSM, widely referred to as a quartz crystal microbalance, is the best-known, oldest, and simplest acoustic wave device. The TSM typically consists of a thin disk of AT-cut quartz with parallel circular electrodes patterned on both sides. The application of a voltage between these electrodes results in a shear deformation of the crystal, originating acoustic waves.

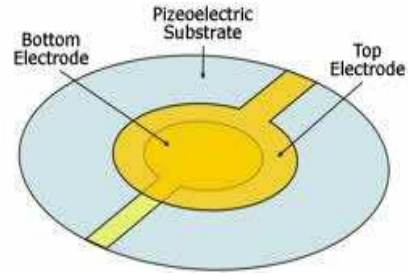

Figure 2-14: TSM representation
[AD35]

These devices are known as resonators because of the crystal that resonates while electromechanical standing waves are created. The displacement is maximized at the crystal faces, making the device sensitive to surface interactions.

The TSM features simplicity of manufacture, ability to withstand harsh environments, temperature stability, and good sensitivity to additional mass deposited on the crystal surface. Because of its shear wave propagation component, the TSM resonator is also capable of detecting and measuring liquids, making it a good candidate for a biosensor. Application as a liquid sensor can be achieved with a sensing film or by direct contact of the liquid onto the surface of the BAW device, as depicted below:

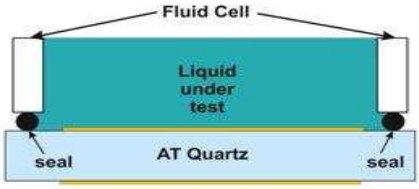

Figure 2-15: BAW device with direct contact with liquids
[AD35]

When in direct contact with the liquid, the mechanical properties of the fluid cause perturbations to the TSM, resulting in resonant frequency changes, which can be interpolated to determine the properties required.

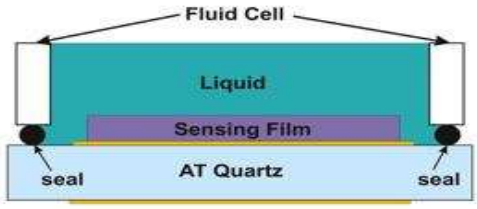

Figure 2-16: BAW device with a thin film acting as contact between electrode and liquid [AD35]

When in contact with a sensing film case, the interaction with the fluids will cause the attachment of molecules to the film, which will result in mechanical perturbations in the TSM, causing changes in the resonant frequency, by which the fluids properties can be determined.

2.4.1.6 Shear-Horizontal Acoustic Plate Mode (SH-APM)

The shear horizontal acoustic plate mode (SH-APM) device combines the best properties of both the BAW and SAW devices. It employs separate input and output transducers in order to allow differential signal measurements like the SAW structures but also allows the sensor crystal to be employed as a physical barrier between the electronics and the sensing medium.

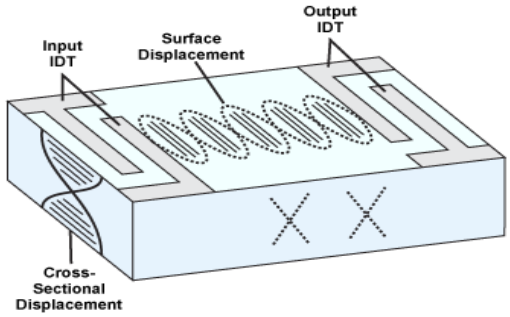

Figure 2-17: Shear-Horizontal Acoustic Plate Mode schematic [AD35]

The substrate acts as a waveguide with energy throughout the bulk of the crystal and is dependent on the thickness of the substrate. Like all previous surface launched acoustic wave devices, the SH-APM device uses input and output IDT to launch and receive the acoustic wave. Similar to the BAW thickness shear mode device, the maximum displacements occur on the top and bottom surfaces of the plate. Similar to the STW devices, the surface displacement is shear and in the plane of the plate so it can be used for liquid-based applications. The waveguide modes have energy distributed between the two surfaces as a standing wave as in the BAW sensor

but traveling along the surface as in a SAW. The continuous exchange of energy between the two surfaces allows the signal between the IDTs to be influenced by changes on the opposite surface.

These devices use a thin piezoelectric substrate, or plate, functioning as an acoustic waveguide that confines the energy between the upper and lower surfaces of the plate. As a result, both surfaces undergo displacement, so detection can occur on either side. This is an important advantage, as one side contains the IDT that must be isolated from conducting fluids or gases, while the other side can be used as the sensor.

2.5 Measuring sugars concentration

The sugars in wine grapes are what make the fermentation process possible. Initially, the sugars in grapes, mostly sucrose, produced by the photosynthesis process and accumulated in the grape during the maturation period. Sucrose will then be hydrolyzed in the grape by the enzyme invertase, producing glucose and fructose. By the time of the harvest, 15-25% of the grape will be composed of sugars, required for the fermentation process.

While fermentation occurs, the sugars molecular chains are broken and the sugars, glucose and fructose, are converted in alcohol and carbon dioxide by yeasts metabolism. Not all sugars present in the grape are broken, as is the case of arabinose, rhamnose and xylose. These sugars always remain in the wine after fermentation and for this reason, no wine is fully fermented and without sugar, since some always remain. Sugars, usually sacarose, may also be added by the winemaker, in case of the grape sugars are not enough to achieve a good fermentation and a proper alcoholic content; in this case, the winemaker must consider not to add too much neither too less sugars, since this may prejudice the fermentation process.

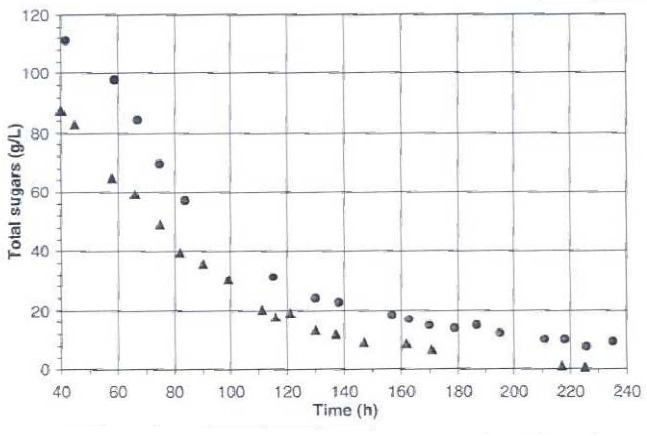

Figure 2-18: Typical normal and stuck (•) fermentations of Cabernet Sauvignon. [RD30]

There are several scales associated with sugar concentrations, others than the traditional g/cm^3. These are the Brix scale, the Balling scale, the Plato scale and the Baume scale. The Brix scale is widely used in food and beverage industry to measure the sugar concentration of products, as in vegetables, fruits, wines, beers, to quote only a few. By definition, one Brix (ºBx) is a measurement of 1g of sugar in 100g of solvent.

Since Brix is related to the concentration of sugars in a fluid, it is therefore related to the specific gravity of the liquid. Because the specific gravity of sucrose solutions is well known, it can also be measured by refractometers. Modern Brix meters are digital refractometers that calculate the Brix value based on refractive index. These meters are typically portable, splash proof and very simple to use, so that they can be operated easily with little training directly in the fied of operation.

When an infrared Brix sensor is used, it measures the vibrational frequency of the sugar molecules, giving a Brix degrees measurement. This will not be the same measurement as Brix degrees using a density measurement because it will specifically measure dissolved sugar concentration instead of all dissolved solids.

2.5.1 Stechiometric measurements

It is possible to determine the sugars concentration by using stechiometric coefficients and by knowing the concentration of one existing product. By knowing, for example, the ethanol concentration, it is possible to know the sugars concentration in real time, simply by relating the stechiometric coefficients:

$$C_6H_{12}O_6 \rightarrow 2\ C_2H_6O + 2\ CO_2$$

Sugars → ethanol + carbon dioxide

Since 1 mol of sugars produce 2 mol of ethanol, then it can be said that [sugars]* V_{tank} origins measured ethanol concentration:

$$[\text{sugars}] = \frac{2 \times V_{tank}}{[\text{Alcoholmeasured}]} \qquad (14)$$

2.5.2 Brix Sensors

Brix sensors are typically refractometers, which are instruments that determine the concentration of an aqueous solution by measuring its refractive index.

2.5.2.1 Refractometry

Refractometry is a technique used to analyse the behaviour of light when it passes through substances, mainly unknown compounds. When light interacts with the substance, it will suffer refractions and it is through these that the refractive index is characterized and measured. This behaviour is mainly because of the different velocity light can have when travelling through different substances. There are several ways to determine the refractive index of a substance:

$$n = \frac{c}{v_{medium}} \tag{15}$$

The refractive index of two different mediums is also related with the incident and with the refracted angles as is given with Snell's law:

$$\frac{sin\theta_1}{sin\theta_2} = \frac{v_1}{v_2} = \frac{n_2}{n_1} \tag{16}$$

Refractive index is a fundamental property of substances and it is often used to identify unknown substances, confirm its purity or even to measure its concentration, being indifferent if the substance is in solid, liquid or gaseous state. This method is widely used to measure the concentration of solutions, in this case, to measure the sugar concentration of the solution.

2.5.2.2 Refractometers

When light enters a liquid, it changes direction; this is the basis of refraction and is the working principle of the refractometers. These devices measure the angle of the diffraction and correlate them to refractive index values, using the Snell's law. Using these values, it is possible to determine the concentrations of solutions, since the refraction of the incident angle will depend of the concentration of the liquid in study.

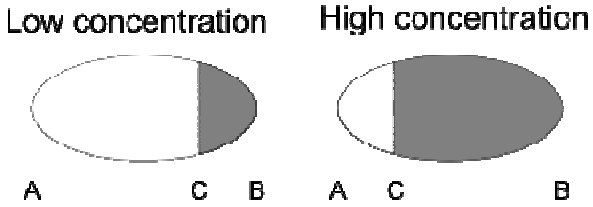

Figure 2-19: Diagram of the refractometer output the white section represents the section with incident light and the dark path represents the area with no incident light

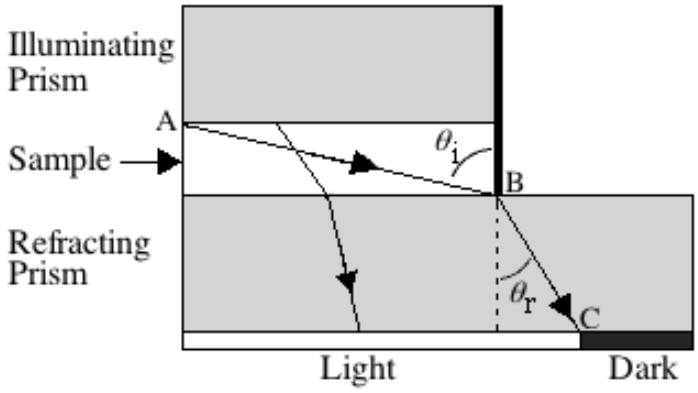

Figure 2-20: Refractometer Sensor schematics

[AD71]

The refractometer architecture is still very similar to the Abbe refractometer, the very first refractometer created. In this architecture, represented in the image above, the liquid sample is placed between two prisms, an illuminating prism and a refractive prism. Usually, the refractive prism is made of materials with a high refractive index and the illuminating prism projects the light source. The light will travel towards the refracting prism, with an incident angle $\theta_i$with the normal to the surface, and inside the refracting prism, the refracted light will make a refracted angle with the normal to the surface, θ_r. Knowing the refractive index of the refractive prism, it is only required to use Snell law to determine the refractive index of the sample. In the bottom of the system, the light shall be acquired, either by analogical methods or digital methods. There is, of course, a dead zone in this area, whose limits are given by the angle with the maximum refractive angle. After this point, there will be no light interacting with the prism and therefore, there will be a dark zone in the system. This edge between both light and dark zone is detected by an image sensor and by knowing it, it is possible to calculate the critical angle of incidence and with this angle and the refractive index, it is possible to determine the Brix in the sample.

However, this relation is not linear. In order to obtain a linear relation, it is necessary to make temperature compensations to all the refractive indexes, as it is demonstrated in the following graphic and expression, which relates the refractive index with the percentage of Brix:

$$Estimate\_RI\_T_2 = (RI\_T_1) - (T_1 - T_2) \times 0.00045 \qquad (17)$$

[AD71]

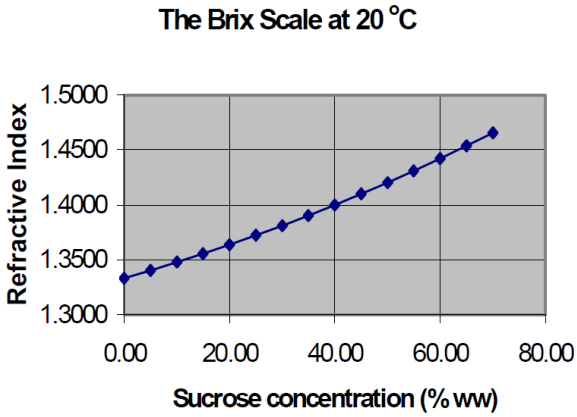

Figure 2-21: Brix (sucrose concentration) relation with the refractive index

[AD78]

The temperature corrections are made using the approved tables “Circular of the National Bureau of Standards C440”, of May 1st, 1942 and the expression above. With these values, it is possible to determine the Brix percentage of the wine.

Brix is also a quality parameter regarding foods and beverages. In this system range, it may also be a measurement of the quality of the grapes used to make the wine. As it can be seen in [AD82], poor quality grape have a Brix concentration below 8% and an excellent quality grape has a Brix concentration greater than 20%.

In case of an analogical brixmeter, the analysis is made visually by the user, with the support of a graduated scale in the eyepiece.

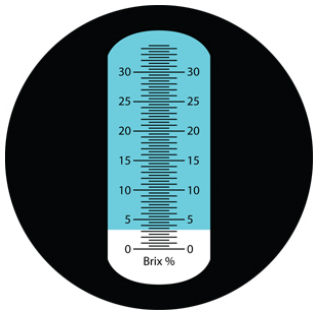

Figure 2-22: Scheme of a solution reading given by an analogical refractometer.

[AD72]

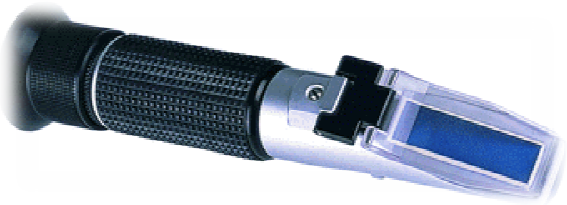

Figure 2-23: Analogical Refractometer

[AD72]

In case of a digital refractometer, the process is similar, differing only in the output. The digital outputs a signal displayed either in an LCD, if it is portable or in an acquisition unit, if it is in-line.

Figure 2-24: Portable Brix Refractometer

[AD55]

Figure 2-25: In line Brix Refractometer

[AD79]

2.6 Measuring Alcoholic concentration

Together with carbon Dioxide (CO_2), ethanol (C_2H_6O) is one of the products of the main reaction that occurs during the fermentation process of wine. This reaction can be described by the following equation:

$$C_6H_{12}O_6 \rightarrow 2\ C_2H_6O + 2\ CO_2$$

Sugars → ethanol + carbon dioxide

The main methods used in industry to measure ethanol concentration are the manual alcoholimeter, which is not an option for this project, and spectrophotometer. It is possible as well to determine the concentration of ethanol by calculating it with the stechiometric coefficients and the initial concentration of grape sugars, however, this method is much more susceptible to errors.

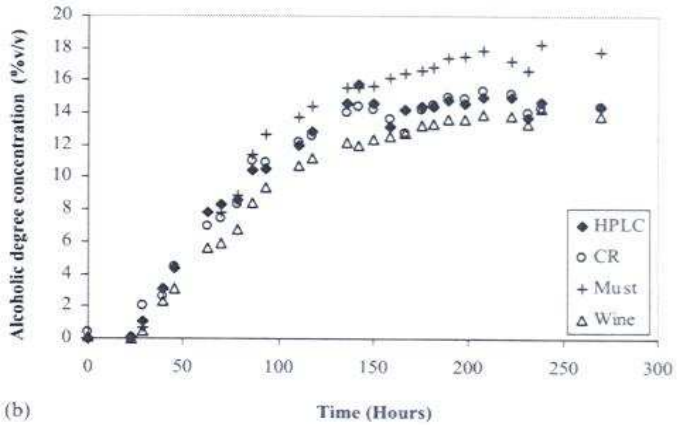

Figure 2-26:Evolution of alcohol content (determined by 4 different methods, HPLC, Must analysis, wine analysis and Concentration Ratio analysis) during the fermentation of a red must of Cabernet Sauvignon
[RD29]

2.6.1 Stechiometric Measurement

As it is known, the density of the grape juice is higher than the density of the wine. This is explained through the fermentation process, during which the sugars in the grape juice ferment, originating ethanol and carbon dioxide. This does not resumes the totality of the fermentation process, since the metabolism of amino acids and breakdown of sugars by yeasts has the effect of creating other biochemical compounds that can contribute to the flavour and aroma of wine. These compounds can be considered "volatile", like aldehydes, ethyl acetate, ester, fatty acids, fusel oils, hydrogen sulfide, ketones and mercaptans or "non-volatile" like glycerol, acetic acid and succinic acid. Yeast also has the effect during fermentation of releasing glycoside hydrolase which can hydrolyse the flavor precursors of aliphatics (a flavor component that reacts with oak), benzene derivatives, monoterpenes (responsible for floral aromas from grapes like Muscat and Traminer), norisoprenoids, and phenols.

Considering these assumptions and knowing that density is given by the expression:

$$\rho = \frac{m}{V} \tag{18}$$

And

$$[C] = \frac{m_s}{M_r V} \tag{19}$$

Therefore

$$[C] = \frac{\rho}{M_r} = \frac{m_s}{V} \quad (20)$$

in which ρ is the measured density, $[C]$ is the concentration in mol/dm^3, M_r is the atomic weight, m_s is the mass of the solute and V is the volume of the tank.

So, considering this assumption, it will be possible to calculate the alcohol concentration using both the concentrations of the sugars, calculated with the variation of the density in fermentation process, and the stechiometric coefficients.

2.6.2 Spectrophotometry

To measure the concentration of ethanol through spectroscopic methods, it is necessary to apply light with a wide spectrum of wavelengths and measure the light detected. The difference of the emitted light and the detected light will give the absorbed light by the ethanol and all other constituents in the wine, showing some maximum of absorption or minimums of absorbance, depending of the spectrum obtained.

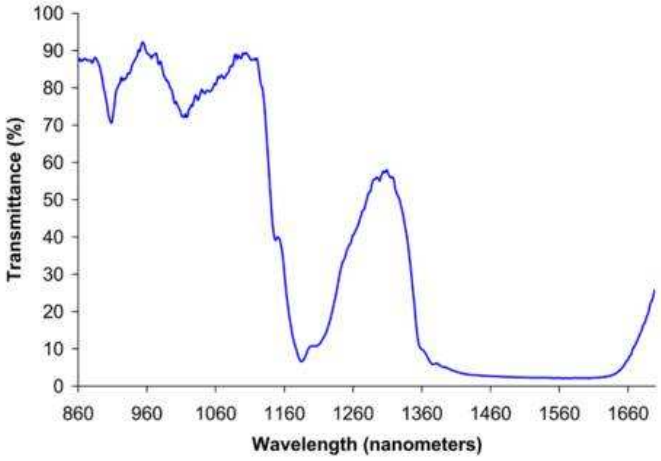

Figure 2-27: Liquid ethanol spectrum in the near IR region [AD77]

As it is seen in 2-27, there is a transmittance minimum to approximately 1160 nm, which means an absorption maximum for this wavelength. By relating the intensity of the beam in the peak and the respective wavelength, it is possible to conclude about the concentration of ethanol in the wine, using

$$\boldsymbol{A = \epsilon . c . L} \quad (21)$$

In which A is the absorbance ϵ is the attenuation coefficient, c is the concentration of the substance we want and L is the total path crossed by the light. By knowing this, c is easily calculated.

2.6.3 Refractometry

As with sugar concentration measurement, it is also possible to use refractometry to measure the alcoholic concentration. The process is the same, differing only in the sensor properties, since this sensor will be more sensitive to alcoholic properties of the solution during the refractive index measurement, as well as the calibration tables to consult.

2.7 Measuring Glucose and Fructose concentration

Glucose and fructose are the main sugars found in grape juices and the responsible for the entire fermentation process, being the ones that are converted in alcohol and carbon dioxide by the yeasts metabolic processes. Glucose and fructose are two very similar compounds; in fact, both substances have the same chemical expression, $C_6H_{12}O_6$, differing only in the molecular chain. In fact, both substances are considered to be stereoisomers, molecules with the same molecular formula and with the same molecular chain differing only in the spatial orientation of the atoms. In fact, these two substances are considered enantiomers, which mean that both stereoisomers that are mirror images of each other. Enantiomers have identical chemical and physical properties, which makes it difficult to distinguish both substances. The most reliable methods to make the distinction are titration or polarimetry and since it is intended to use non-invasive methods to monitorize the wine parameters, it was decided to use a polarimetric approach.

2.7.1 Polarimetry

There are several substances which affect the polarization direction of light. This characteristic is called optical activity and has important applications, such as concentration determination of substances in chemistry, measured by polarization.

The direction of propagation for a electromagnetic wave is given by

$$\vec{S} = \frac{\vec{E} \times \vec{B}}{\mu} \qquad (22)$$

in which $\vec{S}$ is the vector pointing, which has the direction of the wave propagation, $\vec{E}$ is the electrical field component of the wave, $\vec{B}$ is the magnetic field component of the wave and μ is the permeability of the medium in which the wave propagates.

Convention stated that the polarization vector of light is parallel to the wave's electrical field direction. Considering this, it is possible to say that all natural sunlight and most forms of artificial illumination transmit light waves whose electric field vectors vibrate equally in all planes perpendicular to the direction of propagation. The principle of polarimetry requires only the light with specified polarization directions for the application and therefore, the polarizer is inserted in the system. The polarizer is described as being a filter containing a molecule chain orientated in a single direction. Only the incident electromagnetic waves with polarization direction perpendicular to the polarizer's orientation are allowed to pass through it.

To measure the plane polarised light angle, it is used a polarimeter. There are many designs of polarimeters. Some are archaic and some are in current use. The most sensitive polarimeters are based on interferometers, while more conventional polarimeters are based on arrangements of polarising filters, wave plates or other devices.

2.7.2 Polarimeters

A polarimeter is usually depicted as it is depicted in the following figure:

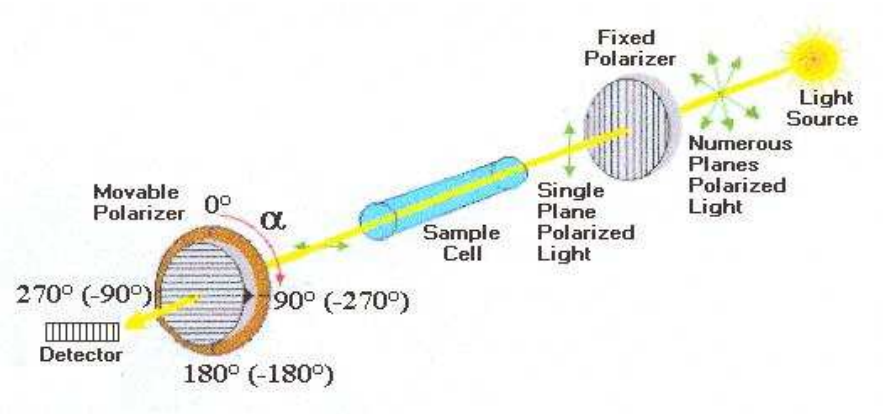

Figure 2-28: Schematic representation of a polarimeter

[AD73]

The light source plays the most important role in the system. Specific wavelengths are required to interact with each substance and because lamps do not emit only in that specific wavelength, but in a range, filters may be used when required to cut all unnecessary wavelengths that may influence the results.

According to all available theoretical and experimental evidence, it is the electric field vector rather than the magnetic field vector of a light wave that is responsible for all the effects of polarization and other observed phenomena associated with light. Therefore, the electric field vector of a light wave, for all practical purposes, can be identified as the light vector.

It is for this reason that it is used a first polarizer after the light source, as it is depicted in Figure 2-28, depicted above. Because the light is emitted to all directions, much of the light that would interact with the sample would not be properly polarized, which could return false results. For this reason, and because electric field (the light component perpendicular to the light propagation) is considered as the light vector, the magnetic component is cut with the polarizer, in order to avoid noises and false results.

With only the electric component of the wave, light will interact with the sample in the sample tube and due to the interactions with the molecules, it will rotate α degrees. Through this rotation value, measured through an analyser, adapted with a protractor, it is possible to identify the sample in study.

Generally, the specific rotation [α] depends on the length of the tube, and the concentration of the optical active compound.

When we are dealing with pure liquids, the equation used is as following:

$$[\alpha] = \frac{\alpha}{d \times L} \qquad (23)$$

[α] =the specific rotation

α = observed rotation

d = the density of the liquid

L = the length of the tube.

When the sample is a solution, different equations are used:

$$[\alpha]_D^{20} = \frac{100.\alpha}{e \times L} \qquad (24)$$

Or

$$[\alpha]_D^{20} = \frac{\alpha}{c \times L} \qquad (25)$$

$[\alpha]_D^{20}$ =the specific rotation

α = observed rotation

e = the concentration of the solution in grams per 100 mililitres

c = the concentration of the solution in grams per millilitre

L = the length of the tube in decimetres.

The main difference between these two equations is solely on the units of concentration we wish to work with, either $\mathrm{g}/100\ \mathrm{ml}$ or g/ml. It is important to refer that $[\alpha]_{\mathrm{D}}^{20}$ is temperature dependant. Knowing this, the specific rotation can be temperature corrected using the expression

$$[\alpha]_{\mathrm{D}}^{\mathrm{T}} = [\alpha]_{\mathrm{D}}^{0} + \mathrm{nT} \quad (26)$$

being only required to know the temperature coefficient n, the temperature T and the specific rotation for both fructose and glucose at a temperature of 0ºC and 589nm.

2.7.2.1 Polarimeter Using Optoelectronic methods

Using purely optoelectronic methods it is possible to calculate the angle of rotation, applying Malus's law,

$$\mathrm{I} = \mathrm{I}_0 \cos^2\theta \quad (27)$$

With this method, all attenuations must be considered and discounted from I_0 and because both polarizers are oriented parallel to each other, the angle calculated with Malus's expression will be the angle of the light plane when exiting the vial with the wine sample.

As it was previously said, the most important component in the light is the electric component, since it is the one that passes through the polarizers. Because of this, and since E_0 is the amplitude of the electrical field, then

$$\mathrm{I}_0 \propto {\mathrm{E}_0}^2 \quad (28)$$

Knowing this, and considering the light decomposition axis represented in the image below, we have

$$\mathrm{I} \infty (\mathrm{E}_0 \cos\theta)^2 \quad (29)$$

$$\frac{\mathrm{I}}{\mathrm{I}_0} = \left(\frac{\mathrm{E}_0 \cos\theta}{\mathrm{E}_0}\right)^2 = \cos^2\theta \quad (30)$$

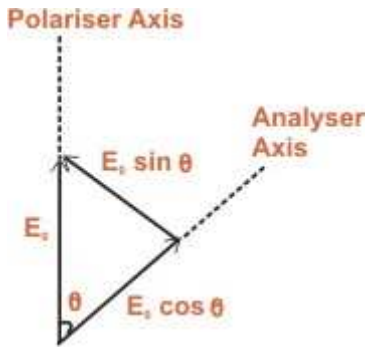

Figure 2-29: Light's electric field vector decomposition [AD74]

which means that the intensity of the beam is proportional to the square of the cosine of the angle. Through these considerations, and knowing that the calculated angle is the difference between the angle of the first polariser and the analyser, it is possible to use Malus's law to determine the rotation angle of light in the polarimeter.

2.7.2.2 Polarimeter Using Mobile parts method

Another possibility for a polarimeter design is to use mobile parts. Using a configuration like this, there would be a rotational system associated with the analyser, in order to rotate it. This rotation is the basis of the polarizers operation, since polarizers must be rotated to the position with maximum light intensity.

The measurement of this angle is the basis of the traditional polarimeter functioning, to measure the rotation angle between the orientation with minimum light intensity and the orientation with the maximum light intensity.

2.7.3 Identifying Fructose and Glucose

Being two very similar sugars, differing only in the molecular chain, fructose and glucose react similarly to polarized light. For fructose and glucose identification, the light source more commonly used is a yellow sodium D, with a wavelength of 589 nm. For this wavelength, the optical rotation of the beam will be -93.0º for fructose and 52.5º for glucose and 66º for sucrose.

When dealing with mixtures of both sugars, as is the case, the optical rotations will increment each other, and the rotation verified in the polarimeter will come affected by both sugars:

$$\alpha = [\alpha]_{gluc}.\,l.\,c_{gluc} + [\alpha]_{fruc}.\,l.\,c_{fruc} \quad (31)$$

in which α is the rotation measured with the polarimeter, $[\alpha]$ is the optical rotation of the sample, l is the length of the sample tube and c_{gluc} and c_{fruc} are the glucose and fructose concentrations, respectively.

In order to determine the concentrations of both enantiomers, we can use Lauer *et al* [RD8] equations:

$$C_{gluc} = \frac{-[\alpha_{fruc}].C_t + \frac{1000}{x}.\alpha}{[\alpha_{gluc}] - [\alpha_{fruc}]} \quad (32)$$

and

$$C_{fruc} = \frac{[\alpha_{gluc}].C_t - \frac{1000}{x}.\alpha}{[\alpha_{gluc}] - [\alpha_{fruc}]} \quad (33)$$

in which C_{gluc} and C_{fruc} are the concentrations (in g/dm^3) of glucose and fructose respectively, C_t is the total concentration of the sugars in the solution (in g/dm^3), $[\alpha_{gluc}]$ and $[\alpha_{fruc}]$ are the optical rotations of glucose and fructose respectively, x is the length of the polarimeter tube in decimetres and α is the rotation of the beam verified in the polarimeter.

2.8 Measuring Conductivity

For this specific project, it is required the monitoring of the electric conductivity, which is a measure of the material's ability to conduct electric current. This parameter can be determined with the expression $\sigma = \frac{E}{J}$, where σ is the electric conductivity, J is the current density in a section of area A of the wire and E is the electric field which generates the voltage imposed at the material's terminals, or with the expression $\sigma = \frac{1}{\rho}$, in which ρ is the resistivity of the material.

Conductivity is an important parameter to measure because it can be related with the concentration of carbon dioxide [RD7].

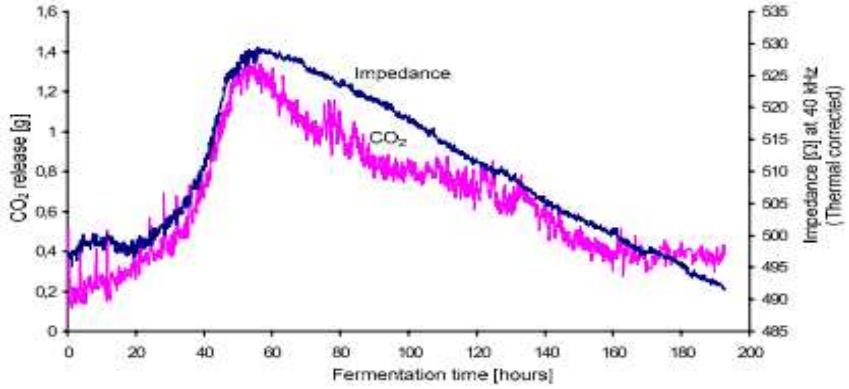

Figure 2-30: Relation between Carbon Dioxide concentration and total wine impedance [RD7]

As it is depicted in the image above, there is a relation between the carbon dioxide concentration and the wine impedance during the fermentation process. With this knowledge, it is possible to qualitatively monitor the carbon dioxide concentration.

2.8.1 Ohm's Law Conductivity Measurement

Experimentally, the electric conductivity of materials can be easily determined with ohm's law, by imposing a known voltage at the conductor terminals and measure the current that passes through it. With this, electric resistance can be easily determined with $V = RI$. Then, as resistivity is proportional to resistance, according with

$$R = \rho \frac{L}{A} \qquad (34)$$

in which L is the length of the conductor, A is the cross section area of the conductor, and ρ is the resistivity. Knowing these parameters, it is easy to determine electric conductivity.

However, this method is not valid for some materials, especially for organic materials and liquids. In these situations, when is required to measure the conductivity of one of these materials, another method is used, which is the method of the four electrodes.

2.8.2 Relaxation Probe Method

The relaxation probe is a device used to measure the conductivity of materials, recently used in the Cassini–Huygens mission to Titan, the Saturn moon. This probe is based in the concept of relaxation time and the intrinsic capacities of materials as working principle. The relaxation time is considered in physics as the time in which a

system changes its state to equilibrium from an excited state. As such, by adapting the relaxation method to a conductivity sensor, this shall be an electrode immersed in a medium that is charged at voltage V. When the power is suddenly cut, the electrode will discharge to the medium during a time τ and that needs to be measured by the acquisition and processing system. In the scheme below, the sensor is represented by an equivalent circuit, in which the first capacitor (C1) is the intrinsic capacity of the connection wire and the parallel association of resistor (R1) and capacity (C2) is the electrode.

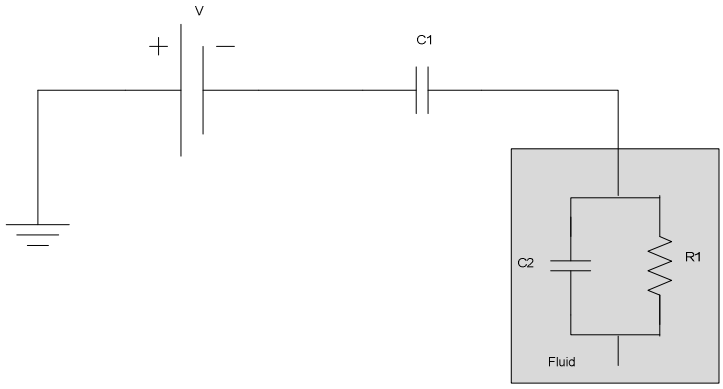

Figure 2-31: Relaxation Probe circuit schematics

By knowing the discharge time, it is possible to calculate the conductivity where the discharge occurs. This relation can be expressed by the equation

$$\sigma = \frac{\varepsilon}{\tau} \qquad (35)$$

Therefore, it is required to know the permittivity of the fluid in order to use this method.

2.9 Measuring Permittivity

Permittivity is a measure of how an electric field interacts with different mediums and is related to the ability of the material to transmit the electric field through itself. The permittivity is directly related with the electric susceptibility, which measures how easy it is to polarize the material in response to the electric field. This relation can be expressed by the relation

$$\varepsilon = \varepsilon_r \varepsilon_0 = (1 + \chi)\varepsilon_0 \qquad (36)$$

in which ε_0 is the permittivity of the vacuum, $8.8 \times 10^{-12} F/m$.

The interest in measuring the electric permittivity of the wine is due to the interest in this value to other measurements, such as conductivity, since the

methodology used, the relaxation technique, requires the permittivity of the wine in order to determine the conductivity.

2.9.1 Mutual Impedance Probe

The mutual impedance probe, also known as the four electrode method, is a method widely used to determine physical properties of materials, namely conductivity and permittivity. This method is mostly used in geology, to determine these parameters for soils study and recently is being applied in space probes to study outer planets atmosphere and soils as well. One recent example is the Huygens-Cassini probe, launched in October 15th, 1997 to study the Saturnian System, especially Titan, Saturn's largest moon. Having completed its mission in June 2008, Cassini is now in a two-year mission extension.

The four electrode method is an evolution of the two electrode method. This was developed after several relations between resistivity, temperature, water concentration and salt concentration, developed by Whitney *et al* (1887), Gardner (1898) e Briggs (1899). However, this method measures sum of the total resistance of the sample and the resistance of the contacts between the electrodes and the soil. This offers some problems when making measurements with this method, leading to unpredictable errors in the results.

Considering these problems, in 1915, Wenner suggested the utilization of four electrodes, separated of equal distances between them, which would minimize the measurement errors. This method was accepted and is still used today in several areas of interest, such as medicine, biology and geology.

The mutual impedance probe is a method widely used in geology and biomedical sciences. This is a non-invasive method, so it can be used to study properties of several materials without causing damages. With this method, material properties can be study to a certain depth, and this depth can be adjusted with the size of the electrodes.

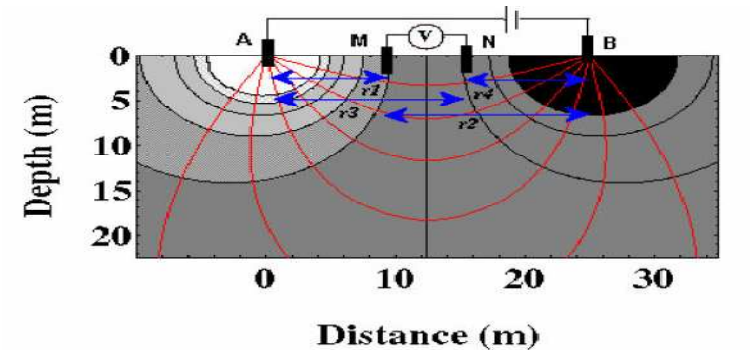

Figure 2-32: Four electrode working schematic

[AD52]

With this system, resistivity can be calculated by

$$\rho = \frac{1}{\sigma} = \frac{AV}{LI} \tag{37}$$

in which L is the length of the conductor wire with section A, V is the voltage and I is the total current. The parameter K, given by

$$K = \frac{A}{L} \tag{38}$$

is a geometric factor, easily calculated. By simplifying, the expressions,

$$\rho = K\frac{V}{I} \tag{39}$$

and

$$\sigma = \frac{I}{VK} \tag{40}$$

The K coefficient depends of the distances between the electrodes. Considering the image above, where the electrodes were identified as being A, M, N and B, where M and N are the sensing electrodes responsible for the voltage measurement, and A and B the current injectors. With AM, NB and MN distances between the same name electrodes and AM=NB, then

$$K = \pi\frac{AM.AN}{MN} \tag{41}$$

The depth of these measures will depend with both resistivity and the geometry of the four electrode probe. If the electrodes are indeed equally spaced with a distance A, then $K = 2\pi A$ and the depth of the measurement will be approximately A.

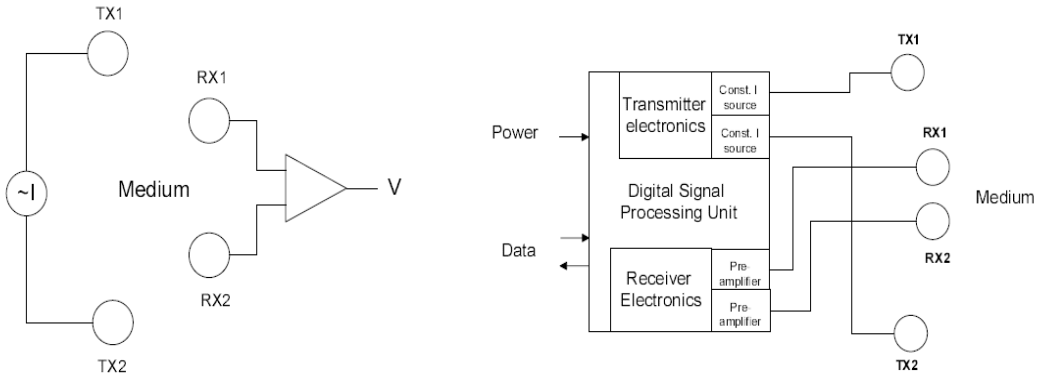

Figure 2-33: Mutual Impedance Probe working schematic

[AD52]

By using this concept, a sinusoidal current I, of frequency w, chosen such that the wavelength is much larger than the size of the electrode array, is injected between two transmitting electrodes, TX1 and TX2, and induces a voltage V between two receiving electrodes, RX1 and RX2. The complex ratio $\frac{V}{I}$ is the mutual impedance of the circuit. All considerations taken previously for the system architecture to conductivity measurement are valid for permittivity measurement. However, for permittivity measurement, it is only required to know amplitude of the signals and respective phases, as is expressed in the expression below:

$$\varepsilon = \frac{V_0}{V}\cos(\varphi - \varphi_0) \tag{42}$$

Through this, it is possible to easily determine permittivity.

To guarantee a good measurement range and a good accuracy of the MIP, it is required that the probe have a good operating frequency range, as well as a good transmitter signal magnitude range and a signal spectral cleanliness. It is required that the receiver has a good SNR, good signal processing capabilities and a limited sensitivity to environmental parameters, such as temperature and humidity.

Permittivity determination is important since this parameter is required to determine the conductivity through the relaxation method. This relation is depicted in the relaxation method section.

3 System Overview

3.1 System Architecture

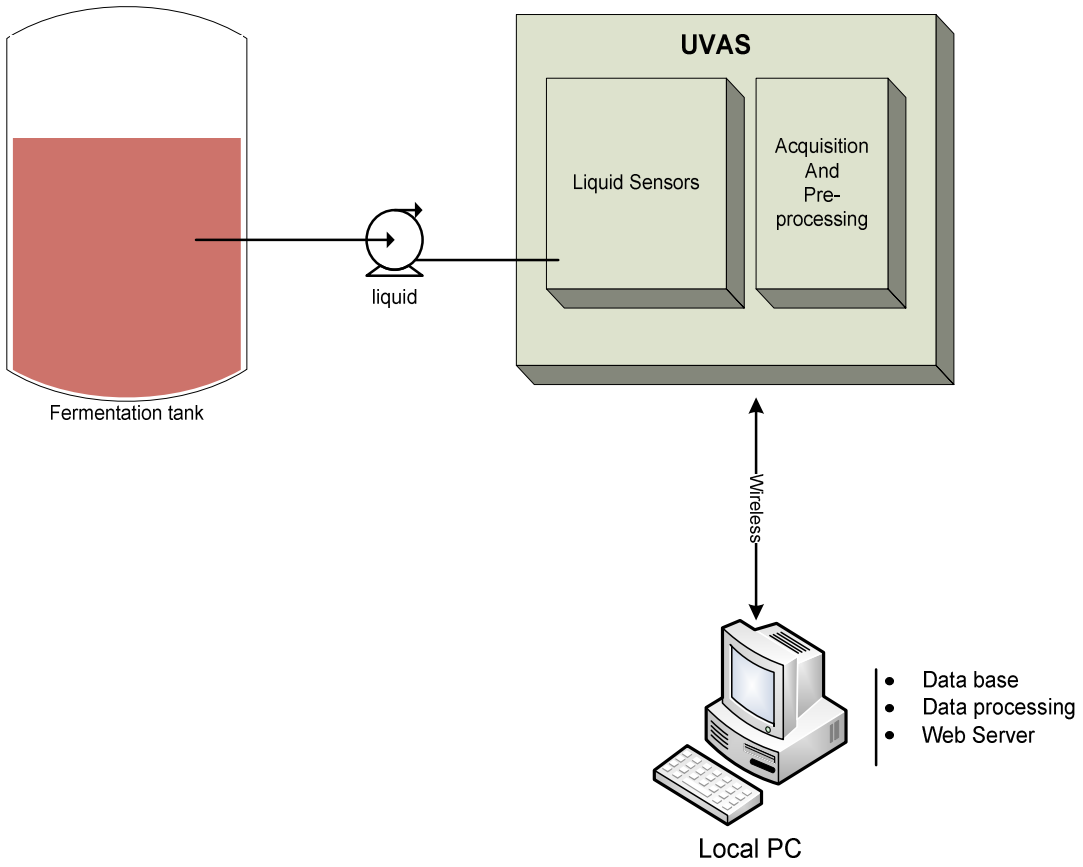

Figure 3-1: UVAS System Architecture

It is intended to apply a great variety of sensors in the UVAS system to measure the different parameters considered as essential in wine fermentation. These sensors acquire data from both the liquid and the gases, by which the fermentation may be characterized and properly monitored. It is intended to have the diverse sensors connected to an acquisition and pre-processing unit, considered as a slave in the computer network, in which the raw data would be properly pre processed, being consequently sent to a local computer, which acts as the master PC of this system, where the data are further processed and presented accordingly in the program GUI.

In Figure 3-1 is also represented a box for actuation control. The actuation over the fermentation will not be implemented in the first stage of the UVAS system, as the first stage intents to develop a system to monitor the fermentation, allowing the user to manually actuate over the process.

Wireless communication was the physical medium selected for master/slave communications. The reason for this choice was mostly to have the master PC in a remote and more secure location, where it would not be susceptible to accidents or spills from the tanks and other hazardous accidents that could occur in wine making industry and could damage the computer.

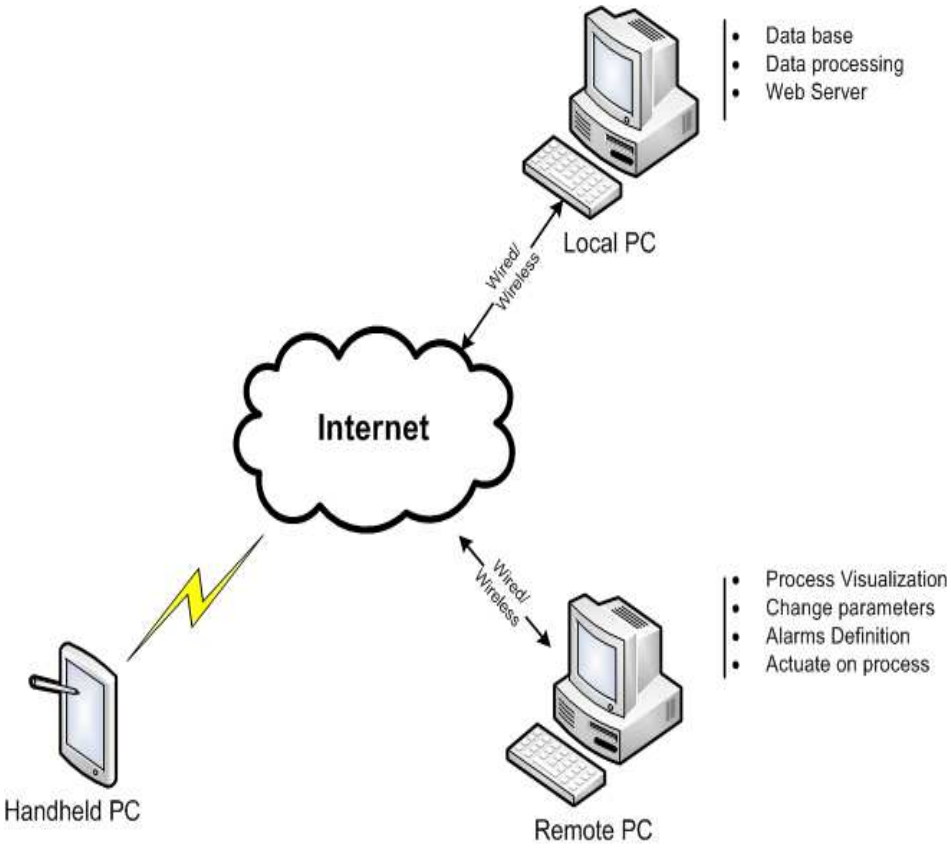

Figure 3-2: UVAS System Network Architecture

Regarding the communication between the Master PC and all other PCs with remote access, it was decided to use a webservice, to make the acquired data available to other users, as long as these users have an authorized access to the webservice. Through this webservice, the data would be available on the web and the user could access them through any kind of proper equipment.

3.2 System Functional Breakdown

The following diagram, presented in figure 3-3, presents all the functions of the UVAS system, which are intended to implement in the system. These diagrams were designed using the UML language program “Enterprise Architect”.

The functional block 1.1 represents the Data Acquisition functionality; within this functional block, the system shall acquire data from the tanks, either by digital or analogue sensors.

The functional block 1.2 represents all support operations the UVAS system has available in order to accomplish its purpose, such as liquid pumping, to force the liquid into the sensors, in order to perform the measurements, system cleaning, after each set of measurements, since it is possible to contaminate the sensors with the wine, requiring these to be washed and returning the analysed liquid back to the tank.

The functional block 1.3 represents all data management functions, since storage of the data and consequent processing, as conversion of the raw data to perceptible information for the user, correlate the information with known data, allowing a better control of the fermentation, management of the system configurations, such as the periodicity of measurements or set milestones for desired fermentation profiles control. The functional block 1.4 represents all communication functions of the UVAS system, more specific internet transmissions and local transmissions between devices, reading and writing between them.

The final functional block, 1.5, is the functional block of the HMI/GUI, which allows data presentation, consult fermentation state, request a desirable acquisition of data, configure the parameters of the monitoring, in case of considering some more essential to monitor than others, present correlations of the present fermentation development and of the theoretical results, in order for the user better actuate over it and present suggestions considering how to better actuate over the fermentation process.

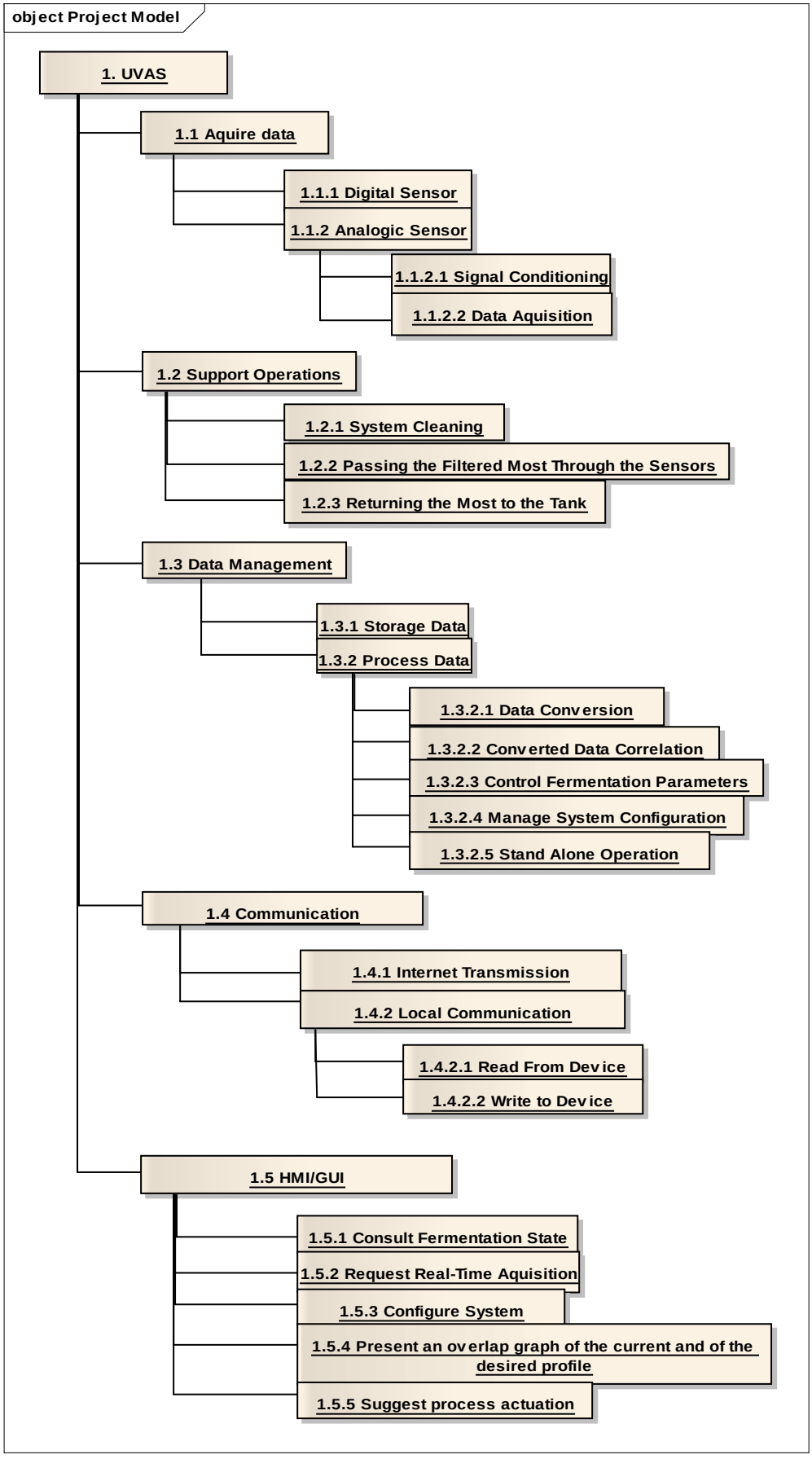

Figure 3-3: UVAS system Functional Breakdown

3.3 System Sequence Diagram

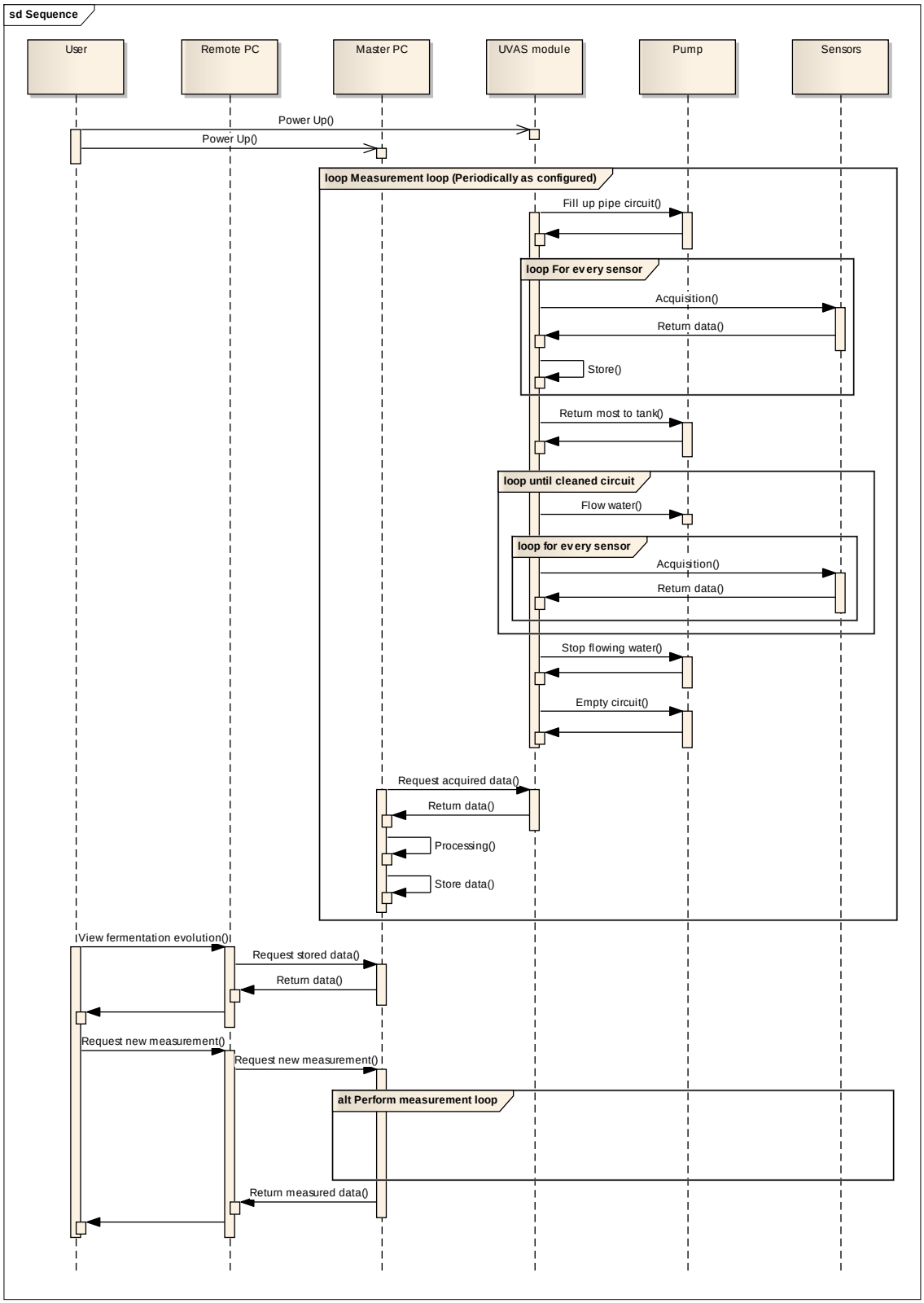

Figure 3-4: UVAS System Sequence Diagram

The previous image, figure 3-4, represents a sequential diagram for the monitoring cycle of the UVAS system, involving all its functionalities, since data acquisition by the sensors, the pumping of the liquid to flow to all sensors, the pre processing of the data, the cleaning of the sensors with water, performing another set of measurements to control the cleaning of the sensors and the consequent transmission of the data to the Master PC, where the data are fully processed and sent through webservices to remote users, which may also request measurements.

3.3.1 Functional Blocks Analysis

In this section the UVAS system functionalities are explored from the following perspectives: inputs (left), outputs (right), constraints (top) and resources (bottom). Function modelling is based on IDEF0 diagrams. IDEF0 (Integration Definition for Function Modeling) is a method to describe functions, being part of the IDEF family of modelling languages, being used to model the decisions, actions, and activities of an organization or system.

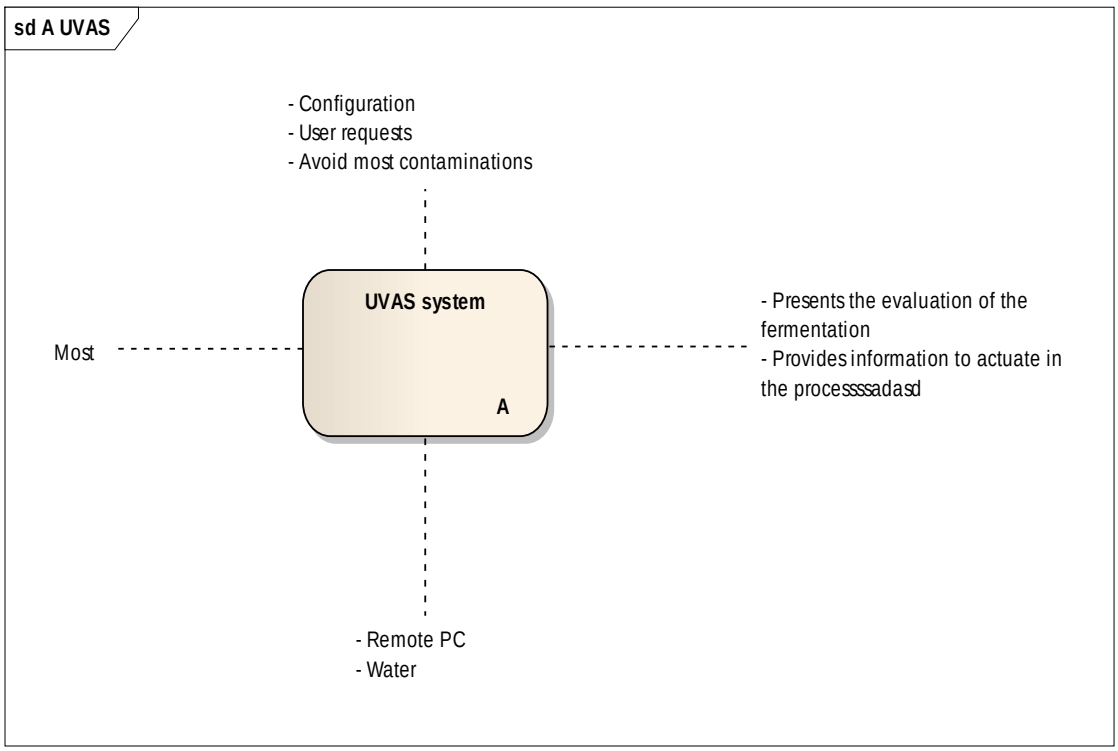

Figure 3-5: Functional block diagram – Top level.

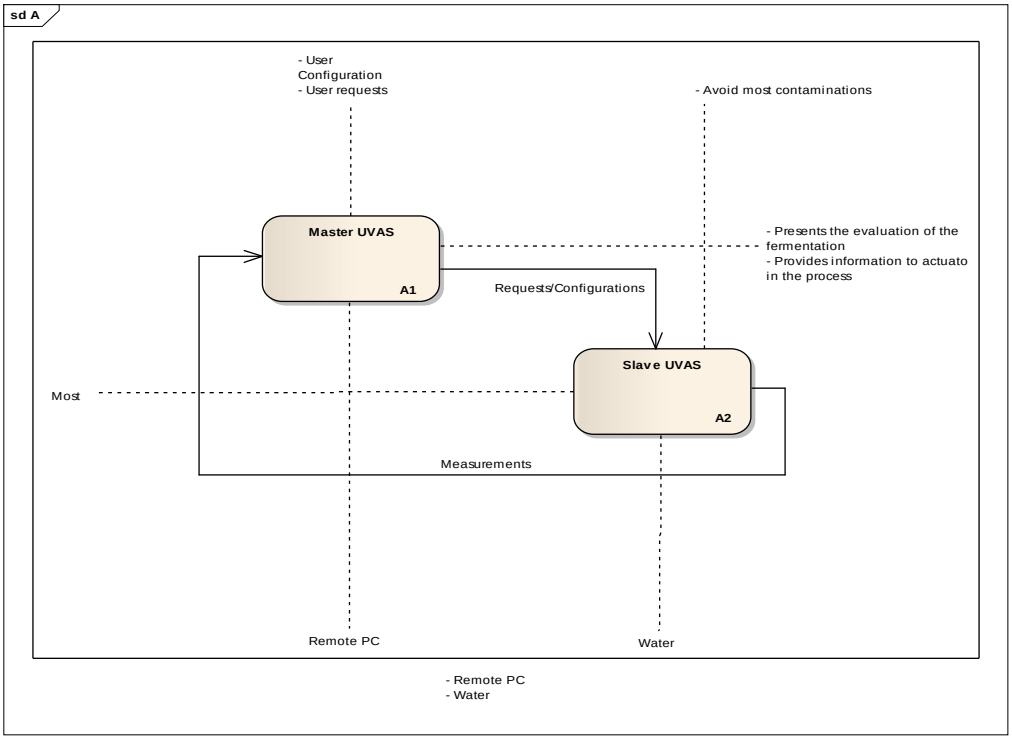

Figure 3-6: Functional block diagram – Tier 1.

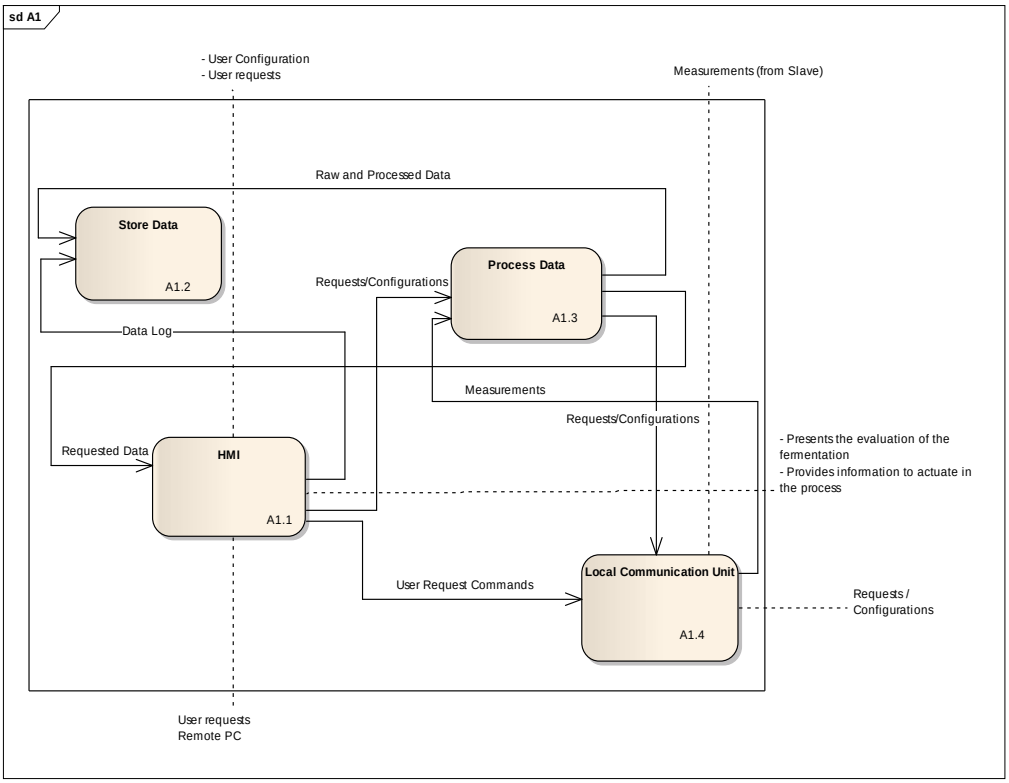

Figure 3-7: Functional block diagram- Tier 2, Master UVAS

The user makes requests through the HMI (A1.1); he may store data and system configurations (A1.2), request process data (A1.3) or send request commands

to the local communication unit (A1.4). These commands are sent to the slave, ordering data acquisition, and the measurements received are sent to the process data block. All processed data are stored in memory (A1.2) and sent to the HMI (A1.1), in order to be displayed.

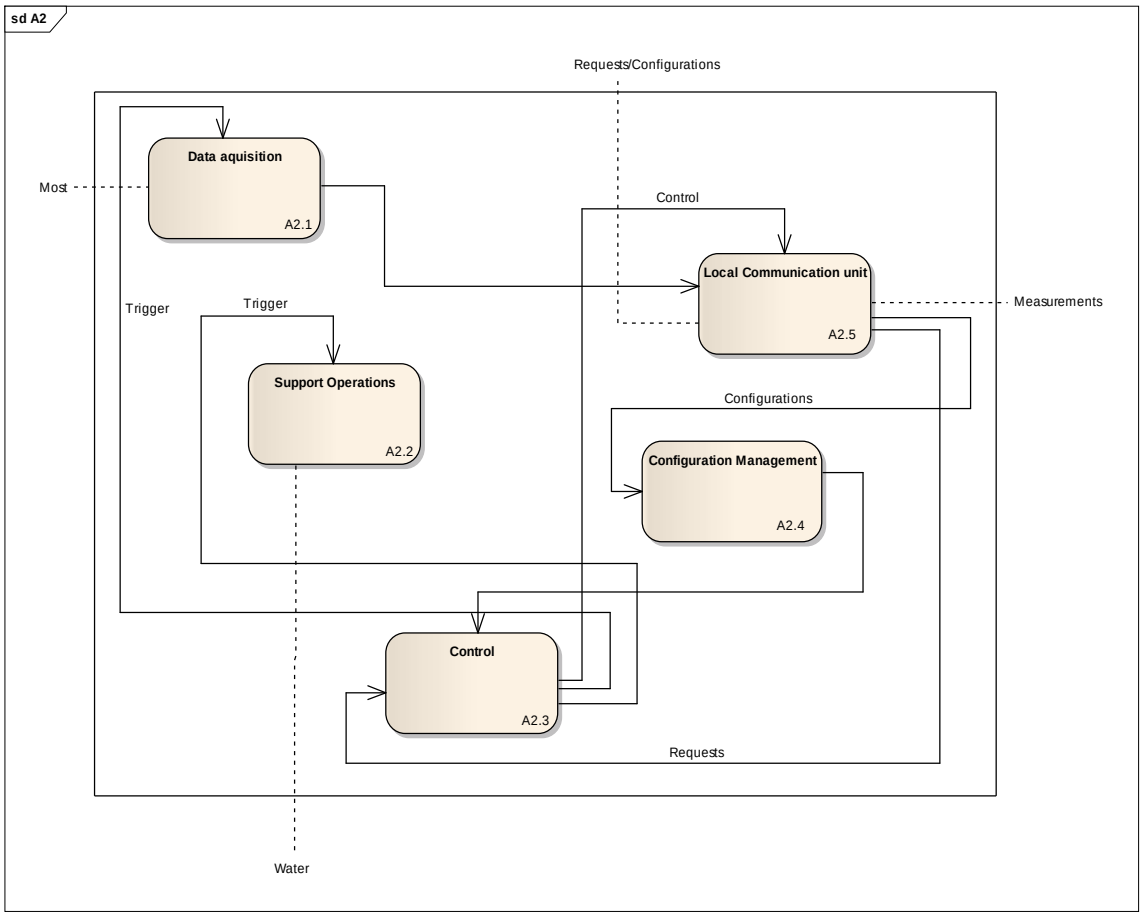

Figure 3-8: Functional block diagram- Tier 2, Slave UVAS.

All data acquired from the most (A2.1) are sent to the local communication unit (A2.5), from which they are sent to the Master. This block (A2.5) is also responsible for receive the requests and the configurations by the user, whose configurations are sent to the configuration management (A2.4), which will constraint the functioning of the control block (A2.3), which also receives requests from the local communication unit. The control block feedbacks to the local communication unit, in order to feedback to the master and is responsible for two trigger signals, one to start acquisitions from the most and other to start the support operations (A2.2).

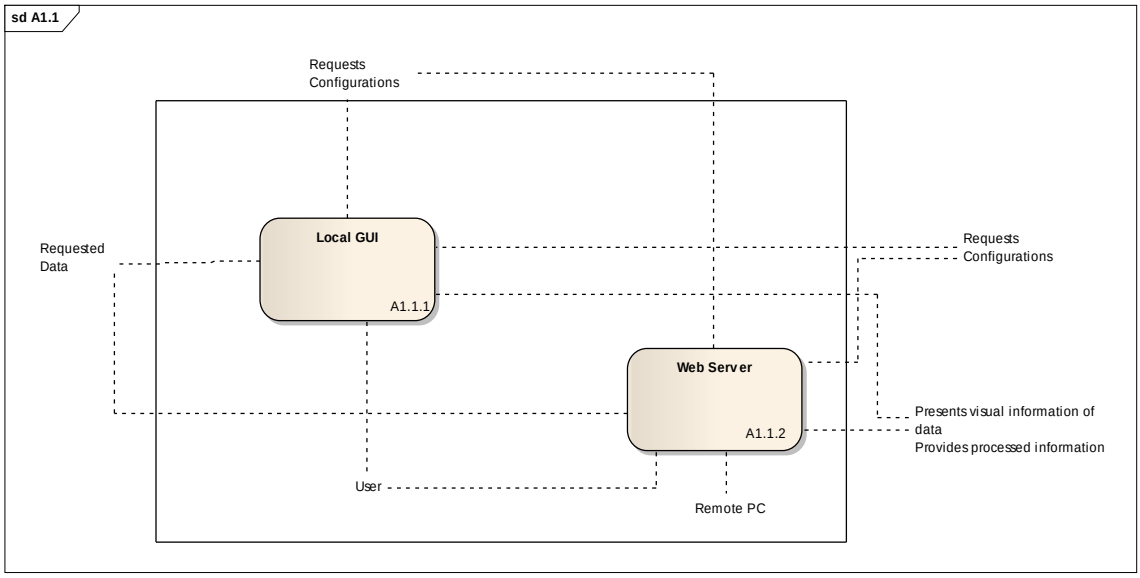

Figure 3-9: Functional Block diagram – Tier 3, Master HMI

The image above depicts a more specific view of the HMI block, from the master. The HMI consists in a local GUI (A1.1.1), which receives requests and configurations from a local user and a Web Server, which also receives requests and configurations from remote users with remote PCs, connected through the web. Both these blocks output requests and configurations as well as present visual interpretation of data and providing processed data to the user.

4 Sensors Development

4.1 Sensors Development Overview

UVAS system requires the implementation of several sensors in order to monitor the diverse parameters. After the research phase, the final choice was made considering several sensor parameters, such as sensor resolution, accuracy, range, price, output signal and composition materials. Several of these parameters were evaluated regarding their definition in [RD5].

There are certain materials to avoid, such as organic materials and glasses. Organic materials can react with the wine, therefore contaminating the solution and glasses are very sensible and are easily damaged. There are some polymers resistant to strong chemical reactions and these may be used. The preferable materials to apply in UVAS system are stainless steel or others equivalent, since these materials offer high resistance to chemical reactions.

Considering these requirements, the chosen solution to monitor each parameter is presented in this chapter, as well as a small description of the development process. Since UVAS system requires a great number of sensors, these were developed in parallel by several team members and because of this work division, only the sensors developed by the trainee Paulo Marques, or those to which development trainee Paulo Marques has contributed will be described in the following sections.

4.1.1 Measuring pH

Both glass and ISFET pH technologies require regular calibration and cleaning of the probes at some point in their useful lives. These calibrations depend greatly of the on the sensor type and frequency of usage. Adding to the fragility of the glass bulb pH sensors, these must also be stored in a solution when not in use because the sensor tip shall never be allowed to get dry.

ISFET sensors eliminate some of these problems associated with the glass bulb sensors, being able to be stored dry and having small requirements in maintenance. These are also excellent for field work, food testing, soil testing and industrial applications.

The sensor body materials are going to be in contact with the solution and cannot introduce additional elements causing contamination. Therefore, robust materials should be used, such as stainless steel or glass, avoiding organic materials and plastics.

However, polymers are widely used in pH ISFET meters. One of these polymers is PEEK, used in the body of the InPro 3300 and Tophit CPS471D. Both these sensors are used in Food and Beverage industries, pharmaceutical industry and hygienic applications and InPro 3300 has achieved excellent performance results and commendations in F&B industries. PEEK has excellent mechanical and chemical resistance properties that are retained to high temperatures, making it a good choice for several applications and should not be ignored.

Considering the project requirements and the technical findings, the best solution for the pH sensor is to use an ISFET type sensor. For this, according with the several requirements, such as the system architecture, device specifications and prices, it was decided to build a suitable sensor probe with Optoi OII1 chips.

Figure 4-1: ISFET Chip OII1

[AD68]

These ISFET chips are n-channel transistors, with small dimensions ($\mathrm{L} = 13\mathrm{mm}, \mathrm{W} = 7.7\mathrm{mm}$), suitable to insertion in the UVAS system, have a sensitivity of $55\ \mathrm{mV/pH}$ and a fast response time of 1-2 seconds and has a pH range from 2-12 pH units.

The analogical circuit assembled to use with this sensor was the one presented in the component's datasheet, which is presented below:

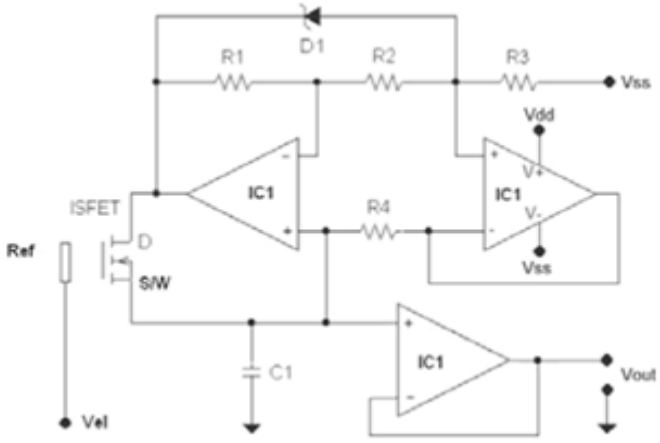

Figure 4-2: ISFET Chip Circuit

[AD68]

In order to assemble the circuit, components were used with the same values as presented in the sensor's datasheet:

R1 = 150kΩ; R2 = 470kΩ; R3 = 10kΩ; R4 = 9.1kΩ; C1 = 470pF; D1 = 1.23V

The operational amplifier used was Microchip's MCP6024, with Vdd = 5.0 V; Vss = 0 V and Vel = $\frac{\mathrm{Vdd}}{2}$.

The reference electrode used, represented in the circuit as Ref, at a voltage Vel, was a simple piece of wire, connected to a power source at a potential Vel = 2.5 V.

4.1.2 Measuring Temperature

In order to monitor the temperature, it was decided to use an RTD sensor. This choice is due to the high accuracy of the RTD, when comparing to NTC and thermocouples, as well as the repeatability and stability achieved, both important requisites for the UVAS system.

The chosen RTD was Labfacility – DM-334, with the Farnell code 8598525. This sensor is a PT100, has a range of 50℃ to +400℃ an d is class A, which has better sensitivity that those of class B, as is demonstrated in the RTD section of chapter 2.2. The sensor has dimensions of 10x2x10 mm (height x width x lead length).

Figure 4-3: RTD sensor image
[AD67]

In order to relate the resistance values with the temperature values, it was made a linear fit with the values presented in the datasheet, some of which are also presented in the table below. With these values, the relation Resistance *vs* Temperature was interpolated:

Table IV: RTD Resistance with Temperature Relation

Temperature (ºC)	Resistance (Ω)
-200	18.52
-100	60.26
0	100
100	138.51
200	175.86
300	212.05

By making a linear fit for these data, it is obtained the RTD characteristic curve, depicted in the image below:

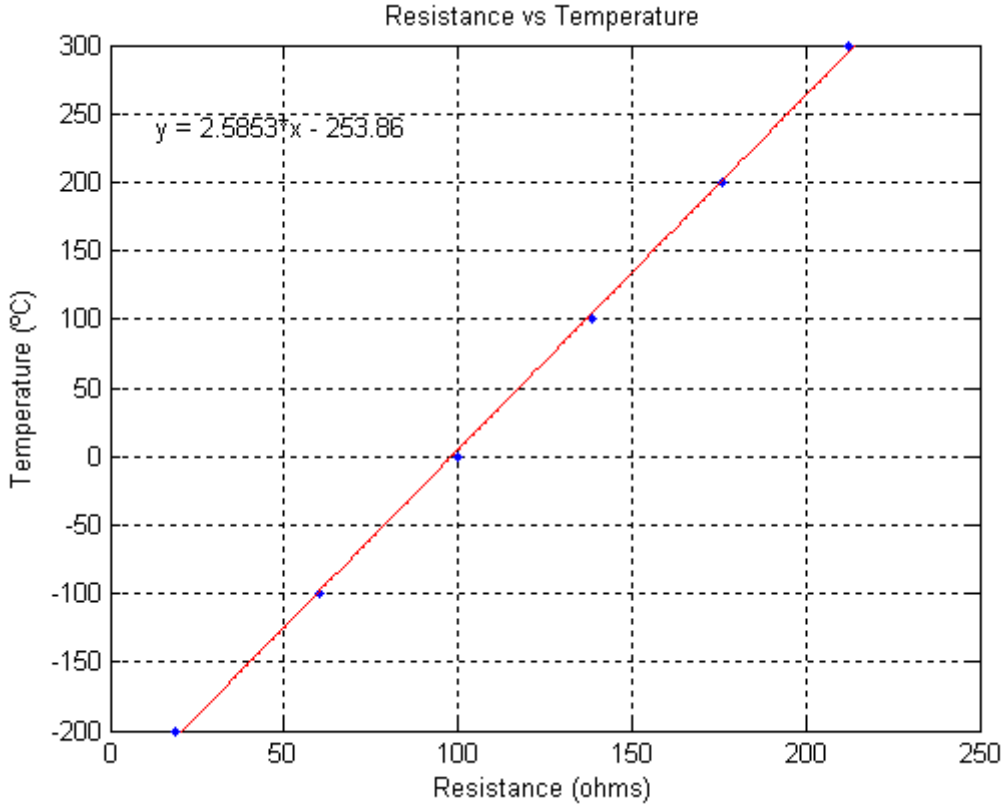

Figure 4-4: RTD relation between Resistance and Temperature

Analysing the graph, it is possible to conclude that

$$Temperature(ºC) = 2.5853 \times Resistance(\Omega) - 253.86$$

This relation was used with all measurements of the system, relating the temperature measured with the resistance of the RTD.

In order to be able to register the temperature of the wine, it was decided to assemble the sensor inside a stainless steel tube and thermal mass. The sensor would be “glued” by the thermal mass to the tube and because of the thermal properties of the two materials, thermal mass and stainless steel, the temperature on the sensor would be roughly the same as the temperature of the medium in contact with, in this case the wine. The plate would merely produce an offset and delay in the sensor, something that can be easily corrected in the temperature sensor programming.

As this sensor has been used in other applications by Activespace Technologies, there is already a fully developed temperature sensor and therefore the development of this sensor was considered complete for the time being.

4.1.3 Measuring Viscosity

The initial choice to assemble a sensor to monitor the viscosity of the wine was to use acoustic wave sensors, from Sengenuity ([AD31] to [AD36]). However, although these sensors are solid state and offer better results, safety and avoid the necessity of maintenance, its price can go up to 5000€. For this reason, it was decided to assemble a mobile parts viscosity sensor, depicted in the image below, designed in CATIA.

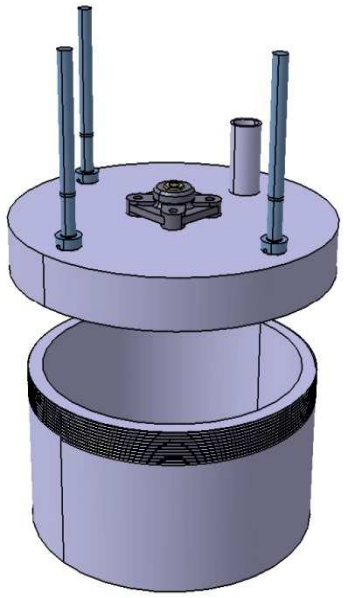

Figure 4-5: Viscosimeter schematic

The working principle for this sensor is to measure the required current to move the paddles and through it, determine the viscosity of the liquid. In order to do this, a small dc motor has to be connected to the paddles array, placed inside of the machined case. This connection must be properly isolated in order to avoid wine losses tooutside. The sensor's case has one entry and one exit, in order to be filled from the top entry and emptied from the bottom exit.

The filling and emptying of the sensor chamber was to be made with a pump and valves. When it is to fill the sensor chamber, the filling valve would allow the wine to pass, while the emptying valve would block the wine to pass. On the other hand, when it is to empty the sensor chamber, the opposite will happen. However, despite having a possible solution, this was not analysed nor properly studied so far. The solution for the viscosimeter is still on hold.

4.1.4 Measuring sugars and alcoholic concentration

In order to measure the Brix concentration in the wine, it was decided to use a refractometer. The choice was ATAGO's PAL-86S. This refractometer is both portable

and digital, with two possible outputs, either Brix scale or Oechsle scale. For the UVAS system, the desired scale is the Brix scale, which has a range of 0.0% to 53.0%, a resolution of 0.1% Brix and an accuracy of ±0.2%. In order to measure the alcoholic concentration, it was decided to use a refractometer. The choice was ATAGO's PAL-34S. As with the brixmeter, this refractometer is also both portable and digital, with a range from 0.0 to 45% ethanol, a resolution of 0.5% and an accuracy of ±1.0%.

As these are portable devices, are odd choices to implement in a standalone system. However, portable refractometers for Brix and alcoholic measurement are far cheaper than probes and other similar systems, costing $330 US dollars, while another type refractometer sensor could cost more than $1000 US dollars. Therefore, some changes would be made, in order to adapt this sensor to the UVAS requirements.

One possible way to extract the signal is from the LCD entry. The refractometer makes all the analyzing in an internal microcontroller and sends the Brix scale and the alcoholic concentration value into the device LCD. It is possible to intercept this signal at the LCD entry and send it to another microcontroller. Here, the signal can either be further processed, converting it from string to number, or be simply sent to display in another GUI.

Figure 4-6: Atago Pal-86S Brixmeter

[AD55]

Figure 4-7: Atago Pal-34S Alcoholmeter

[AD54]

These sensors require two AAA batteries as power supply, therefore, another change is required to apply an external power supply, avoiding the need for batteries.

Another sensor alteration to be made is in the case. In order to turn these sensors in a more probe like sensor, as it was previously said, there is the need to place it in flow; therefore, it is required a case made from compatible materials that do not react with the wine and respect the conditions stated before. It was decided to make a new casing from either aluminium or stainless steel.

With all these alterations, a more probe like sensor can be achieved to implement on the UVAS system.

As of the date of delivery of the present document, there was no development regarding this sensor beyond this point.

4.1.5 Measuring Glucose and Fructose concentration

In order to measure glucose and fructose concentrations during the fermentation, it was decided to use a polarimeter. Considering this solution, it was decided to make a fully automatic device for application in the UVAS system.

Considering these requirements, it was required to develop full mechanical, electronic and optoelectronic systems. The responsibility for the development of this sensor was given to trainee Paulo Marques.

The development of this sensor was based in the considerations approached in chapter 2.7, whose applications are evaluated in this section.

As it is said, there are two possible methods to develop the polarimeter: to use the mobile parts, in which there is a motor rotating the analyser and the optoelectronics method, in which only optoelectronic properties are used. It was decided to evaluate both methods; however, the present work only discusses the development of the mobile parts polarimeter, since it was not possible to assemble and validate the architecture of the optoelectronic architecture polarimeter.

Considering the need of flexibility in this prototype, a guide through with respective skates was used, considering the need to move the components to optimize the response of the sensor. The several components required to assemble the polarimeter were separated in different mounts, in order to evaluate each component application independently. Cell mounts brackets were designed and fabricated specifically of the application in the polarimeter, as it is explained in the following sections.

In order to perform the rotation of the analyser, it is intended to use a stepper motor. Through the relation between the steps and the step angle, it is possible to

determine the angle of rotation. For this development, a schematic of the polarimeter was designed in CATIA, which is depicted in the image below, figure 4-8.

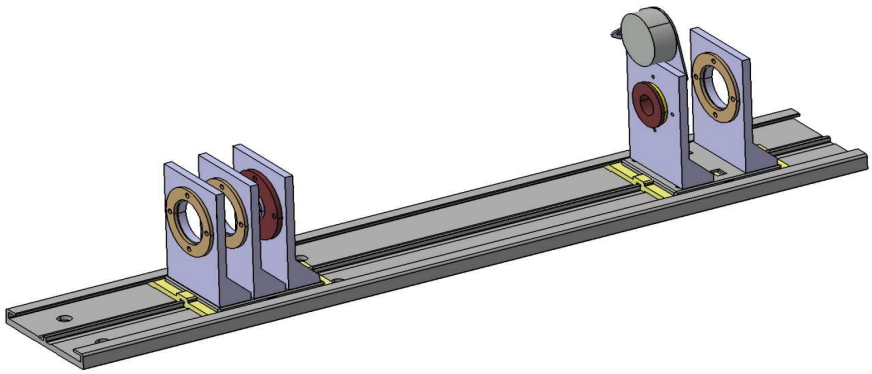

Figure 4-8: Polarimeter schematics

4.1.5.1 Sample Vial

Ideally, the sample vial would be connected to valves, which would be responsible for filling and emptying the sample vial. For prototype development, however, considering costs and practicability, it was decided to use a small vial with parallelepiped shape, of 100x50x50 mm, manually filled with liquid.

In polarimetry, the dimension of the vial most relevant is the length travelled by light. Considering this, the justification for these measures is presented with the following calculations: using equation (31) and substituting with the minimum and maximum values for the concentrations of glucose and fructose in wine, as represented in table 3, the specific rotation of glucose and fructose and the dimensions of the sample vial, it is possible to measure the maximum and minimum rotations angles:

For a minimum concentration of 50g/l of glucose and fructose, the minimum angle to measure is approximately:

$$\alpha = \left(\frac{52.7 \times 50}{1000} \times 1\right) - \left(\frac{92.4 \times 50}{1000} \times 1\right)$$

$$\Leftrightarrow \alpha = -1.985^{o}$$

For a maximum concentration of 180g/l of glucose and fructose, the maximum angle to measure becomes:

$$\alpha = \left(\frac{52.7 \times 180}{1000} \times 1\right) - \left(\frac{92.4 \times 180}{1000} \times 1\right)$$

$$\Leftrightarrow \alpha = -7.146\ ^{o}$$

If the vial had a length of 200 mm, then the respective angles for minimum and maximum concentrations would be $\alpha = -4º$ and $\alpha = -14.292º$.

Although small, both these angles are easily measured with the selected approach of the stepper motor.

Figure 4-9: Polarimeter sample vial

Using a vial with this length, it is possible to develop a small system, although it would be possible to develop an even smaller, with a smaller vial. However, since the costs of making a smaller vial would increase with the decrease in dimensions, it was decided to use a vial of 100 mm, since it allows distinguishing good variations of polarization angles.

4.1.5.2 Guide Troughs and Mounts

To create a first prototype, it is required a system to move the several components, if required, for testing purposes. In order to do this, it was decided to use a guide trough. The biggest component used in the prototype is the sample vial, with parallelepiped shape of 100x50x50 mm. For this reason, in order to have space to move the components (collimator, polarizers, light source) or substitute the sample vial to a bigger one, if required, it is intended to use a guide trough with 500 mm. In order to housing the sample vial, the DryLin® N - Low profile linear guide system NK-02-80, consisting of a guide trough and two skates was chosen to be used in the prototype.

Figure 4-10: DryLin® N - Low profile linear guide system with one skate

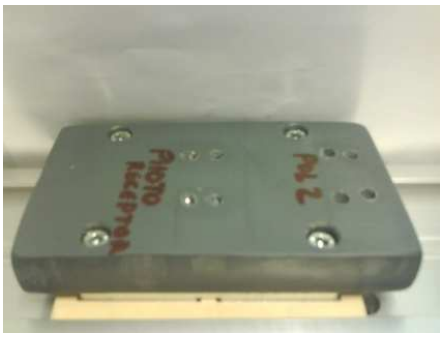

Figure 4-11: Skate mount used

In order to fix the components in the guide trough, optical cell mounts were applied. These mounts were machinated from stainless steel according with the need and were screwed to the skates using a small piece of PVC as support, as shown in 4-11.

The analyser, which is the designation given to the last polarizer in the system, the one that rotates and from which the angle of rotation will be measured, was placed in a special mount. As it was previously said, the analyser requires to be rotated. Considering this requirement, a special mount was assembled, allowing the rotation of the analyser with the stepper motor movement transference. These two types of mounts are shown in the following images:

Figure 4-12: Optical mounts used in the polarimeter: a) Standard mount; b) Analyser mount

4.1.5.3 Light Source and Light Detector

The light source mostly used in this type of application, more specifically, to measure concentrations of glucose and fructose using polarimetry, is a sodium light source that emits in the wavelength of 589 nm, also referred to as the sodium D line.

In the modern automated polarimeters, the light source is usually a laser with all the previous stated characteristics, but due to difficulties associated with the pricing of such devices and of laser diodes, which emit in the sodium D line and also because of

the difficulty to find a device with the specified parameters, it was decided to use LEDs that emits in the 589 nm wavelength.

It was decided to use the LED AND180HYP from AND OPTOELECTRONICS, with Farnell code 1703499 which has a luminous intensity of 9750 mcd and a viewing angle of 6º.

Figure 4-13: LED used as light source in the polarimeter

[AD58]

Research was made for a device with a higher spectral sensitivity in the needed range, but because these were too expensive, it was decided to use one with a good spectral sensitivity around the sodium D line. Considering this, it was decided to use OSRAM Optoelectronics Silicon NPN Phototransistor SFH 3310. Phototransistors work as ordinary transistors, however the base is exposed to the incident light and like ordinary transistors, phototransistors act as an amplifier for the base signals. Because of this, the phototransistor is a good choice to detect small variations of light, as it is the case.

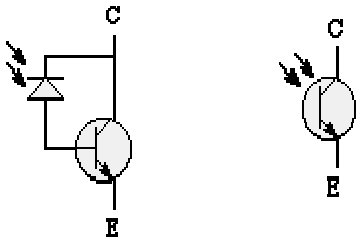

Figure 4-14: Photodiode and transistor circuit comparison with the phototransistor

[AD63]

Figure 4-15: Phototransistor used as photodetector in polarimeter

[AD59]

The selected phototransistor has an absorption maximum for 560 nm, as it is depicted in the respective graphic of spectral sensitivity:

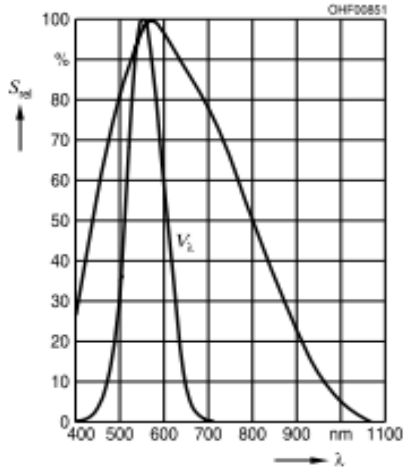

Figure 4-16: Osram 3310 phototransistor relative sensitivity graphic
[AD59]

For the needed wavelength of 589 nm, the phototransistor has a spectral sensitivity around 65%.

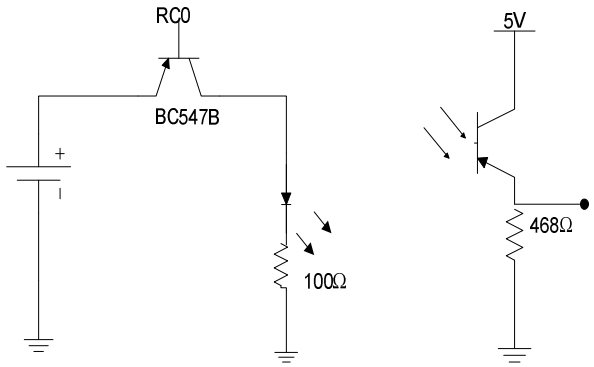

Figure 4-17: LED and phototransistor circuits

Both LED and phototransistor circuits were assembled in protoboards, in order to fix them in the respective mounts, for better system stability.

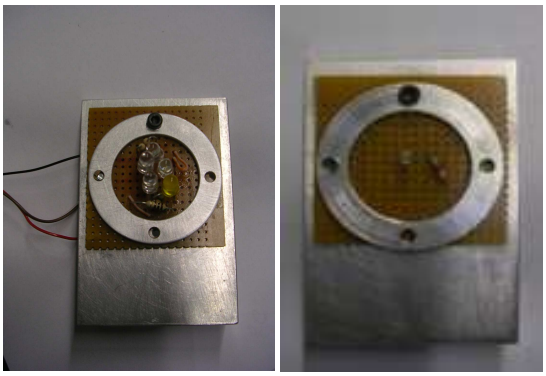

Figure 4-18: LED array and phototransistor circuits in protoboards assemblies

In an initial approach, it was considered to apply an array of LEDs as the light source of the polarimeter. This requirement was due to have a great amount of light to perform the measurements. However, because the LEDs have a viewing angle of only 6º, the array proved to be ineffective, unless the phototransistor receives the light of all LEDs in an angle of 6º. If this does not happen, then the LEDs will be useless in the application.

Considering this, only one LED was used as the light source of the polarimeter.

4.1.5.4 Collimator

The use of the collimator is only required if there is the need to straighten the light into a light beam. If the light source emits in a large area, the optical power will be spread over the same area and in order to maximize the effects of the light, it is used a collimator to straighten the light into a beam. The necessity of the collimator started with the idea of the array of LEDs. As the array of LEDs proved to be ineffective, so did the collimator proved to be unnecessary.

Since the light source in the polarimeter is only one LED, it is not required to use a collimator. However, the collimator could still be applied in the system if there is the need to straighten the beam. Considering this, it was decided to apply the collimator to the system.

The chosen collimator was Edmund Optics' NT56-291, with a pinhole aperture of 1mm.

Figure 4-19: Precision pinhole collimator mount
[AD70]

As with the LED and phototransistor, the collimator must be properly aligned with both emitter and receptor, to allow the passing of the light and a direct beam of light into the phototransistor.

4.1.5.5 Polarizers

The polarizers are the components responsible for the light polarization. These are responsible for cutting all wave fronts with different orientations than that of the polarizer, which will reduce the light intensity and will cut all unnecessary wave fronts that could act as noise in the readings. The chosen polarizers were linear polarizers from Edmund Optics, more specifically TECHSPEC® Linear Polarizing Laminated Film, Edmund Optics NT45-668, with a transmission of single sheet of 38%, transmission of two parallel sheets of 27% and transmission of two crossed sheets of 0.04%, as well as polarizing efficiency greater than 99%. Since these sheets come with 8.5" x 15" dimensions, these may easily be cut into the desired dimensions.

Figure 4-20: Techspec Linear Polarizing Laminated Film sheet
[AD69]

In the images below, are shown the polarizer mounts that were used for the polarimeter: the first polarizer sheet was cut with dimensions of 5cm by 5.5cm and the second polarizer was cut with dimensions 3cm by 3.2cm.

Figure 4-21: a) First polarizer mount; b) Analyser mount

4.1.5.6 Detector/ Analyzer

In standard polarimeters, the polarized light detection is made with another polarizer, which is called the analyser. This is placed in a crossed position with the first polarizer, allowing no light to pass at all, considering this position to be position 0. When a optical active sample is placed between both polarizers, this position suffers a small rotation and must be found again; the system rotates to this new point where the new minimum is and the variation between the initial and the final position is the desired angle that gives the orientation of the light plane.

To implement this, the analyser must be placed in a mount able to rotate.

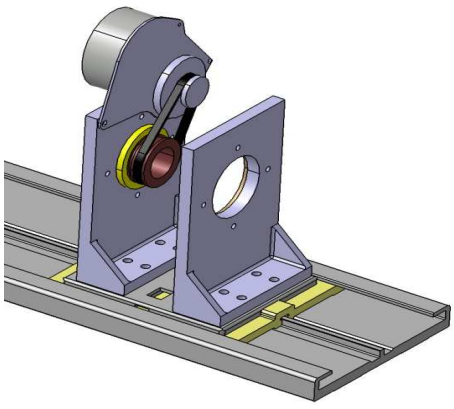

Figure 4-22: Schematics of the analyser rotation system

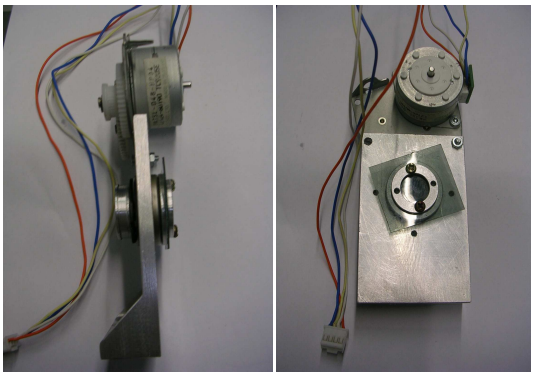

Figure 4-23: Analyser Bracket Assembly from different views

In order to have a fully automated system, avoiding the need to manually rotate the analyser, as well as to be able to rotate small angles, it is intended to apply a small motorized system. In order to do this, it was decided to use a DC stepper motor. This choice is justified with the ability of the motor to make small steps, easily reduced to smaller steps with the application of gearheads. The control of these motors is also easier than the control of the DC motors. These last require encoders to make the control while a stepper motor require only to commute the state of the windings, accordingly with the tables of control for stepper motors [RD12].

Since the values of glucose and fructose concentrations are limited between 50-180 g/l, it was decided that the system must have a precision of 1g/l. In order to do this and using (31):

$$\alpha = \left(\frac{52.7 \times 1}{1000} \times 1\right) - \left(\frac{92.4 \times 1}{1000} \times 1\right)$$

$$\Leftrightarrow \alpha = -0.04^{o}$$

then it is calculated that in order to have a precision of 1g/l, the system must be able to perform steps of 0.04^{o}. Using these values, then the step motor must have a step angle of 0.04º.

The chosen motor was PM35S-048-HPP6, [AD81], a 48 step motor from NMB-MAT, Mineba Motor Manufacturing Corporation, with a step angle of 7.5º, assembled with a gearhead which makes a reduction of approximately 9.42:1. Using this gearhead, it is possible to obtain step reductions to 0.796º. Using the belt of the motor to transmit the movement of the gearhead to the analyser, a reduction of 2:1 will be achieved, which will allow the system to give steps of 0.398º. However, as it was stated before, in order to have a precision of 1g/l it is required to have step angles of 0.04º. For this reason, it is necessary to use another gearhead.

$$\frac{7.5}{reduction} = 0.04 \Leftrightarrow reduction \sim 188$$

Considering these requirements, in order to have a precision of 1g/l, it is necessary to use a reduction gearhead with a minimum of 188:1. Using the gearhead that makes the reduction of 9.42:1 and having the belt assembled, making the motor give steps of 0.398º, the precision achieved, calculated using equation (31), is approximately 10 g/l, ten times the desired.

For this reason, a reduction gearhead to reduce the step motor step at least 188:1 is desired or an equivalent that can be associated with the one of 9.42:1 in order to achieve the desired reduction.

In order to make the stepper motor control, it was decided to use a L239E, Full H bridge. The circuit used is represented in the following diagram, taken from the component's datasheet:

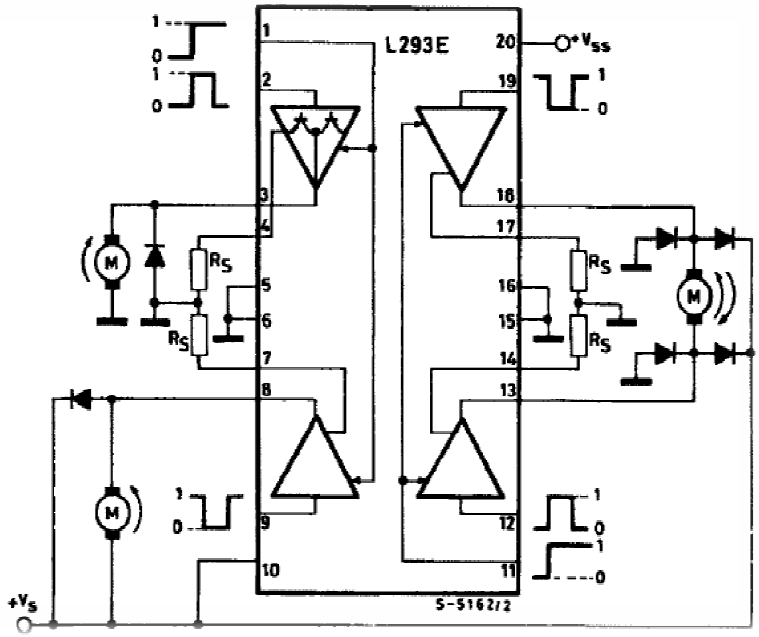

Figure 4-24: L293E and stepper motor circuit schematic

[AD57]

It is required the application of a full H bridge because the selected motor is a bipolar stepper motor. This means that all windings must be commutated accordingly with the table of movements of the stepper motor in order to be able to move. This is better explained in [RD12], where an overview of stepper motor and their functioning methods is explained. A bipolar stepper motor, as is the case of the selected motor for the polarimeter, has two poles for each winding and a single winding per phase. Considering this, it requires to have all windings connected to the bridge, each terminal

to a port of the H-Bridge, in order to commute the state of the windings between 0 and 1. This is valid as well to reverse the direction of the movement: it is required to reverse the direction of the current in the windings of the motor. These motors have typically 4 wires and are more powerful than the unipolar stepper motors:

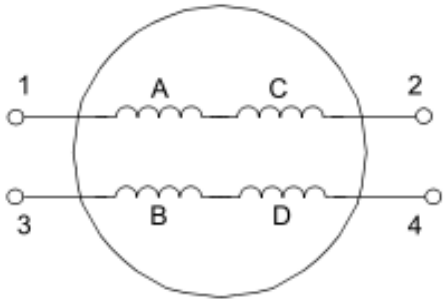

Figure 4-25: Bipolar Stepper Motor Schematics
[RD12]

If the stepper motor is unipolar, then it may have 5 to 6 wires. In these motors, to reverse the direction of the motor is not required to reverse the direction of the current, unlike the bipolar motors. Unipolar stepper motors have two windings per phase and one of this windings ends is made common; this way, it is only requires a half bridge circuit to control the motor and it is possible to have a 2-phase motor much easier than with the bipolar stepper motor.

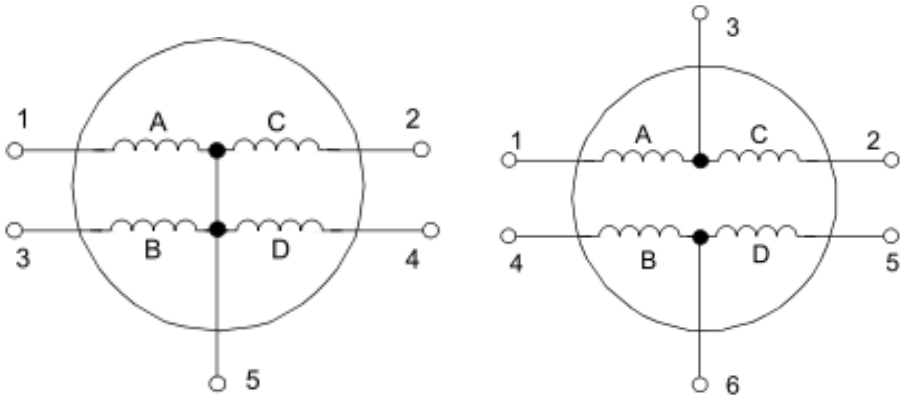

Figure 4-26: Unipolar Stepper Motor schematics with 5 and 6 wires

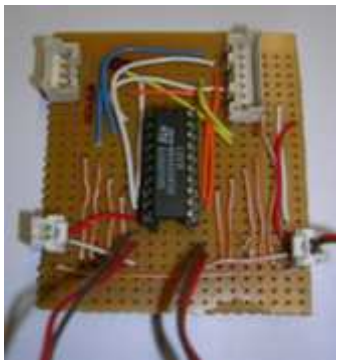

Figure 4-27: Step motor drive circuit assembled

Considering the backlash of the motor, which may prevent steps to occur and considering as well current peeks that may occur, causing the motor to jump steps during the movement, it was decided to apply a position sensor to the motor gears. This position sensor was placed to force the zero position on the stepper motor, in case of a detected malfunction, as a safety measure. The sensor consisted of an infrared LED and an infrared photodiode, pointing to the white gears.

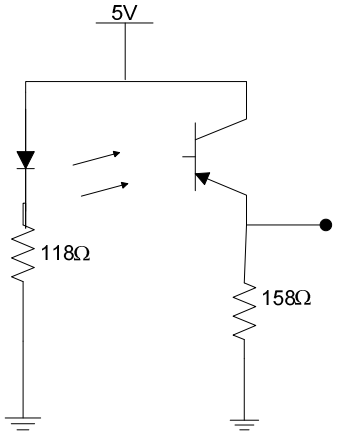

Figure 4-28: Position Sensor circuit schematics

In one of the gear teeth it was made a black line; based in the reflection properties, when the light hits the white surface, it would reflect back to the photodiode; if the light hits the black line, the light would be absorbed and the photodiode would not detect anything. In case of either backlash or current peeks, which may cause the motor to loose or jump steps, the motor routine will reach the zero position before it was supposed to and if this happens, the programming will cause the sensor to re*set al*l acquired data and restarts an acquisition all over again.

Figure 4-29: Position sensor circuit

4.1.5.7 Polarimeter Assembly and Programming

The full circuit diagram for the polarimeter is presented in the image below, depicting the connections between the stepper motor, the L293E, the microcontroller PIC18F2455, the LEDs, the photodetector and the system assembled for the position sensor:

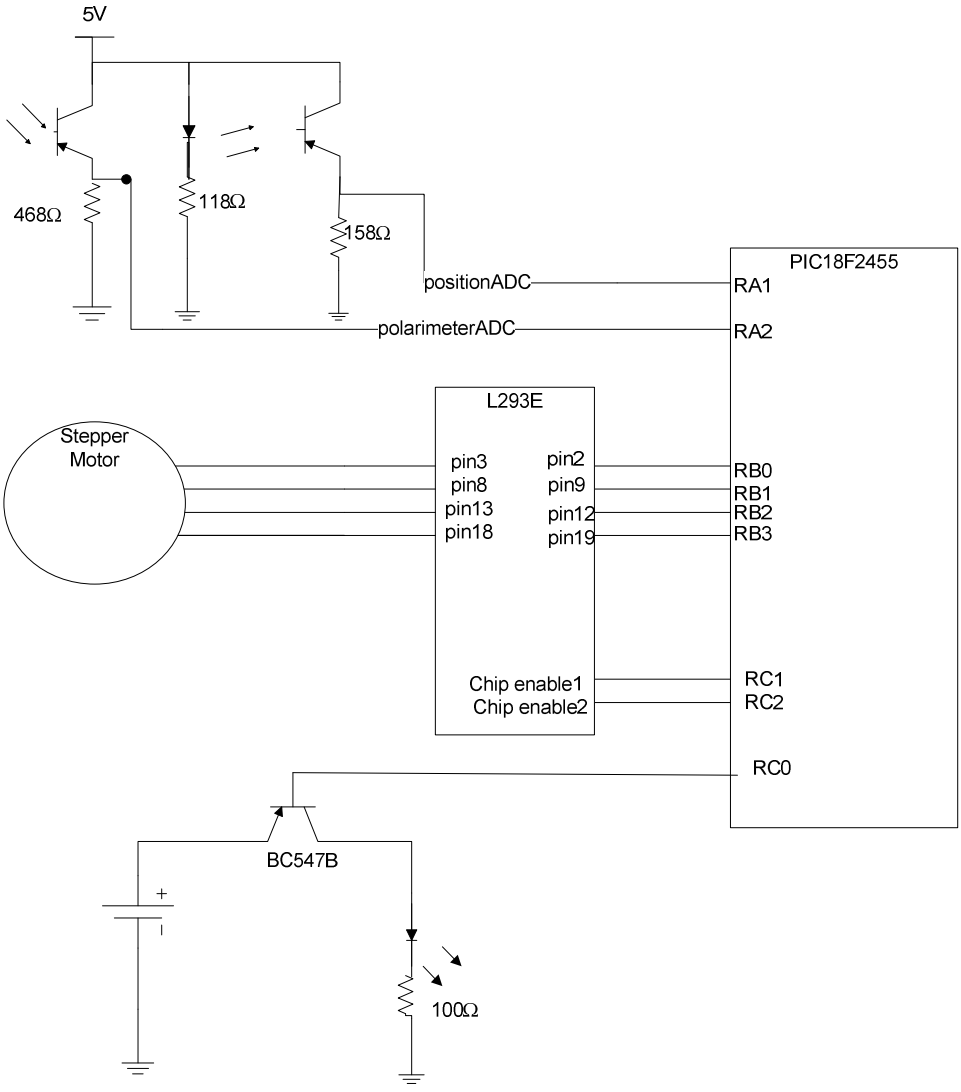

Figure 4-30: Polarimeter circuit schematic

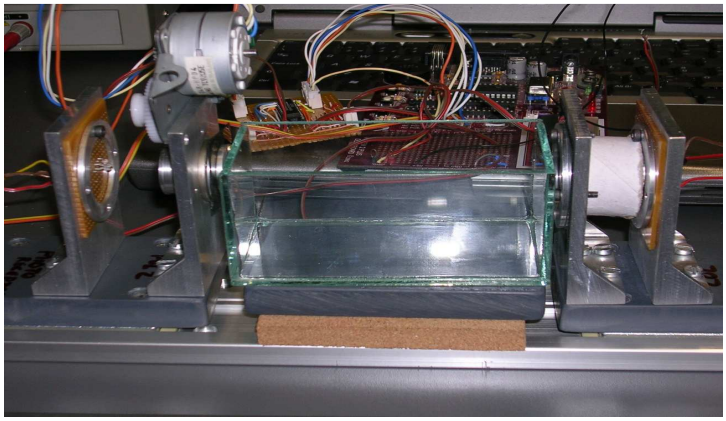

Figure 4-31: Polarimeter full prototype assembly

The software for the polarimeter was developed using Microchip MPLAB and MCC18 compiler, Pickit 3 debugger/programmer and PICDEM 2 Plus demo board, using PIC18F2455.

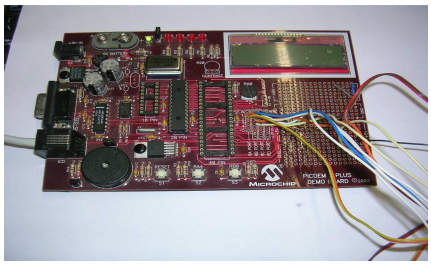

Figure 4-32: PICDEM 2 Plus Demo Board

The software was developed using functional programming for ADC acquisition, data analysis, turn the system on and off and move the step motor, as it is depicted in the diagram below, in figure 4-33.

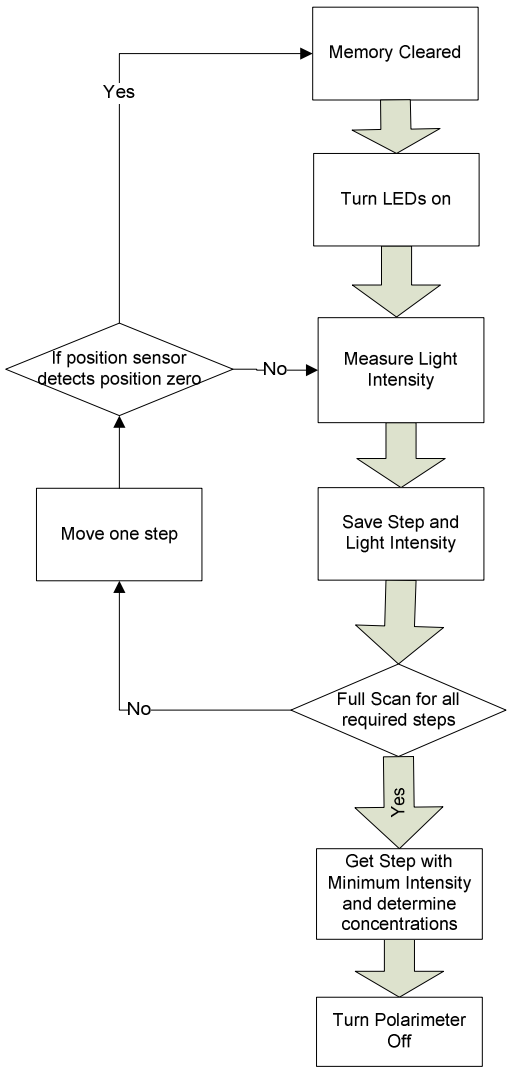

Figure 4-33: Polarimeter software flow diagram

The system starts its acquisition in a position zero, being this position the position of the minimum light detected when the vial is empty in the system. When an acquisition is started, with a properly filled vial, the memory is cleared, having no data regarding previous acquisitions. After this, the system turns all LEDs, the light source and the position sensor IR LED, on, initiating the light acquisition at the phototransistor. While a scan and an acquisition occur, an array with the dimensions of the required number of steps, given by equation (43) is filled with the photovoltage values detected at the phototransistor.

$$required\ moving\ angle = steps \times\ angle\_per\_step \qquad (43)$$

in which $angle\_per\_step$ corresponds to the movement of one step with a fully assembled motor system with gearhead and belt.

The photovoltage measured at the phototransistor is saved with its corresponding step number in the respective array in the memory of the PIC18 and if a full scan has not already occurred, then system will move one more step. If with this step the position sensor detects the position zero before expected, then all measured data is erased from the memory of the PIC; if the position sensor does not detect the position zero, then the system will continuing to acquire the light intensity for the new step.

Considering the minimum and maximum values of rotation, calculated previously in chapter 4.1.6.1, it is required that in order to move approximately 7º, the motor must move approximately 18 steps. Having acquired data for all steps required during the movement, the system will get the step where the minimum light intensity was detected. Using (43), the angle of the plane light direction is easily calculated and knowing this angle and recalling expressions (32) and (33), the values for the concentrations of glucose and fructose are easily calculated. In the end of the calculations, the concentrations are sent by the microcontroller USART to the HyperTerminal of the computer, where the results may be viewed by the user.

Something that must be taken into consideration is the ambient light incident in the phototransistor; this light generates additional photovoltage, considered as noise in the application. However, as it was explained, the photovoltage is not considered for quantitative analysis, but only for qualitative analysis.

The software for the polarimeter was developed accordingly with the diagram depicted in figure 4-33. All developed software is presented within the CD-ROM, delivered with the present report at the Department of Physics.

4.1.5.8 Tests and Validation

After the assembly of the polarimeter, validation tests were made, considering all requirements previously specified. Using the components referred through this chapter, it is possible to preview the results obtained with the polarimeter: knowing that the minimum concentrations of glucose and fructose in wine are approximately 50 g/l and that the maximum concentrations are around 180 g/l, then, using the expression (31), it is possible to theorize the minimum and the maximum angular rotation. For a vial length of 1dm, and knowing that the optical power of glucose is 52.7º and the optical power of the fructose is -92.5º, the minimum rotation calculated for fructose and glucose is approximately $-1.985º$, while the maximum rotation calculated is $-7.146º$. For minimum concentrations of 50g/l:

$$\alpha = \left(\frac{52.7 \times 50}{1000} \times 1\right) - \left(\frac{92.5 \times 50}{1000} \times 1\right)$$

$$\Leftrightarrow \alpha = -1.985^{o}$$

For maximum concentrations of 180g/l:

$$\alpha = \left(\frac{52.7 \times 180}{1000} \times 1\right) - \left(\frac{92.4 \times 180}{1000} \times 1\right)$$

$$\Leftrightarrow \alpha = -7.146\ ^{o}$$

For testing purposes, however, it was used an aqueous solutions of sucrose, using tap water and ordinary sugar, which was easier to acquire. Following the same procedure, then:

$$\alpha = [\alpha]_{\text{sucrose}}.\,\text{l}.\,\text{c}_{\text{sucrose}} \qquad (44)$$

in which $[\alpha]_{\text{sucrose}} = 66^{o}$, and l is 1 dm, for the minimum concentration of 50 g/l:

$$\alpha = \left(\frac{66 \times 50}{1000} \times 1\right)$$

$$\Leftrightarrow \alpha = 3.3^{o}$$

And for the maximum concentration of 180 g/l:

$$\alpha = \left(\frac{66 \times 180}{1000} \times 1\right)$$

$$\Leftrightarrow \alpha = 11.88\ ^{o}$$

With these calculations, it is possible to predict that the minimum rotation would be 3.3º and the maximum rotation would be 11.88º. Using this knowledge, it is possible to evaluate the results of the polarimeter. The measurements made for the system testing and validation are depicted in the following table:

Table V: Sucrose concentration Measurement Using Polarimetry

Sucrose Mass (g)	Volume (ml)	Calculated concentration with formula (g/ml)	Angle (º)	Calculated Calculation with polarimetry (g/ml)
14.00 ± 0.50	91.00 ± 0.50	0.154 ± 0.006	10.0 ± 1.0	0.151 ± 0.028
14.00 ± 0.50	153.50 ± 0.50	0.091 ± 0.003	6.0 ± 1.0	0.091 ± 0.024
28.00 ± 0.50	153.50 ± 0.50	0.182 ± 0.003	12.0 ± 1.0	0.182 ± 0.030

The quantities of sugar were measured in a precision scales, available in Activespace Technologies, SA laboratory, and the volume was measured with graduated pipettes, allowing to determine the concentration. In order to measure the error of the calculated concentration and knowing that

$$c = \frac{m}{V} \tag{45}$$

it is used the error propagation equation:

$$\Delta c = \sqrt{\left(\Delta \mathrm{m}^2 \left(\frac{\delta \mathrm{c}}{\delta \mathrm{m}}\right)^2 + \Delta \mathrm{V}^2 \left(\frac{\delta \mathrm{c}}{\delta \mathrm{V}}\right)^2\right)} \Leftrightarrow \Delta c = \sqrt{\left(0.5^2 \left(\frac{1}{\mathrm{V}}\right)^2 + 0.5^2 \left(\frac{\mathrm{m}}{\mathrm{V}^2}\right)^2\right)}$$

In order to measure the angle measured at the polarimeter, it was used a protractor, since there had been a problem concerning the motor belt, which prevented the use of the polarimeter automatic process. Using this method, the obtained values are represented in Table V above, as well as the respective errors, determined with the error propagation equation for the measured concentration through polarimetric methods, recalling (25) and (44), for sucrose concentration measurement ($[\alpha]_{\mathrm{D}}^{20} = 66º$) and a distance L of one decimetre and a respective error of $\pm 0.5\ dm$:

$$\Delta c = \sqrt{\left(\Delta \alpha^2 \left(\frac{\delta \mathrm{c}}{\delta \alpha}\right)^2 + \Delta \mathrm{L}^2 \left(\frac{\delta \mathrm{c}}{\delta \mathrm{L}}\right)^2\right)} \Leftrightarrow \Delta c = \sqrt{\left(1^2 \left(\frac{1}{66 \times \mathrm{L}}\right)^2 + 0.5^2 \left(\frac{\alpha}{66 \times \mathrm{L}^2}\right)^2\right)}$$

Considering the obtained results, it was possible to draw the graphic of the transfer function for the polarimeter:

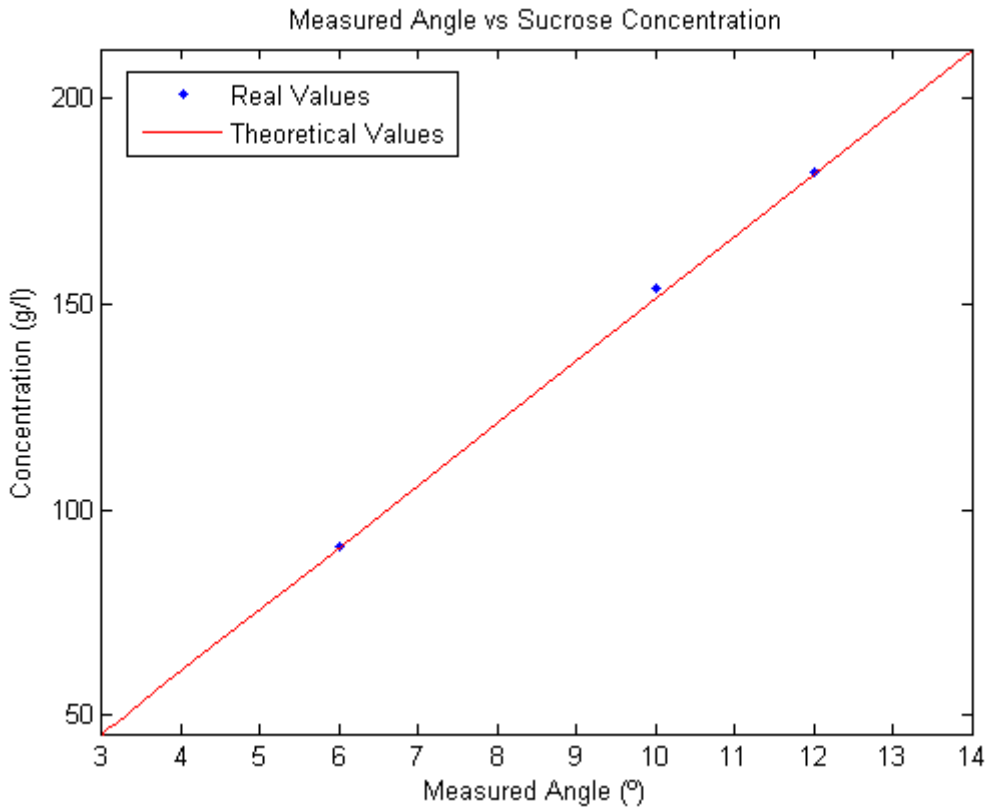

Figure 4-34: Results of the Polarimeter

In the graphic, the enhanced blue points represent the relation between the concentrations calculated with (45) and the measured angle at the polarimeter, while the red line represents the expected concentration values for each angle, calculated with (44).

As it is seen in the graph, the values for concentration obtained with (45) are very similar to those expected with (44). The errors between both measurements of concentration are respectively 0.0020 g/ml, 0.000296 g/ml and 0.0001 g/ml for each measurement. Because it is desired a resolution of 1g/l, or 0.001g/ml, these values for errors are considered acceptable and therefore, according with the performed tests, the polarimeter prototype is considered to be both functional and providing reliable values for concentrations.

4.2 Sensor’s placement and liquid isolation

The sensors will be in contact with the wine, in order to measure the respective parameters. For this, it was decided to use tubes connections in “+” and “T” shape, made of stainless steel, to place the sensors inside and perform the measurements. These pipes are depicted in the following image:

Figure 4-35: Tube connections used for sensors implementation

In order to proper isolate the screws of the pipes, it was decided to use food grade silicone. This is still under research and analysis for application.

5 Conclusions

For the UVAS project, it was necessary to analyze a list of physical and chemical parameters (Table III; contact Activespace Technologies, SA for more information) and find a solution with which was possible to measure that specific parameter. Of all presented parameters, it was not possible to find solutions for all chemical parameters, being possible to find solutions to all desirable physical parameters.

After the initial research phase, it became the responsibility of trainee Paulo Marques to develop the polarimeter sensor. In the development of the polarimeter, there were some considerations that require to be analysed, in order to be able to develop a better product in phase two. The main problem to consider is no doubt the alignment of the light source and of the phototransistor. These two components must be properly aligned in order to detect the light. Associated with this, there is the problem of the light source; considering the analysis made, only one LED must be used as light source. Although only one of the used LED proved to be bright enough for the application, it may be desirable to find other LED that emits in the wavelength of 589 nm, with a light intensity superior to 9.750 cd. Another consideration is the requirement to have the polarimeter completely light isolated, because external light sources add noise to the signals.

Two possible architectures were proposed to develop the UVAS system: to use mobile parts and to use optoelectronic methods. As it was presented in this document, the selected approach was the mobile parts polarimeter. Using this method, a precision in concentration measurement of 1g/l was achieved and good results with small errors were determined for sucrose concentrations. The optoelectronic polarimeter was intended to be assembled and tested, but due to delays, this was not possible. In phase two, it is intended to assemble an optoelectronic polarimeter and validate its application in the UVAS system.

It was intended to have a full prototype with all functionalities presented as of the date of disclosure of the present document. However, due to several delays in the implementation of the sensors, it was not possible to fully accomplish it and because of this, it was given a greater importance in the assembly and validation of the sensors for the UVAS system. These are currently being developed and all functionalities presented but not developed in phase one will be fully implemented in phase two of the UVAS system, starting in October of the present year.

6 Glossary

6.1 Terms and Definitions

Acoustic Viscosity	Acoustic viscosity is a measure of absolute viscosity times specific gravity.
cP	Centipoises – Viscosity measurement unit
cSt	Centistokes – Viscosity measurement unit
mPas	Milipascals – Viscosity measurement unit
IDT	Interdigital transducer or interdigitated transducer, is a device which consists of two interlocking comb-shaped metallic coatings (in the fashion of a zipper) which are applied to a piezoelectric substrate, such as quartz or lithium niobate. IDTs are primarily used to convert microwaves to surface acoustic waves
AT-Cut	Cut made in crystals with an angle θ with the transversal
cP	Centipoises – viscosity unit
cc	Cubic centimetre – volume unit
IDEF0	IDEF0 is part of the IDEF family of modelling languages in the field of software engineering, and is built on the functional modelling language Structured Analysis and Design Technique (SADT).
cd	candela
Brix	Sugar Concentration Measurement Unit

6.2 Acronyms

AD	Applicable Document
AST	ActiveSpace Technologies, SA
AV	Acoustic Viscosity
BAW	Bulk Acoustic Wave

CVD	Chemical Vapour Deposition
DV	Dynamic Viscosity
GUI	Graphical User Interface
HMI	Human Machine Interface
IDEF	Integration Definition for Function Modelling
IDT	Interdigital transducers
ISFET	Ion Sensitive Field Effect Transistor
KV	Kinematic Viscosity
MIP	Mutual Impedance Probe
MOSFET	Metal Oxide Semiconductor Field Effect Transistor
NA	Not Applicable
NTC	Negative Temperature Coefficient
PEEK	Polyether ether ketone
PTC	Positive Thermal Coefficient
PWA	Permittivity, Waves and Altimetry
RD	Reference Document
RD	Relative Density
RTD	Resistive Thermal Devices
SADT	Structured Analysis and Design Technique
SAW	Surface Acoustic Wave
SG	Specific Gravity
SH-APM	Shear-Horizontal Acoustic Plate Mode
SNR	Signal to Noise Ratio
STW	Surface Transverse Wave
SVN	Subversion

SW	Specific Weight
TBD	To Be Defined
TSM	Thickness Shear Mode
UVAS	Unidade Vinícola Automatizada por Sondagem
CATIA	Computer Aided Three-dimensional Interactive Application

7 Applicable and Reference Documents

7.1 Applicable Documents

[AD1]	Mike Coope, “Sensorland.com,” June 2000. [Online]. Available: http://www.sensorland.com [Accessed: Sept., 2009].
[AD2]	“ISFET”. [Online]. Available: http://www.wikipedia.org. [Accessed: Oct., 2009].
[AD3]	PASCO, “Products PS-2102 – ENGLISH DOCUMENTS”, [Online]. Available: http://store.pasco.com [Accessed: Oct, 2009].
[AD4]	ENVCO-Environmental Equipment, “Greenspan pH1200 pH Sensor”, [Online], Available: http://www.envcoglobal.com/catalog/product/digital-ph-sensors [Accessed: Oct, 2009].
[AD5]	Metler-Toledo, “InPro3300”, [Online], Available: http://us.mt.com/us/en/home.html [Accessed: Oct, 2009]
[AD6]	Campbell Scientific, “CS525 Submersible ISFET pH Probe”, [Online], Available: http://www.campbellsci.com/cs525 [Accessed: Oct,2009]
[AD7]	Hach, “PH77-SS”[Online], Available: http:// http://www.hach.com/ [Accessed: Oct,2009]
[AD8]	Hach, “PH37-SS” Available: http:// http://www.hach.com/ [Accessed: Oct,2009]
[AD9]	Prof. Dr. Ir. P. Bergveld Em, “ISFET, Theory and Practice”, University of Twente, IEEE Sensor Conference, Toronto, Oct 2003, Available: http://www.ewh.ieee.org/tc/sensors/Tutorials/ISFET-Bergveld.pdf. [Accessed: Oct 2009]
[AD10]	Endress+Hauser,”Tophit CPS471D”, [Online], Available: http://www.us.endress.com/ [Accessed: Oct,2009]
[AD11]	Monarch Instrument, “PHTEMP101”, [Online], Available: http://www.monarchinstrument.com/dcloggers.htm?ID=PH/ [Accessed: Oct 2009]
[AD12]	“Thermoelectric Effect”. [Online]. Available: http://www.wikipedia.org. [Accessed: Nov., 2009].
[AD13]	“Thermocouple”. [Online]. Available: http://www.wikipedia.org. [Accessed: Nov., 2009].
[AD14]	“Resistive Thermal Device”. [Online]. Available: http://www.wikipedia.org. [Accessed: Nov., 2009].
[AD15]	“Negative Thermal Coefficient”. [Online]. Available: http://www.wikipedia.org. [Accessed: Nov., 2009].

[AD16]	“Temperature/Resistance Table for Platinum Sensors”, [Online], Available: http://www.lakeshore.com [Accessed: Nov., 2009]
[AD17]	“5618B Small Diameter Industrial RTD”, Fluke, Hart Scientific, [Online], Available: http://www.hartscientific.com/products/5618.htm [Accessed: Nov 2009]
[AD18]	“Precision Industrial RTDs – Model 5627A”, Fluke, Hart Scientific, [Online], Available: http://www.hartscientific.com/products/5627A.htm [Accessed: Nov 2009]
[AD19]	“Viscosity”, [Online]. Available: http://www.wikipedia.org. [Accessed: Nov., 2009].
[AD20]	“Viscosity”, [Online]. Available: http://wiki.xtronics.com/, [Accessed: Nov., 2009].
[AD21]	Glenn Elert, “Viscosity”, [Online], The Physics Hypertextbook, 1998, Available: http://physics.info/, [Accessed: Nov., 2009].
[AD22]	Brookfield Enginneering, “Why Measure Viscosity?, [Online], Brookfield Engineering Available: http://www.brookfieldengineering.com [Accessed: Nov. 2009].
[AD23]	Sengenuity, Sensor Engine Technology, “Acoustic Wave Technology For Viscosity Measurement Using the ViSmart Viscosity Sensor”, [Online], Sengenuity, Sensor Engine Technology, Available: http://www.sengenuity.com/tech_ref [Accessed: Nov. 2009].
[AD24]	Kerem Durdag, “Viscosity Monitoring With a Solid-state Embedded Probe”, [Online], Vectron Machinery Lubrication Magazine, September 2007, Available: http://www.machinerylubrication.com [Accessed: Nov.2009]
[AD25]	“M10 Viscosity Sensor”, Norcross, [Online], Available: http://www.viscosity.com/ne_pr13.html, [Accessed: Nov 2009]
[AD26]	“Model M50”, Norcross, [Online], Available: http://www.viscosity.com/p_sensors_il.html, [Accessed: Nov 2009]
[AD27]	“Model M24”, Norcross, [Online], Available: http://www.viscosity.com/p_sensors_il.html, [Accessed: Nov 2009]
[AD28]	“XL7”, Hydramotion, [Online], Available: http://www.hydramotion.com/, [Accessed: Nov 2009]
[AD29]	Sofraser, “MIVI”, [Online], Available: http://www.sofraser.com/viscometer_mivi.htm, [Accessed: Nov 2009]
[AD30]	Sofraser, “CIVI”, [Online], Available: http://www.sofraser.com/ink_process_viscometer_polymer_principle.htm , [Accessed: Nov 2009]
[AD31]	L. M. Reindl, “Wireless Passive SAW Identification Marks and sensors”, Institute of Electrical Information Technology, Clausthal University of Technology, [Online], Available: http://ewh.ieee.org/tc/sensors/Tutorials/reindl-tutorial-NewOrleans.pdf,

	[Accessed: Nov 2009]
[AD32]	Bill Drafts, “Acoustic Wave Technology Sensors”, Sensors, Oct 2000 [Online], Available: http://www.sensorsmag.com/sensors/acoustic-ultrasound/acoustic-wave-technology-sensors-936, [Accessed: Nov 2009]
[AD33]	“Surface Acoustic Wave”, [Online]. Available: http://www.wikipedia.org. [Accessed: Nov., 2009].
[AD34]	Sengenuity Acoustic Viscosity Sensors Video Presentation, [Online], Available: http://www.sengenuity.com/video.html, [Accessed: Nov. 2009]
[AD35]	Sengenuity, “The Technology”, [Online], Available: http://www.sengenuity.com/technology.html, [Accessed: Nov. 2009]
[AD36]	Sengenuity, “ VISmart™ Solid-State Low Shear Bolt Sensor”, [Online], Available: http://www.sengenuity.com/prods_spec_sheets.html, [Accessed: Nov. 2009]
[AD37]	C-N Kim and Y-M Park, “An investigation on the in situ measurement of oil concentration”, International Journal of Air conditioning and Refrigeration, vol. 9 no.1, pp 20-28, 2001.
[AD38]	Steve Baum, “Fluid Density and Hydrostatic Pressure”, Dec 1997. [Online]. Available: http://stommel.tamu.edu/~baum/reid/book1/book/node52.html [Accessed: Nov. 2009].
[AD39]	The Engineering Toolbox, “Buoyancy”, The Engineering Toolbox, 2005. [Online] Available: http://www.engineeringtoolbox.com/buoyancy-force-d_1485.html [Accessed: Nov, 2009].
[AD40]	The Engineering Toolbox, “Density, Specific Weight and Specific Gravity”, The Engineering Toolbox, 2005 [Online] Available: http://www.engineeringtoolbox.com/density-specific-weight-gravity-d_290.html [Accessed: Nov, 2009].
[AD41]	The Engineering Toolbox, “Density of Fluids – Changing Pressure and Temperature”, The Engineering Toolbox, 2005 [Online] Available: http://www.engineeringtoolbox.com/fluid-density-temperature-pressure-d_309.html [Accessed: Nov, 2009].
[AD42]	Kerem Durdag, Vectron “Viscosity Monitoring With a Solid-state Embedded Probe”, Practicing Oil Analysis Magazine. September 2007 [Online] Available: http://www.oilanalysis.com/ [Accessed: Nov, 2009]
[AD43]	“Buoyancy”, Wikipedia, [Online] Available: http://www.wikipedia.org [Accessed: Nov, 2009]
[AD44]	FMC Technologies, “Model S50-D Density Sensor”, datasheet, [Online] Available: http://info.smithmeter.com/literature/docs/ss0m020.pdf, [Accessed: Nov, 2009]

[AD45]	Thermo Scientific, " Thermo Scientific, Sarasota FD900, Sarasota ID900, Sarasota PD900 Gas Density Meters", datasheet, [Online] Available: http://info.smithmeter.com/literature/docs/ss0m020.pdf, [Accessed: Nov, 2009]
[AD46]	Lemis Process, "In-tank Density Meters DC-40 SERIES", datasheet, [Online] Available: http://www.lemis-process.com/?mid=41&measure=40&pid=13, [Accessed: Nov, 2009]
[AD47]	Lemis Process, "In-tank Density and Viscosity Meters DC-42 SERIES", datasheet, [Online] Available: http://www.lemis-process.com/?mid=41&measure=40&pid=1, [Accessed: Nov, 2009]
[AD48]	Lemis Process, " In-tank Density Meter DC-40 TRIO", datasheet, [Online] Available: http://www.lemis-process.com/?mid=41&measure=40&pid=26, [Accessed: Nov, 2009]
[AD49]	Lemis Baltic, "In-flow Density and Viscosity Meter DC-52", datasheet, [Online] Available: http://www.lemis-baltic.com/pages/index.php?murl=products&psg=15, [Accessed: Nov, 2009]
[AD50]	Ronan Engineering, "Density", Technical document [Online] Available: http://www.ronanmeasure.com/tn_dens.html [Accessed: Nov,2009]
[AD51]	"Electrical conductivity", [Online]. Available: http://www.wikipedia.org. [Accessed: Nov., 2009].
[AD52]	"Permittivity"", [Online]. Available: http://www.wikipedia.org. [Accessed: Nov., 2009].
[AD53]	"Physics Forum: Relation between conductivity and permittivity", [Online], Available: http://www.physicsforums.com/showthread.php?t=265516. [Accessed: Nov. 2009]
[AD54]	Atago, "Digital Hand-held "Pocket" Ethyl alcohol Meter PAL-34S", [Online], Available: http://www.atago.net/english/pop_pal_34s.html, [Accessed: May 2010]
[AD55]	Atago, "Digital Hand-held "Pocket" Wine Refractometer", [Online], http://www.atago.net/USA/products_wine.php#wp5, [Accessed: May 2010]
[AD56]	"Basic stepper control - PIC18F and L293D", [Online], Available: http://www.electro-tech-online.com/robotics-mechatronics/20759-basic-stepper-control-pic18f-l293d.html, [Accessed: June 2010]
[AD57]	SGS-Thompson Microelectronics, "L293B/L293E, Push-Pull four channel Drivers", [Online], Available: http://www.st.com, [Accessed: June 2010]
[AD58]	Andptoelectronics, "AND180HYP InGaAlP High Brightness Yellow Light Emission" [Online], Available: http://www.purdyelectronics.com/pdf/AND180HYP.pdf, [Accessed: June 2010]

[AD59]	OSRAM, “NPN-Si-Fototransistor SFH 3310”, [Online], Available: http://www.osram.com/osram_com/, [Accessed: June 2010]
[AD60]	NDT Resource Center, “Acoustic Impedance”, [Online], Available: http://www.ndt-ed.org/EducationResources/CommunityCollege/Ultrasonics/Physics/acousticimpedance.htm, [Accessed: July 2010
[AD61]	Cole Parmer, “Cole-Parmer Technical Library, Refractometers”, [Online] Available: http://www.coleparmer.com/techinfo/techinfo.asp?htmlfile=Refractometers.htm&ID=633, [Accessed: July, 2010]
[AD62]	ESA, “Polarimetry Tutorial”, [Online] Available: http://earth.esa.int/polsarpro/tutorial.html, [Accessed: July, 2010]
[AD63]	Eric Seale, “Phototransistors”, July 12, 2003, [Online] Available: http://encyclobeamia.solarbotics.net/articles/phototransistor.html [Accessed: July, 2010]
[AD64]	Murdoch University Library, “How to Cite References – IEEE Style”, February 2008, [Online] Available: http://wwwlib.murdoch.edu.au/find/citation/ieee.html [Accessed: September 2009]
[AD65]	National Semiconductor, Application Note 31, “Op Amp Circuit Collection” September 2002, [Online] Available: http://www.national.com/an/AN/AN-31.pdf, [Accessed: May 2010]
[AD66]	National Instruments, “Measuring Temperature with an RTD or Thermistor”, 13th November 2009, [Online] Available: http://zone.ni.com/devzone/cda/tut/p/id/3643, [Accessed: December, 2009]
[AD67]	Labfacility, “Temperature and Process Technology, Platinum RTD” [Online] Available: http://www.farnell.com/datasheets/22128.pdf, [Accessed: May 2010]
[AD68]	Optoi, “Microelectronics – pH sensor”, [Online] Available: http://www.optoi.com/, [Accessed: Nov 2009]
[AD69]	Edmund Optics, “TECHSPEC® Linear Polarizing Laminated Film”, [Online], Available: http://www.edmundoptics.com/, [Accessed: June 2010]
[AD70]	Edmund Optics, “Precision Pinholes”, [Online], Available: http://www.edmundoptics.com/, [Accessed: June 2010]
[AD71]	John Hanson, “Chemistry Lab Techniques - Refractometry”, last updated 01/09/04, [Online], Available: http://www2.ups.edu/faculty/hanson/labtechniques/refractometry/intro.htm, [Accessed: June 2010]
[AD72]	Grapestompers, “How To Use A Refractometer in Winemaking”, [Online], Available: http://www.grapestompers.com/articles/refractometer_use.asp,

	[Accessed: May 2010]
[AD73]	Dr. E. Thall, Thall's Website, Florida State College, "Stereochemistry", [Online], Available: http://web.fccj.org/~ethall/stereo/stereo.htm/, [Accessed: May 2010]
[AD74]	Physics Handbook, "Malus's Law", [Online] Available: http://www.physicshandbook.com/laws/maluslaw.htm, [Accessed: May 2010]
[AD75]	Scienceworld, Wolfram Research, [Online] Available: http://scienceworld.wolfram.com/physics/MalussLaw.html, [Accessed: May 2010]
[AD76]	Eric Weisstein, "World of Science, Wolfram Web Resource", [Online] Available: http://scienceworld.wolfram.com/, [Accessed: June 2010]
[AD77]	"Ethanol"", [Online], Available: http://www.wikipedia.org. [Accessed: March., 2009].
[AD78]	Bellingham+Stanley Technical Bulletin, R016, Refractometer Scales, Misconceptions, [Online], Available: http://www.bellinghamandstanley.com/, [Accessed: July 2010]
[AD79]	Hydronix, "Measuring Moisture in Sugar", [Online], Available: http://www.hydronix.com/applications/moisture_in_sugar.php?gclid=CIK84LDm1KMCFan-2AodkCMdbw, [Accessed: June 2010]
[AD80]	Brix Refractometer, http://www.bombayharbor.com/Product/31513/Brix_Refractometer.html
[AD81]	"PM35l048", NMB-MAT, [Online] Available: http://www.datasheetarchive.com/PM35S-048-datasheet.html [Accessed May 2010]
[AD82]	"Refractive Index of Crop Juices -- Calibrated In % Sucrose Or ºBrix", [Online] Available:http://www.highbrixgardens.com/pdf/brix-chart.pdf, [Accessed July 2010]

7.2 Reference Documents

[RD1]	P. Steendijk, G. Mur, E. T. Van Der Velde, and L. Baan, "The four-electrode resistivity technique in anisotropic media: theoretical analysis and application on myocardial tissue in vivo," IEEE Transactions on Biomedical Engineering, vol.40, pp. 1138-1148, 1993.
[RD2]	P. N. Robillard and D. Poussart, "Spatial Resolution of Four Electrode Array," IEEE Transactions on Biomedical Engineering, vol. 26, pp. 465-470,1979.
[RD3]	C. Korasli, "A New Method For Measuring Earth Electrode Resistance in Low-Voltage Distribution Systems", University of Bahrain, Dept. of Electrical Engineering, Isa Town, Kingdom of Bahrain.
[RD4]	M.A. Omar, "Elementary Solid State Physics", Addison Wesley Publishing Company, 1975

[RD5]	J. Fraden, “Handbook of Modern Sensors”, 3rd ed., Springer, 2003.
[RD6]	G.K. Batchelor, “An introduction to Fluid Dynamics”, Cambridge University Press, 1967
[RD7]	M. A. Pérez, R. Muñiz, C. de la Torre, B. Garcia, C. E. Carleos, R. Crespo, L.M. Cárcel “Impedance Spectrometry For Monitoring Alcoholic Fermentation Kinetics Under Wine-Making Industrial Conditions”, XIX IMEKO World Congress, Fundamental and Applied Metrology, September 6-11, 2009, Lisbon, Portugal
[RD8]	K. Lauer, *et al*, "Process for the Simultaneous Determination of Glucose and Fructose", Sep 1972, Available: googlebooks , [Accessed: June 2010]
[RD9]	eXtreme Electronics, “Controlling DC Motors, AVR Tutorial Series”, [Online], Available: http://extremeelectronics.co.in/, [Accessed: June 2010]
[RD10]	D. W. Jones, University of Iowa, “Stepping Motors Fundamentals, AN907”, Reston Condit, Microchip Technology Inc, Microchip Technology Inc, [Online], Available: http://www.microchip.com/, [Accessed: June 2010]
[RD11]	B. C. Baker, "Precision Temperature-Sensing With RTD Circuits, AN687", Microchip Technology Inc, [Online], Available: http://www.microchip.com/, [Accessed: June 2010]
[RD12]	P. Yedamale, S. Chattopadhyay, “Stepper Motor Microstepping with PIC18C452, AN822”, Microchip Technology Inc, [Online], Available: http://www.microchip.com/, [Accessed: June 2010]
[RD13]	F. J. Bates and Associates “Polarimetry, Sacharimetry and the Sugars” Conversion tables, , Circular of the Bureau of Standards C440, [Online], Available: http://www.boulder.nist.gov/div838/SelectedPubs/Circular%20440%20Table%20114.pdf [Accessed: June 2010]
[RD14]	C. Raynal, C. Bonnefond, F. Raginel, D. Granès, A. Ortiz-Julien, “Wine fermentation with a new, 100% organic nutrient”, [Online], Available: http://www.lallemandwine.com/IMG/pdf_Fermaid_O_eng.pdf, [Accessed: May 2010]
[RD15]	D. Wang, Y.Xu, J.Hu, G.Zhao, “Fermentation Kinetics of different sugars by apple wine yeast Saccharomyces cerevisiae”, [Online], Available: http://www.scientificsocieties.org/jib/papers/2004/G-2004-1304-255.pdf, [Accessed: May 2010]
[RD16]	C-N Kim and Y-M Park, “An investigation on the in situ measurement of oil concentration”, International Journal of Air conditioning and Refrigeration, vol. 9 no.1, pp 20-28, 2001.
[RD17]	Organization International de la Vigne et du Vin, “Compendium of International

	Methods of Wine and Must Analysis", Volume 1, Edition of 2010.
[RD18]	Organization International de la Vigne et du Vin, "Compendium of International Methods of Wine and Must Analysis", Volume 2, Edition of 2010.
[RD19]	Anelli G. 1977, The proteins of must, Am. J. Enol. Vitic. 28:200-203
[RD20]	Bely, J.M. Sablayrolles and P. Barre, Automatic detection of assimilable nitrogen deficiencies during alcoholic fermentation in enological conditions, J. Ferm. Bioeng. 70 4 (1990), pp. 246–252.
[RD21]	Bisson, L.F., 1999, Stuck and sluggish fermentations. Am. J. Enol. Vitic. 50, 107-119.
[RD22]	Cardoso, A.D.; Carvalheira, J., Coimbra M.A., Rocha S. (2005) Tecnologia dos Vinhos Tintos. Cardoso A.D.(Ed.) DRABL.
[RD23]	Curvelo-Garcia A. (1988) Controlo de Qualidade dos Vinhos. Química Enológica. Métodos Analíticos. IVV.
[RD24]	Esti M., Volpe G., Micheli L., Delibato E. Compagnone D., Moscone D., Palleschi G. (2004) Electrochemical biosensors for monitoring malolactic fermentation in red wine using two strains of Oenococcus oeni Anal. Chim. Acta 513: 357-364
[RD25]	Goelzer A., Charnomordic B., Colombié S., Fromion V. Sablayrolles J.M. 2009 Simulation and optimization software for alcoholic fermentation in winemaking conditions Food Control 20(7):635-642
[RD26]	Molina A.M., Swiegers J. H., Varela C., Pretorius I. S., Agosin E. (2007) Influence of wine fermentation temperature on the synthesis of yeast-derived volatile aroma compounds Appl Microbiol Biotechnol 77:675–687
[RD27]	Ribéreau-Gayon P., Dubourdieu D. Donéche B., Lonvaud A., (1999) Traité d´Œnologie. 2. Chimie du vin. Stabilisation et traitments . Dunod , Paris.
[RD28]	Ribéreau-Gayon P., Glories Y., Maujean A., Dubourdieu D. (1998) Traité d´Œnologie. 2. Chimie du vin. Stabilisation et traitments . Dunod , Paris.
[RD29]	Urtubia A., Pérez-Correa J.R., Meurens M., Agosin E. (2004) Monitoring large scale wine fermentations with infrared spectroscopy . Talanta 64: 778-784
[RD30]	Urtubia A., Pérez-Correa J.R., Soto A. Pszczólkowski P. (2007) Using data mininig techniques to predict industrial wine problems fermentations Food Control 18: 1512-1517.
[RD31]	Vicente, António Madrid (1987) Manual de Enologia Practica. A. Madrid Vicente,

	Ediciones Madrid.
[RD32]	Amerine M.A. & OUGH C.S. Methods For Analysis of Musts and Wines, Etobicoke, Canada, Wiley, 1980.